Quantum Electrodynamics of Excitons with Radiative Relaxation

A dissertation submitted to

THE GRADUATE SCHOOL OF ENGINEERING SCIENCE
OSAKA UNIVERSITY

in partial fulfillment of the requirements for the degree of

DOCTOR OF PHILOSOPHY IN SCIENCE

by

Motoaki BAMBA

March 2009

Abstract

An electron and a hole attract each other due to the Coulomb interaction, and they behave as a quasi-particle called exciton. An exciton can be created by a photon which is incident into the material, and the created exciton collapses into a photon with a finite life time. After that, the emitted photon can also create another exciton at other position. In this way, the exciton and photon propagate as a quasi-particle in the material, and it is called an exciton-polariton. Because of the Coulomb interaction and the Pauli exclusion principle, excitons interact with each other, and then optical response of excitons has been discussed for several decades not only in its linear (one-exciton) process but also in nonlinear (many-exciton) processes. However, such discussions have been mainly performed in the semiclassical framework, where the light is classically treated based on the Maxwell equations. The construction of full quantum theories for exciton optical processes is currently a developing theme, and attracts an attention due to the recent development of quantum information technologies and the recent observation of nonclassical states of exciton-polaritons, such as entanglement, squeezing, Bose-Einstein condensation, and so on.

Although the quantum electrodynamics (QED) in vacuum was established in the 1940s, the QED of excitonic materials has been discussed for only about 15 years. Compared to the vacuum situation, we must consider the frequency dependence of the dielectric function of the materials due to the polariton effect in addition to the nonradiative damping of excitons, which is inevitable to discuss their resonance processes. The QED of such dispersive and absorptive media has been discussed in the pioneering work by Huttner and Barnett in 1992. Its theoretical framework can be interpreted by the relation with the fluctuation dissipation theorem, and has a good correspondence with the classical electrodynamics based on the Maxwell equations. Currently, this QED theory has been extended to inhomogeneous, anisotropic, magnetic, and nonlinear media. However, there remains a task to consider the nonlocal susceptibility originating from the exciton center-of-mass motion, which has been discussed in the semiclassical framework for about 50 years.

The nonlocal optical susceptibility is a general property derived from the linear response theory, and its nonlocality should be explicitly considered in nano-scale systems in order to describe the confinement of the exciton center-of-mass motion. While the nonlocality has been discussed in relation with additional boundary condition (ABC) problem, K. Cho has proposed a theoretical framework which requires no ABC in 1986. This is called an ABC-Free theory or a microscopic nonlocal theory, and has been applied to linear and nonlinear optical processes of excitons confined in nano-scale materials. However, this theory has been discussed in the semiclassical framework.

One of the main subjects in this thesis is the construction of a QED theory for excitons in arbitrary-structured 3D materials with considering the nonlocality and nonradiative damping of excitons. This theory maintains good correspondences with its underlying theories, the QED theory for dispersive and absorptive media and the semiclassical microscopic nonlocal theory. Although the same kind of theories

have already been proposed in line with the series of QED theories, the present QED theory provides a practical calculation method for arbitrary-structured excitonic materials from nano- to macro-scale by using the same calculation idea as the microscopic nonlocal theory. On the other hand, from the viewpoint of extending the nonlocal theory, the present theory enables us to consider the quantum fluctuation of the electromagnetic fields and to describe nonclassical states of light. Furthermore, it has been revealed in the present thesis that the nonlocal theory can provide the retarded correlation functions of excitons and of electromagnetic fields.

Another subject in the present thesis is the analysis of exciton-photon coupled modes in excitonic finite systems, whose resonance frequency and radiative decay rate can be obtained as poles of the exciton correlation functions derived in the nonlocal theory. Especially, I have focused on the material-size dependence of the exciton radiative decay rate. According to Fermi's golden rule, increasing the material size, the radiative decay rate becomes higher because of the increment of the interaction volume between excitons and radiation field. This is called exciton superradiance, and has been discussed theoretically and experimentally for more than 20 years. On the other hand, in a thick film where the exciton-polariton picture is suitable, we can consider that the radiative decay time of polaritons is proportional to the time of flight in the film. Therefore, the radiative decay rate is inversely proportional to the film thickness in contrast to the exciton superradiance. This contradiction reflects a breakdown of Fermi's golden rule in the exciton-photon interaction. The crossover between the two radiative decay schemes has been theoretically discussed in some works previously, and it is interpreted as the crossover of exciton-photon coupled modes from exciton-/photon-like to polariton modes. However, the crossover condition has not been completely clarified. By using a rigorous calculation method based on the microscopic nonlocal theory, which can connect the two decay schemes, I have calculated the exciton radiative decay rate in a CuCl film with continuously changing the thickness from nano- to macro-scale, and then the crossover behavior has been numerically obtained. For the analysis, I have intuitively introduced another calculation method, which is based on the dispersion relation and resonance condition and can reproduce the results of the rigorous method. From the simplified equation in the intuitive method, I have derived the crossover condition between the two radiative decay schemes. Briefly speaking, the crossover occurs when an apparent propagation speed of superradiant excitons reaches the group velocity of polaritons. This is a reasonable condition in the viewpoint of the breakdown of Fermi's golden rule in exciton-photon interaction.

The other subject in the present thesis is deriving the analytical expression of the excitons' retarded correlation functions, which is written with the information of their poles derived by the intuitive calculation method. The exciton correlation functions renormalize the exciton-photon interaction, and then they reflect the radiative energy shift, retarded interaction via the electromagnetic fields, radiative and nonradiative relaxation processes. According to the quantum theory of many-particle systems, time-ordered and thermal correlation functions can be obtained by the analytic continuation with the retarded ones. Therefore, the analytical expression of the correlation functions is useful for systematic discussion of a variety of nonlinear, relaxation, and emission processes of excitons in arbitrary-structured materials. As a demonstration, I consider a CuCl film with exciton center-of-mass motion, and solve an ABC problem to calculate the poles, i.e., the exciton-photon coupled modes, including polariton-field wavefunctions in these modes. By a intuitive consideration of the analytical expression, the retarded correlation functions have been reproduced with good precision.

Acknowledgements

This thesis is based on my research works under the supervision of Professor Hajime Ishihara, Department of Physics and Electronics, Osaka Prefecture University. I would like to express my sincere gratitude for his advice and discussions throughout the study and for his supervision of publishing and presenting the research works.

Further, I am also grateful to variable discussions with Professor Kazumasa Miyake, Professor Tadashi Itoh, and Professor Nobuyuki Imoto, Osaka University. Prof. Miyake have also given a generous support to me during my research life as a special research student at Osaka Prefecture University.

I also acknowledge to Professor Kikuo Cho, Osaka University, for his fruitful comments and discussions to my research and also his supervision to my bachelor study at Osaka University. I also express thanks to Prof. Hiroshi Ajiki (Osaka University) and Prof. Kazuki Koshino (Tokyo Medical and Dental University) for their helpful comments and discussions from the theoretical viewpoints.

I have also obtained fruitful advice and comments from the experimental research groups of Prof. Tadashi Itoh & Prof. Masaaki Ashida (Osaka University), Prof. Keiichi Edamatsu & Prof. Hideo Kosaka (Tohoku University), Prof. Masaaki Nakayama (Osaka City University), and Prof. Kohji Mizoguchi (Osaka Prefecture University). I would like to thank all the staffs and students in these groups.

I also wish to thank the discussions with Dr. Takuya Iida, Dr. Hisaki Oka, Dr. Akira Ishikawa, and Dr. Seiji Uryu in the research group of Prof. Ishihara. Further, I also wish to acknowledge with gratitude the hearty support of Ms. Hidemi Deguchi, Ms. Etsuko Hazama, Ms. Nobuko Fukuda, and Ms. Ikuko Uchida. I thank faithfully all the members of the research group of Prof. Ishihara for their fruitful discussions.

The present research works were partially supported by the Japan Society for the Promotion of Science (JSPS); a Grant-in-Aid for Creative Science Research, 17GS1204, 2005; and a Grant-in-Aid for JSPS Research Fellows.

Table of Contents

Chapter 1

Introduction

1.1 Background

In conventional theories for optical processes in condensed matters, the light has been mainly treated classically regardless of whether the matter systems are described in quantum mechanical terms (semiclassical theory) or classical ones. These theories have successfully explained a variety of optical phenomena regarding the classical light or the coherent state of photons. However, there is growing interest in the quantum electrodynamics (QED) of elementary excitations in condensed matters in order to discuss optical processes of nonclassical light such as entangled states, single photons, squeezed states, cavity photons, and so on. The relevant experiments have already been reported, for example, the entangled-photon generation via biexcitons (excitonic molecules) [1], triggered single photon generation from bound excitons in a semiconductor [2], and the squeezing of cavity polaritons in semiconductor microcavities [3, 4]. On the other hand, the Bose-Einstein condensation (BEC) of excitons has been discussed as a principle theme concerning the bosonic properties of excitons [5, 6]. Recently, the BEC of exciton-polaritons in semiconductor microcavities has been reported in some experimental works [7, 8, 9, 10], and theoretical analysis of the BEC of excitons interacting with cavity photons is also a hot topic [11, 12, 13, 14, 15].

The quantization of the radiation field has been studied for a long time not only in vacuum [16] but also in a medium characterized by a frequency independent dielectric constant (see introductions and references in Refs. 17 and 18). Further, dispersive dielectric media, which have a frequency dependent dielectric function, has also been considered in some works (see references in Ref. 18). In particular, concerning elementary excitations in condensed matters, Hopfield has discussed eigenstates of exciton-photon systems or exciton-polaritons [19], where their dispersive properties are reflected through the susceptibility $\chi(\omega)$, dielectric function $\varepsilon(\omega) = 1 + \chi(\omega)$, or dispersion relation $\varepsilon(\omega) = c^2k^2/\omega^2$. However, it is well known that the susceptibility is generally represented as a complex function satisfying the Kramers-Kronig relations (see App. A.2). Furthermore, its imaginary part, which characterizes the absorption in medium, cannot be neglected in the discussion of resonant optical processes of elementary excitations in condensed matters.

In the classical and semiclassical frameworks for optical processes in condensed matters, the absorption is reflected mainly through the susceptibility or damping rates of elementary excitations. However, in full quantum frameworks, the absorption significantly modifies the discussion for considering the electromagnetic fluctuation in the same manner as the appearance of fluctuation operator in the Langevin equation (see App. A.3), although the statistical average of the fluctuation itself vanishes and it does not affect the (semi)classical discussions. The theoretical framework for QED of dispersive and absorptive media

has been established by the work of Huttner and Barnett [20, 21] and the successive studies (see a review by Knöll et al. [18]). I will explain the outline of those theories in Sec. 1.3.

On the other hand, the relaxation dynamics of elementary excitations is a significant subject in the solid state optics. Although the relaxation of elementary excitations is mainly caused by the absorption in the case of nearly-infinite crystals, the radiative relaxation should also be considered in inhomogeneous media, especially in nano-structured materials. However, in discussing the optical processes of excitons in inhomogeneous media, it is well known that, in addition to the Maxwell boundary conditions, some additional boundary conditions (ABCs) are required in the traditional calculation method based on connecting the electromagnetic fields at interfaces of different materials [22]. This ABC problem is caused by the spatial nonlocality of excitonic susceptibility $\chi(\boldsymbol{r}, \boldsymbol{r}', \omega)$ originating from their center-of-mass motion, and the nonlocal effects significantly appear in nano-structured materials as the center-of-mass confinement of excitons. In order to avoid the ABC problem, we must explicitly consider the nonlocal susceptibility in inhomogeneous systems. Along the same lines as the above QED theories, the electromagnetic field quantization in such nonlocal systems has also been performed in some works [23, 24, 25, 26, 27, 28]. However, for applying these theories into actual problems, we must solve an integro-differential equation as will seen in Eq. (1.55). Instead of solving this complicated equation, as indicated by Cho in the semiclassical framework [29, 30, 31], we can reduce the problem into a linear equation set by using the microscopic representation of the nonlocal susceptibility. I will explain above-mentioned studies concerning the nonlocality in Sec. 1.4.

Based on the microscopic nonlocal theory [30, 31], some anomalous optical phenomena in nano-structured materials have been predicted theoretically [32, 33, 34, 35, 36, 37, 38, 39], and actually the following experimental works have revealed that the nano-structures show peculiar responses and rapid radiative decay in nonlinear optical processes of excitons. In 1999, a large nonlinearity has been observed for the degenerate four-wave mixing in GaAs film with 110 nm thickness [40, 41]. Further, an energy interchange of exciton's center-of-mass quantum states has been observed by the nondegenerate two-photon excitation scattering in CuCl films with 19.3 nm and 35.3 nm thicknesses in 2004 [42]. Most recently, in 2006, a fast decay time of about 100 fs has been observed for the degenerate four-wave mixing in CuCl film with 187 nm thickness [43]. These anomalous optical responses originate from the long-range interaction between the electromagnetic fields and the excitons with center-of-mass motion coherently spreading in whole crystal. Therefore, in order to discuss these phenomena, we must explicitly consider the exciton center-of-mass motion yielding the nonlocal susceptibility.

1.2 Motivation and purpose of this thesis

The entangled-photon generation via biexcitons in semiconductors was experimentally reported by Edamatsu et al. in 2004 [1], and this has been previously proposed in the theoretical work by Savasta et al. in 1999 [44, 45]. The authors considered a CuCl film with micrometer-order thickness, and also a CuCl crystal with thickness of about 100 μm was used in the actual experiment. On the other hand, in other nonlinear processes of excitons as mentioned in the previous section, some theoretical and experimental studies have revealed that nanometer-order semiconductor films show peculiar and rapid optical responses compared to bulk crystals. The first motivation of the research in this thesis is discussing the entangled-photon generation from nano-structured materials, where a high generation efficiency and anomalous generation properties were expected in the same manner as the above experiments

for nanofilms.

In order to analyze the entangled-photon generation via biexcitons in nano-structured materials, we need a QED theory for excitons confined in nano-structures, i.e., nonlocal inhomogeneous systems. Further, the theory must provide a practical calculation method for inhomogeneous systems in contrast to the previously discussed QED theories [23, 24, 25, 26, 27, 28], in which we must solve the integro-differential equation. One of the purposes in this thesis is to construct such a QED theory applicable to actual material structures including a substrate, outside media, distributed Bragg reflector (DBR) cavity, and so on. This kind of theories is required for the detailed analysis of experimental results and the practical proposition of suitable material structures for the entangled-photon generation or other optical processes, while modelized systems are usually considered in the theoretical framework of quantum optics. In contrast that the modelized calculation is suitable for qualitative discussion, the detailed calculation of the present theory is useful for quantitative discussion. In other words, the theories applicable to actual material structure are essential to verify calculation results obtained from the model calculations. In Chap. 2, I try to apply the calculation idea of the microscopic nonlocal theory by Cho [30, 31] into the QED theory for excitonic media with nonlocal susceptibility in order to reduce the integro-differential equation into a linear equation set, which can be performed for arbitrary-structured 3D materials.

On the other hand, we must also consider exciton-exciton interactions to describe the entangled-photon generation by the scattering via biexciton states. The QED theory discussed in Chap. 2 has already been applied to the theoretical study of the entangled-photon generation from a CuCl nanofilm [46], and it has been elucidated that a good signal-to-noise ratio with maintaining a signal intensity can be obtained from nanometer-order thickness, in addition to the anomalous exciton-exciton scattering via biexcitons reflecting the above-mentioned anomalous exciton mode structure [42]. On the other hand, although the present QED theory was extended under a phenomenological approximation to describe the biexciton scattering in Ref. 46, its approximation cannot be applied to the entangled-photon generation from semiconductor microcavity proposed in Refs. 47 and 48, because we must consider the recreation of biexcitons from the emitted entangled pairs in the cavity. Therefore, more systematic technique for perturbation calculation should be constructed for the further discussion of the entangled-photon generation and of other processes of excitons in nano-structured materials. One of the candidates for such a perturbation method is the Feynman diagram technique with exciton correlation functions in exciton-photon inhomogeneous systems, which are obtained by the present QED theory (and also by the semiclassical microscopic nonlocal theory [30, 31]) as revealed in the present research. The next purpose is to construct a calculation method applicable to general perturbation in exciton-photon inhomogeneous systems. Such method would be a powerful tool for discussing the nonclassical light generation from condensed matters with practical structure and nonclassical states of polaritons, such as entangled photons, single photons, squeezed states and BEC of cavity polaritons as mentioned above. Further, such a general perturbation method is also useful for other nonlinear, dephasing, and emission processes of excitons in inhomogeneous systems, especially for discussing nano-structured materials, where the center-of-mass confinement and radiative decay of excitons significantly appear. The present theory is required for the detailed analysis of experimental results and proposing suitable material structures for these discussions in the future.

In order to construct the general perturbation theory for exciton-photon inhomogeneous systems, time-ordered and thermal correlation functions of excitons should be derived from the analytic continuation with the retarded ones obtained from the QED theory of this thesis. First, we must obtain the information of poles in the exciton-photon inhomogeneous systems to analytically express the retarded correlation

functions, although the functions can be numerically evaluated for a given frequency. This is the another subject of this thesis and will be discussed in Chap. 3. One pole is characterized by a complex frequency, and its real and imaginary parts represent a resonance frequency and a radiative decay rate of a exciton-photon coupled mode, respectively. The crystal-size dependence of this radiative decay rate has been discussed in relation to the crossover between the exciton superradiance and the polariton radiative decay scheme. A comprehensive interpretation of the crystal-size dependence of the exciton-photon coupled modes is also a subject of this thesis, and it will also be discussed in detail in Chap. 3. After the calculation of the poles, the analytical expression of the retarded correlation functions must be derived for the continuation to the time-ordered and thermal ones. This is the other subject of this thesis, and will be discussed in Chap. 4.

1.3 QED of dispersive and absorptive media

In this section, I explain the outline of QED theories of dispersive and absorptive media. The pioneering work has been performed by Huttner and Barnett [20, 21]. As reviewed in Ref. 18, the successive works have revealed its interpretation and the relationship with the fluctuation-dissipation theorem, and also applied the theory into some actual problems. Further, the QED theory has been generalized for inhomogeneous media in some works.

1.3.1 Huttner-Barnett theory

The quantization of the electromagnetic fields in dispersive and absorptive dielectrics has been systematically carried out by Huttner and Barnett [20, 21]. The authors discussed homogeneous systems, and the dispersive property is described by using the classical Hopfield polariton model [19], i.e., polarizable harmonic oscillators interacting with the radiation field. Further, the absorption is considered by using a reservoir of oscillators interacting with the polarizable ones. First, the authors diagonalized the Hamiltonian, and derived the eigenoperators $\{\hat{C}_\lambda(\boldsymbol{k},\omega)\}$, where the quantum numbers λ, $\boldsymbol{k}$, and ω represent the polarization direction, wavevector, and frequency, respectively. This operator satisfies the Bosonic commutation relation as

$$\left[\hat{C}_\lambda(\boldsymbol{k},\omega),\hat{C}^\dagger_{\lambda'}(\boldsymbol{k}',\omega')\right] = \delta_{\lambda,\lambda'}\delta(\boldsymbol{k}-\boldsymbol{k}')\delta(\omega-\omega'), \tag{1.1a}$$

$$\left[\hat{C}_\lambda(\boldsymbol{k},\omega),\hat{C}_{\lambda'}(\boldsymbol{k}',\omega')\right] = 0, \tag{1.1b}$$

and describes the Hamiltonian as

$$H = \sum_{\lambda=1,2}\int \mathrm{d}\boldsymbol{k}\int_0^\infty \mathrm{d}\omega\ \hbar\omega\ \hat{C}^\dagger_\lambda(\boldsymbol{k},\omega)\hat{C}_\lambda(\boldsymbol{k},\omega). \tag{1.2}$$

Further, the authors represented the vector potential by using the eigenoperators. The most useful expression is its frequency Fourier component defined as

$$\hat{\boldsymbol{A}}^\pm(\boldsymbol{r},\omega) = \frac{1}{2\pi}\int_{-\infty}^\infty \mathrm{d}t\ \mathrm{e}^{\pm\mathrm{i}\omega t}\boldsymbol{A}(\boldsymbol{r},t), \tag{1.3}$$

which gives its Heisenberg representation as

$$\boldsymbol{A}(\boldsymbol{r},t) = \int_0^\infty \mathrm{d}\omega\left[\mathrm{e}^{-\mathrm{i}\omega t}\hat{\boldsymbol{A}}^+(\boldsymbol{r},\omega)+\mathrm{e}^{\mathrm{i}\omega t}\hat{\boldsymbol{A}}^-(\boldsymbol{r},\omega)\right]. \tag{1.4}$$

Here, $\hat{\boldsymbol{A}}^{+}(\boldsymbol{r},\omega)$ and $\hat{\boldsymbol{A}}^{-}(\boldsymbol{r},\omega)$ are respectively called positive- and negative-frequency components, and they have a relation as

$$\hat{\boldsymbol{A}}^{\pm}(\boldsymbol{r},\omega)=\hat{\boldsymbol{A}}^{\mp}(\boldsymbol{r},-\omega)=\{\hat{\boldsymbol{A}}^{\pm}(\boldsymbol{r},-\omega^{*})\}^{\dagger}. \tag{1.5}$$

By using the eigenoperators $\{\hat{C}_{\lambda}(\boldsymbol{k},\omega)\}$ (here, ω is a quantum number in the system), the positive-frequency component of the vector potential is represented as

$$\hat{\boldsymbol{A}}^{+}(\boldsymbol{r},\omega)=\int \mathrm{d}\boldsymbol{k}\ \frac{\mathrm{e}^{\mathrm{i}\boldsymbol{k}\cdot\boldsymbol{r}}}{(2\pi)^{3/2}}\sum_{\lambda=1,2}\boldsymbol{e}_{\lambda}(\boldsymbol{k})\ \frac{\omega}{c^{2}}\sqrt{\frac{\hbar}{\pi\varepsilon_{0}}\mathrm{Im}[\varepsilon(\omega)]}\ \frac{\hat{C}_{\lambda}(\boldsymbol{k},\omega)}{\varepsilon(\omega)\omega^{2}/c^{2}-k^{2}}, \tag{1.6}$$

where $\boldsymbol{e}_{\lambda}(\boldsymbol{k})$ is the unit vector in the polarization direction, and $\varepsilon(\omega)$ is the complex dielectric function represented by system parameters, i.e., coupling parameters between the radiation field and the polarizable oscillators and between the polarizable oscillators and the reservoir ones. Further, the authors showed that $\varepsilon(\omega)$ satisfies the Kramers-Kronig relations. This function just characterizes the quantum fluctuation of the electromagnetic fields in the dispersive and absorptive media. On the other hand, the other electromagnetic fields are described as

$$\hat{\boldsymbol{E}}^{+}(\boldsymbol{r},\omega)=\mathrm{i}\omega\hat{\boldsymbol{A}}^{+}(\boldsymbol{r},\omega), \tag{1.7}$$

$$\hat{\boldsymbol{B}}^{+}(\boldsymbol{r},\omega)=\boldsymbol{\nabla}\times\hat{\boldsymbol{A}}^{+}(\boldsymbol{r},\omega), \tag{1.8}$$

$$\hat{\boldsymbol{D}}^{+}(\boldsymbol{r},\omega)=\varepsilon_{0}\varepsilon(\omega)\hat{\boldsymbol{E}}^{+}(\boldsymbol{r},\omega)-\frac{1}{\mathrm{i}\omega}\hat{\boldsymbol{J}}_{\mathrm{NT}}(\boldsymbol{r},\omega). \tag{1.9}$$

Here, $\hat{\boldsymbol{J}}_{\mathrm{NT}}(\boldsymbol{r},\omega)$ is the fluctuation operator governing the absorption in media, which does not appear in the classical electrodynamics, and it is defined as

$$\hat{\boldsymbol{J}}_{\mathrm{NT}}(\boldsymbol{r},\omega)=-\omega\sqrt{\frac{\varepsilon_{0}\hbar}{\pi}\mathrm{Im}[\varepsilon(\omega)]}\int \mathrm{d}\boldsymbol{k}\ \frac{\mathrm{e}^{\mathrm{i}\boldsymbol{k}\cdot\boldsymbol{r}}}{(2\pi)^{3/2}}\sum_{\lambda=1,2}\boldsymbol{e}_{\lambda}(\boldsymbol{k})\ \hat{C}_{\lambda}(\boldsymbol{k},\omega). \tag{1.10}$$

This operator is called noise current density, and, from commutation relation (1.1), it satisfies

$$\left[\hat{\boldsymbol{J}}_{\mathrm{NT}}(\boldsymbol{r},\omega),\{\hat{\boldsymbol{J}}_{\mathrm{NT}}(\boldsymbol{r}',\omega'^{*})\}^{\dagger}\right]=\delta(\omega-\omega')\boldsymbol{\delta}_{\mathrm{T}}(\boldsymbol{r}-\boldsymbol{r}')\frac{\varepsilon_{0}\hbar\omega^{2}}{\pi}\mathrm{Im}[\varepsilon(\omega)], \tag{1.11}$$

where $[\hat{\boldsymbol{J}},\{\hat{\boldsymbol{J}}\}^{\dagger}]$ is a 3×3 tensor whose (ξ,ξ') element implies $[\hat{J}_{\xi},\{\hat{J}_{\xi'}\}^{\dagger}]$ for $\xi=x,y,z$, and $\boldsymbol{\delta}_{\mathrm{T}}(\boldsymbol{r}-\boldsymbol{r}')$ is the dyadic Dirac delta function extracting the transverse component (see App. F).

1.3.2 Relationship with fluctuation-dissipation theorem

As indicated by Matloob and Loudon [49], the commutation relation [Eq. (1.11)] of the noise current density $\hat{\boldsymbol{J}}_{\mathrm{NT}}(\boldsymbol{r},\omega)$ can be understood from the fluctuation-dissipation theorem (see, for example, Chap. XII of Ref. 50). Eq. (1.9) means that the induced current density in the medium is written as

$$\hat{\boldsymbol{J}}^{+}(\boldsymbol{r},\omega)=-\mathrm{i}\omega\left[\hat{\boldsymbol{D}}^{+}(\boldsymbol{r},\omega)-\varepsilon_{0}\hat{\boldsymbol{E}}^{+}(\boldsymbol{r},\omega)\right]=\varepsilon_{0}\omega^{2}\chi(\omega)\hat{\boldsymbol{A}}^{+}(\boldsymbol{r},\omega)+\hat{\boldsymbol{J}}_{\mathrm{NT}}(\boldsymbol{r},\omega), \tag{1.12}$$

where $\chi(\omega)=\varepsilon(\omega)-1$ is the optical susceptibility. In the same manner as the Langevin equation (App. A.3), the noise operator $\hat{\boldsymbol{J}}_{\mathrm{NT}}(\boldsymbol{r},\omega)$ appears due to the absorption in the medium. When we consider the subspace H_{ex} excluding the radiation field, from the interaction Hamiltonian

$$H_{\mathrm{int}}=-\int \mathrm{d}\boldsymbol{r}\ \boldsymbol{J}(\boldsymbol{r})\cdot\boldsymbol{A}(\boldsymbol{r}), \tag{1.13}$$

the susceptibility $\chi(\omega)$ corresponds to the retarded Green's function of the polarization in $H_{\rm ex}$ system as

$$\boldsymbol{\delta}_{\rm T}(\boldsymbol{r}-\boldsymbol{r}')\varepsilon_0\omega^2\chi(\omega) = \frac{-1}{\mathrm{i}\hbar}\int_{t'}^{\infty} \mathrm{d}t\ \mathrm{e}^{\mathrm{i}\omega(t-t')}\,\langle[\boldsymbol{J}_0(\boldsymbol{r},t),\boldsymbol{J}_0(\boldsymbol{r}',t')]\rangle_{\rm ex}\,, \tag{1.14}$$

where the time-dependent operator is defined as

$$\boldsymbol{J}_0(\boldsymbol{r},t) \equiv \mathrm{e}^{\mathrm{i}H_{\rm ex}t/\hbar}\boldsymbol{J}(\boldsymbol{r})\mathrm{e}^{-\mathrm{i}H_{\rm ex}t/\hbar}. \tag{1.15}$$

In the same manner that the Langevin equation has the fluctuation operator to maintain the equal-time Schrödinger commutation relation, $\hat{\boldsymbol{J}}^{+}(\boldsymbol{r},\omega)$ must have the noise operator $\hat{\boldsymbol{J}}_{\rm NT}(\boldsymbol{r},\omega)$ in order to maintain the identity (1.14), because $\hat{\boldsymbol{A}}(\boldsymbol{r},\omega)$ is considered to be an external field or a c-number in the subspace. Actually, by using Eq. (A.20) and the Kramers-Kronig relation [Eq. (A.23)], the commutation relation (1.11) of $\hat{\boldsymbol{J}}_{\rm NT}(\boldsymbol{r},\omega)$ provides Eq. (1.14).

On the other hand, as indicated by Matloob et al. [51] and by Gruner and Welsch [52], using expression (1.10) of $\hat{\boldsymbol{J}}_{\rm NT}(\boldsymbol{r},\omega)$, the vector potential [Eq. (1.6)] is rewritten as

$$\hat{\boldsymbol{A}}^{+}(\boldsymbol{r},\omega) = -\mu_0\int \mathrm{d}\boldsymbol{r}'\ G_0(\boldsymbol{r},\boldsymbol{r}',\omega)\hat{\boldsymbol{J}}_{\rm NT}(\boldsymbol{r}',\omega), \tag{1.16}$$

where the function $G_0(\boldsymbol{r},\boldsymbol{r}',\omega)$ is defined as

$$G_0(\boldsymbol{r},\boldsymbol{r}',\omega) = \int \frac{\mathrm{d}\boldsymbol{k}}{(2\pi)^3}\ \frac{\mathrm{e}^{\mathrm{i}\boldsymbol{k}\cdot(\boldsymbol{r}-\boldsymbol{r}')}}{\varepsilon(\omega)\omega^2/c^2-k^2} = -\frac{\exp\left[\mathrm{i}\sqrt{\varepsilon(\omega)}(\omega/c)|\boldsymbol{r}-\boldsymbol{r}'|\right]}{4\pi|\boldsymbol{r}-\boldsymbol{r}'|}. \tag{1.17}$$

Since this is just the Green's function satisfying

$$\left[\boldsymbol{\nabla}^2+\frac{\omega^2}{c^2}\varepsilon(\omega)\right]G_0(\boldsymbol{r},\boldsymbol{r}',\omega) = \delta(\boldsymbol{r}-\boldsymbol{r}'), \tag{1.18}$$

we can find that the vector potential [Eq. (1.16)] satisfies the following wave equation:

$$\left[\boldsymbol{\nabla}^2+\frac{\omega^2}{c^2}\varepsilon(\omega)\right]\hat{\boldsymbol{A}}(\boldsymbol{r},\omega) = -\mu_0\hat{\boldsymbol{J}}_{\rm NT}(\boldsymbol{r},\omega). \tag{1.19}$$

This has the same form as the Maxwell wave equation in the classical electrodynamics except the noise current density $\hat{\boldsymbol{J}}_{\rm NT}(\boldsymbol{r},\omega)$.

On the other hand, when we focus on the transverse field propagating in the z direction, Eq. (1.19) reduces to

$$\left[\frac{\partial^2}{\partial z^2}+\frac{\omega^2}{c^2}\varepsilon(\omega)\right]\hat{A}(z,\omega) = -\mu_0\hat{J}_{\rm NT}(z,\omega), \tag{1.20}$$

where the fields are integrated over the x-y plane with the normalization area S as

$$A(z) = \frac{1}{\sqrt{S}}\int \mathrm{d}x\int \mathrm{d}y\ A(\boldsymbol{r}), \tag{1.21}$$

$$\hat{J}_{\rm NT}(z,\omega) = \frac{1}{\sqrt{S}}\int \mathrm{d}x\int \mathrm{d}y\ \hat{J}_{\rm NT}(\boldsymbol{r},\omega). \tag{1.22}$$

Further, Eq. (1.16) is rewritten as

$$\hat{A}^{+}(z,\omega) = -\mu_0\int \mathrm{d}z'\ G_0(z,z',\omega)\hat{J}_{\rm NT}(z',\omega), \tag{1.23}$$

where the Green's function $G_0(z,z',\omega)$ satisfies

$$\left[\frac{\partial^2}{\partial z^2}+\frac{\omega^2}{c^2}\varepsilon(\omega)\right]G_0(z,z',\omega) = \delta(z-z'), \tag{1.24}$$

and is represented as

$$G_0(z,z',\omega)=\int_{-\infty}^{\infty}\frac{\mathrm{d}k}{2\pi}\,\frac{\mathrm{e}^{\mathrm{i}k(z-z')}}{\varepsilon(\omega)\omega^2/c^2-k^2}=\frac{\mathrm{e}^{\mathrm{i}n(\omega)(\omega/c)|z-z'|}}{\mathrm{i}2n(\omega)\omega/c}. \tag{1.25}$$

In this situation, the commutation relation [Eq. (1.11)] of $\hat{J}_{\mathrm{NT}}(\boldsymbol{r},\omega)$ reduces to

$$\left[\hat{J}_{\mathrm{NT}}(z,\omega),\{\hat{J}_{\mathrm{NT}}(z',\omega'^{*})\}^{\dagger}\right]=\delta(\omega-\omega')\delta(z-z')\frac{\varepsilon_0\hbar\omega^2}{\pi}\mathrm{Im}[\varepsilon(\omega)], \tag{1.26}$$

and that of the vector potential is obtained as

$$\left[\hat{A}^{+}(z,\omega),\hat{A}^{-}(z',\omega')\right]=-\delta(\omega-\omega')\frac{\mu_0\hbar}{\pi}\,\mathrm{Im}[G_0(z,z',\omega)]. \tag{1.27}$$

This result can be understood from the linear response theory as discussed in Chap. 6 of Ref. 53. This means that the Green's function $G_0(z,z',\omega)$ corresponds to the retarded correlation function of the vector potential as

$$\mu_0 G_0(z,z',\omega)=\frac{1}{\mathrm{i}\hbar}\int_{t'}^{\infty}\mathrm{d}t\;\mathrm{e}^{\mathrm{i}\omega(t-t')}\,\langle[A(z,t),A(z',t')]\rangle \tag{1.28}$$

We can verify that Eq. (1.28) actually provides Eq. (1.27). It is worth to note that, although $\hat{\boldsymbol{J}}_{\mathrm{NT}}(\boldsymbol{r},\omega)$ [Eq. (1.10)] and its commutator [Eq. (1.11)] vanishes in the limit of no absorption $\mathrm{Im}[\varepsilon(\omega)]\to 0$, the commutator [Eq. (1.27)] of the vector potential does not vanish as discussed by Gruner and Welsch [54]. The remains just represent the quantum fluctuation of the electromagnetic fields, or the vacuum fluctuation (see App. B).

1.3.3 Field quantization in inhomogeneous media

The pioneering work by Huttner and Barnett [20, 21] stimulated various theoretical studies associated with the QED of dispersive and absorptive dielectrics, for example, the spontaneous decay in dielectrics [55, 56], quantum input-output relations [51, 57, 58], and quantization in amplifying, anisotropic, magnetic, or nonlinear media [18, 59, 60, 27, 28]. However, in order to extend the Huttner-Barnett theory for inhomogeneous 3D dielectrics, we must consider the Coulomb potential induced by the polarization charge in addition to the vector potential. In the study of Dung, Knöll, and Welsh [61], the extension has been performed by phenomenologically introducing the noise current density and its commutation relation. On the other hand, Suttorp and Wubs have systematically done by using the Laplace transformation technique [62, 63], and Suttorp and van Wonderen also did by the diagonalization method [64]. In these schemes, the complex dielectric function $\varepsilon(\boldsymbol{r},\omega)$ depends on the spatial position $\boldsymbol{r}$ of the medium and the radiation frequency ω. I show the outline of these works in the following paragraphs.

Instead of the vector potential in the Huttner-Barnett work, the field quantization in inhomogeneous media is described in terms of the electric field, which is written as

$$\boldsymbol{E}(\boldsymbol{r},t)=-\frac{\partial}{\partial t}\boldsymbol{A}(\boldsymbol{r},t)-\boldsymbol{\nabla}\phi(\boldsymbol{r},t), \tag{1.29a}$$

$$\hat{\boldsymbol{E}}^{+}(\boldsymbol{r},\omega)=\mathrm{i}\omega\hat{\boldsymbol{A}}^{+}(\boldsymbol{r},t)-\boldsymbol{\nabla}\hat{\phi}^{+}(\boldsymbol{r},\omega). \tag{1.29b}$$

Compared to Eq. (1.7) in the Huttner-Barnett work, the Coulomb potential $\phi(\boldsymbol{r})$ is added in this scheme. When we use the Coulomb gauge, the vector potential is a transverse field satisfying $\boldsymbol{\nabla}\cdot\boldsymbol{A}(\boldsymbol{r})=0$, and the second term of Eqs. (1.29) represents the longitudinal field. In the same manner as the Huttner-Barnett

work, the motion equation of the electric field is obtained as

$$\boldsymbol{\nabla}\times\boldsymbol{\nabla}\times\hat{\boldsymbol{E}}^{+}(\boldsymbol{r},\omega)-\frac{\omega^2}{c^2}\varepsilon(\boldsymbol{r},\omega)\hat{\boldsymbol{E}}^{+}(\boldsymbol{r},\omega)=\mathrm{i}\mu_0\omega\hat{\boldsymbol{J}}_{\mathrm{N}}(\boldsymbol{r},\omega). \tag{1.30}$$

This also has the same form as the Maxwell wave equation in the classical electrodynamics, and has a fluctuation operator $\hat{\boldsymbol{J}}_{\mathrm{N}}(\boldsymbol{r},\omega)$, whose commutation relation is written as

$$\left[\hat{\boldsymbol{J}}_{\mathrm{N}}(\boldsymbol{r},\omega),\{\hat{\boldsymbol{J}}_{\mathrm{N}}(\boldsymbol{r}',\omega'^{*})\}^{\dagger}\right]=\delta(\omega-\omega')\delta(\boldsymbol{r}-\boldsymbol{r}')\frac{\varepsilon_0\hbar\omega^2}{\pi}\mathrm{Im}[\varepsilon(\boldsymbol{r},\omega)]\mathbf{1}. \tag{1.31}$$

Compared to Eq. (1.11) in the Huttner-Barnett work, the commutator becomes isotropic because of considering the longitudinal field or the Coulomb potential. According to the fluctuation dissipation theorem, this commutation relation has been phenomenologically introduced by Dung, Knöll, and Welsh [61]. On the other hand, from the Laplace-transformed motion equations of system variables, Suttorp and Wubs [63] have systematically derived the representation of $\hat{\boldsymbol{J}}_{\mathrm{N}}(\boldsymbol{r},\omega)$, which is written in terms of the canonical variables and momenta of the system at $t=0$. From the commutation relations between them, that of $\hat{\boldsymbol{J}}_{\mathrm{N}}(\boldsymbol{r},\omega)$ have been derived. Around the same time, Suttorp and Wanderen [64] have diagonalized the Hamiltonian, and represented $\hat{\boldsymbol{J}}_{\mathrm{N}}(\boldsymbol{r},\omega)$ in terms of the eigenoperators in the same manner as Eq. (1.10).

On the other hand, by introducing the dyadic Green's function $\mathsf{G}_0(\boldsymbol{r},\boldsymbol{r}',\omega)$ satisfying

$$\boldsymbol{\nabla}\times\boldsymbol{\nabla}\times\mathsf{G}_0(\boldsymbol{r},\boldsymbol{r}',\omega)-\frac{\omega^2}{c^2}\varepsilon(\boldsymbol{r},\omega)\mathsf{G}_0(\boldsymbol{r},\boldsymbol{r}',\omega)=\delta(\boldsymbol{r}-\boldsymbol{r}')\mathbf{1}, \tag{1.32}$$

we can rewrite the Maxwell wave equation, Eq. (1.30), as

$$\hat{\boldsymbol{E}}^{+}(\boldsymbol{r},\omega)=\mathrm{i}\mu_0\omega\int\mathrm{d}\boldsymbol{r}'\;\mathsf{G}_0(\boldsymbol{r},\boldsymbol{r}',\omega)\cdot\hat{\boldsymbol{J}}_{\mathrm{N}}(\boldsymbol{r}',\omega). \tag{1.33}$$

From commutation relation (1.31) of $\hat{\boldsymbol{J}}_{\mathrm{N}}(\boldsymbol{r},\omega)$, that of $\hat{\boldsymbol{E}}^{\pm}(\boldsymbol{r},\omega)$ can be derived as

$$\left[\hat{\boldsymbol{E}}^{+}(\boldsymbol{r},\omega),\hat{\boldsymbol{E}}^{-}(\boldsymbol{r}',\omega')\right]=\delta(\omega-\omega')\frac{\mu_0\hbar\omega^2}{\mathrm{i}2\pi}\left[\mathsf{G}_0(\boldsymbol{r},\boldsymbol{r}',\omega)-\mathsf{G}_0^{*}(\boldsymbol{r},\boldsymbol{r}',\omega)\right], \tag{1.34}$$

where I use the equivalence shown in Eq. (1.54) of Ref. 18 as

$$\int\mathrm{d}\boldsymbol{s}\;\frac{\omega^2}{c^2}\left[\varepsilon(\boldsymbol{s},\omega)-\varepsilon^{*}(\boldsymbol{s},\omega)\right]\mathsf{G}_0(\boldsymbol{r},\boldsymbol{s},\omega)\cdot\mathsf{G}_0^{*}(\boldsymbol{s},\boldsymbol{r}',\omega)=\mathsf{G}_0(\boldsymbol{r},\boldsymbol{r}',\omega)-\mathsf{G}_0^{*}(\boldsymbol{r},\boldsymbol{r}',\omega), \tag{1.35}$$

and the reciprocity relation in the isotropic system as

$$\mathsf{G}_0(\boldsymbol{r},\boldsymbol{r}',\omega)=\{\mathsf{G}_0(\boldsymbol{r}',\boldsymbol{r},\omega)\}^{\mathrm{t}}. \tag{1.36}$$

In the same manner as Sec. 1.3.2, commutation relation (1.34) can be understood by the fact that the dyadic Green's function $\mathsf{G}_0(\boldsymbol{r},\boldsymbol{r}',\omega)$ satisfying Eq. (1.32) corresponds to the retarded correlation function of the electric field as

$$-\mu_0\omega^2\mathsf{G}_0(\boldsymbol{r},\boldsymbol{r}',\omega)=\frac{1}{\mathrm{i}\hbar}\int_{t'}^{\infty}\mathrm{d}t\;\mathrm{e}^{\mathrm{i}\omega(t-t')}\left\langle[\boldsymbol{E}(\boldsymbol{r},t),\boldsymbol{E}(\boldsymbol{r}',t')]\right\rangle. \tag{1.37}$$

The information of the material structure is reflected through the dielectric function $\varepsilon(\boldsymbol{r},\omega)$, and it uniquely determines $\mathsf{G}_0(\boldsymbol{r},\boldsymbol{r}',\omega)$. The form of the dyadic Green's function has already been known for various structures with high symmetry [65], and also can be numerically calculated for arbitrary 3D structures [66].

1.4 Semiclassical theory of excitons

In this section, I focus on the theoretical treatment of optical processes of excitons, especially on the nonlocal susceptibility originating from their center-of-mass motion. Because of this nonlocality, we require some additional boundary conditions (ABCs) in some calculation method. On the other hand, I also explain a method without any ABCs.

1.4.1 Nonlocal susceptibility

In the above QED theories and also in semiclassical ones, the dielectric function is usually treated as a local form as $\varepsilon(\boldsymbol{r},\omega)$ with respect to the spatial position. However, from the microscopic point of view, the optical susceptibility generally has a nonlocal form as $\boldsymbol{\chi}(\boldsymbol{r},\boldsymbol{r}',\omega)$, which characterizes the polarization $\boldsymbol{P}_{\rm ex}(\boldsymbol{r},\omega)$ at a position $\boldsymbol{r}$ induced by electric field $\boldsymbol{E}(\boldsymbol{r}',\omega)$ at a different position $\boldsymbol{r}'$ as

$$\boldsymbol{P}_{\rm ex}(\boldsymbol{r},\omega) = \varepsilon_0 \int \mathrm{d}\boldsymbol{r}'\ \boldsymbol{\chi}_{\rm ex}(\boldsymbol{r},\boldsymbol{r}',\omega)\cdot\boldsymbol{E}(\boldsymbol{r}',\omega). \tag{1.38}$$

When we consider the interaction Hamiltonian between the electromagnetic field and the excitation as

$$H_{\rm int} = -\int \mathrm{d}\boldsymbol{r}\ \hat{\boldsymbol{P}}_{\rm ex}(\boldsymbol{r})\cdot\boldsymbol{E}(\boldsymbol{r}), \tag{1.39}$$

the representation of the dyadic susceptibility $\boldsymbol{\chi}(\boldsymbol{r},\boldsymbol{r}',\omega)$ is derived from the linear response theory (App. A.1) as

$$\boldsymbol{\chi}_{\rm ex}(\boldsymbol{r},\boldsymbol{r}',\omega) = \frac{\mathrm{i}}{\varepsilon_0\hbar}\int_{-\infty}^{\infty}\mathrm{d}t\ \mathrm{e}^{\mathrm{i}\omega(t-t')}\theta(t-t')\left\langle\left[\hat{\boldsymbol{P}}_{\rm ex}(\boldsymbol{r},t),\hat{\boldsymbol{P}}_{\rm ex}(\boldsymbol{r}',t')\right]\right\rangle \tag{1.40}$$

$$= \frac{\mathrm{i}}{\varepsilon_0\hbar}\int_{0}^{\infty}\mathrm{d}t\ \mathrm{e}^{\mathrm{i}\omega t}\left\{\langle 0|\hat{\boldsymbol{P}}_{\rm ex}(\boldsymbol{r})\ \mathrm{e}^{-\mathrm{i}H_{\rm ex}t/\hbar}\ \hat{\boldsymbol{P}}_{\rm ex}(\boldsymbol{r}')|0\rangle - \langle 0|\hat{\boldsymbol{P}}_{\rm ex}(\boldsymbol{r}')\ \mathrm{e}^{\mathrm{i}H_{\rm ex}t/\hbar}\ \hat{\boldsymbol{P}}_{\rm ex}(\boldsymbol{r})|0\rangle\right\} \tag{1.41}$$

$$= \frac{1}{\varepsilon_0}\sum_{\lambda}\left\{\frac{\langle 0|\hat{\boldsymbol{P}}_{\rm ex}(\boldsymbol{r})|\lambda\rangle\,\langle\lambda|\hat{\boldsymbol{P}}_{\rm ex}(\boldsymbol{r}')|0\rangle}{\hbar\omega_\lambda-\hbar\omega-\mathrm{i}\delta} + \frac{\langle 0|\hat{\boldsymbol{P}}_{\rm ex}(\boldsymbol{r}')|\lambda\rangle\,\langle\lambda|\hat{\boldsymbol{P}}_{\rm ex}(\boldsymbol{r})|0\rangle}{\hbar\omega_\lambda+\hbar\omega+\mathrm{i}\delta}\right\}, \tag{1.42}$$

where I denote the excitation eigenstates by λ, and their eigenfrequency by ω_λ. This nonlocality originates from the spatial spreading of the wave function of elementary excitations, or, particularly for excitons in semiconductors, their center-of-mass motion with a finite translational mass. If we consider that the excitation is localized at an excited position, the susceptibility reduces to the local form as Eq. (1.14). Usually, the nonlocality is not considered to be important for macroscopic materials, because the coherence length of elementary excitations is usually much shorter than the light wave length. Therefore, only the averaged values of physical quantities over the coherence volume are reflected in observation, and the nonlocal effect is not apparent. However, in high-quality samples with few defects and impurities, the motion of excitons could have a considerably long coherence, and the electromagnetic fields vary in a considerably short distance in the resonance condition. In such cases, the nonlocality becomes important even for bulk materials, as explained below.

In the case of homogeneous and isotropic media, the exciton center-of-mass wavefunctions are expanded by plane waves as

$$\langle\eta,\boldsymbol{k}|\hat{\boldsymbol{P}}_{\rm ex}(\boldsymbol{r})|0\rangle = \boldsymbol{\mathcal{P}}_\eta\frac{\mathrm{e}^{\mathrm{i}\boldsymbol{k}\cdot\boldsymbol{r}}}{\sqrt{V}}, \tag{1.43}$$

where η and $\boldsymbol{k}$ are indices of relative and center-of-mass motions of excitons, respectively. Substituting Eq. (1.43) into Eq. (1.42), we can find that the nonlocal susceptibility depends only on the difference

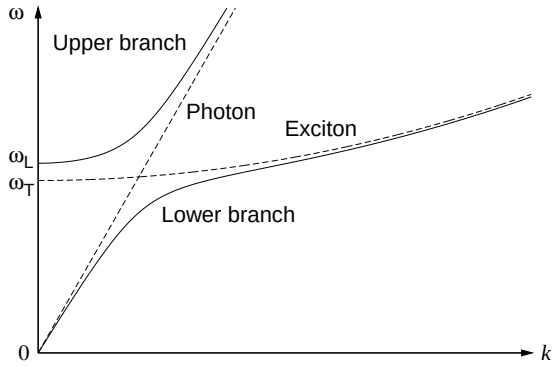

Figure 1.1: Dispersion curves of exciton polariton. Solid lines represent the polariton dispersion [Eq. (1.49)] and dashed lines are those of bare exciton [Eq. (1.50)] and photon [$\omega = ck/\sqrt{\varepsilon_{\rm bg}}$].

$\boldsymbol{r} - \boldsymbol{r}'$ of the two positions as

$$\chi_{\rm ex}(\boldsymbol{r}, \boldsymbol{r}', \omega) = \sum_{\eta,\boldsymbol{k}} \frac{|\boldsymbol{\mathcal{P}}_\eta|^2}{\varepsilon_0 V} \left\{ \frac{\mathrm{e}^{\mathrm{i}\boldsymbol{k}\cdot(\boldsymbol{r}-\boldsymbol{r}')}}{\hbar\omega_{\eta,\boldsymbol{k}} - \hbar\omega - \mathrm{i}\delta} + \frac{\mathrm{e}^{-\mathrm{i}\boldsymbol{k}\cdot(\boldsymbol{r}-\boldsymbol{r}')}}{\hbar\omega_{\eta,\boldsymbol{k}} + \hbar\omega + \mathrm{i}\delta} \right\}. \tag{1.44}$$

Therefore, Eq. (1.38) is rewritten in the reciprocal space as

$$\boldsymbol{P}(\boldsymbol{k}, \omega) = \varepsilon_0 \chi(\boldsymbol{k}, \omega) \boldsymbol{E}(\boldsymbol{k}, \omega), \tag{1.45}$$

and the susceptibility is represented as

$$\chi_{\rm ex}(\boldsymbol{k}, \omega) \equiv \int \mathrm{d}\boldsymbol{r}\ \mathrm{e}^{-\boldsymbol{k}\cdot(\boldsymbol{r}-\boldsymbol{r}')}\ \chi_{\rm ex}(\boldsymbol{r}, \boldsymbol{r}', \omega) = \sum_{\eta} \frac{|\boldsymbol{\mathcal{P}}_\eta|^2}{\varepsilon_0} \frac{2\hbar\omega_{\eta,\boldsymbol{k}}}{(\hbar\omega_{\eta,\boldsymbol{k}})^2 - (\hbar\omega + \mathrm{i}\delta)^2}. \tag{1.46}$$

In this manner, even for homogeneous media, when it has the nonlocality, the susceptibility $\chi(\boldsymbol{k}, \omega)$ depends on the wavevector $\boldsymbol{k}$ in addition to the frequency ω, i.e., the excitonic media have both spatial and temporal dispersions in general. This $\boldsymbol{k}$-dependence leads to more than one propagating or evanescent modes for a given frequency satisfying the dispersion relation

$$\frac{\omega^2 k^2}{c^2} = \varepsilon(\boldsymbol{k}, \omega) = \varepsilon_{\rm bg}(\omega) + \chi(\boldsymbol{k}, \omega), \tag{1.47}$$

which is obtained by substituting Eq. (1.45) into the Maxwell wave equation

$$\boldsymbol{\nabla} \times \boldsymbol{\nabla} \times \boldsymbol{E}(\boldsymbol{r}, \omega) - \frac{\omega^2}{c^2} \varepsilon_{\rm bg}(\omega) \boldsymbol{E}(\boldsymbol{r}, \omega) = \mu_0 \omega^2 \boldsymbol{P}_{\rm ex}(\boldsymbol{r}, \omega). \tag{1.48}$$

Especially, when we consider only one relative motion of exciton, the dispersion relation reduces to

$$\frac{c^2 k^2}{\omega^2} = \varepsilon(\boldsymbol{k}, \omega) = \varepsilon_{\rm bg} + \frac{f_{\boldsymbol{k}}}{\omega_{\boldsymbol{k}}{}^2 - (\omega + \mathrm{i}\delta')^2}. \tag{1.49}$$

Here, $f_{\boldsymbol{k}} = 2\omega_{\boldsymbol{k}} |\boldsymbol{\mathcal{P}}|^2 / \varepsilon_0 \hbar$ is called oscillator strength (but there are some other definition), and the bare exciton frequency is written as

$$\hbar\omega_{\boldsymbol{k}} = \hbar\omega_{\rm T} + \frac{\hbar^2 |\boldsymbol{k}|^2}{2m_{\rm ex}}, \tag{1.50}$$

where $\omega_{\rm T}$ is the transverse exciton frequency at the band edge, and $m_{\rm ex}$ is the exciton translational mass. The two solutions of Eq. (1.49) are shown in Fig. 1.1 by solid lines, and they are called upper and lower

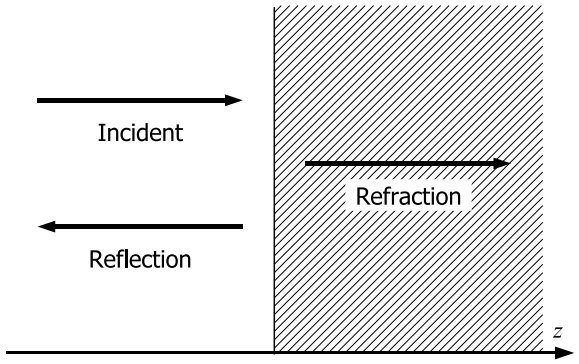

Figure 1.2: Schematic view for boundary problem that requires only the Maxwell boundary conditions.

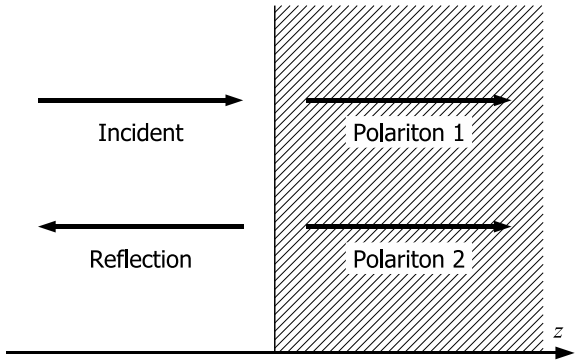

Figure 1.3: Schematic view for boundary problem that requires an ABC.

polariton branches. On the other hand, one dashed line represents the photon dispersion $\omega = ck/\sqrt{\varepsilon_{\mathrm{bg}}}$, and the other is the bare exciton one, Eq. (1.50). In particular, we obtain two solutions of Eq. (1.49) at $k = 0$: One is $\omega = 0$ and the other is equal to the longitudinal exciton frequency as

$$\omega_{\mathrm{L}} = \sqrt{{\omega_{\mathrm{T}}}^2 + f_0/\varepsilon_{\mathrm{bg}}} \simeq \omega_{\mathrm{T}} + \frac{f_0}{2\varepsilon_{\mathrm{bg}}\omega_{\mathrm{T}}} = \omega_{\mathrm{T}} + \frac{|\boldsymbol{\mathcal{P}}|^2}{\varepsilon_0\varepsilon_{\mathrm{bg}}\hbar}, \tag{1.51}$$

which actually provides $\varepsilon(0, \omega_{\mathrm{L}}) = 0$. As seen in Fig. 1.1, we can find two propagating polariton modes for $\omega > \omega_{\mathrm{L}}$, and one propagating mode even at the polariton band gap $\omega_{\mathrm{T}} < \omega < \omega_{\mathrm{L}}$ in addition to an evanescent mode. On the other hand, only one polariton mode is obtained in the classical Hopfield model [19], because the excitons were assumed to have infinite translational mass.

1.4.2 Additional boundary condition

When we consider a material with the polariton dispersion as discussed in the previous section, as first indicated by Pekar [67], we must introduce some additional boundary conditions (ABCs) in addition to the Maxwell boundary conditions in order to uniquely connect the polariton modes inside of the material and the external ones at the interfaces. This kind of problems is known as ABC problems (see, for example, Ref. 22), and it arises when the translational symmetry is broken due to the material interfaces. The Maxwell boundary conditions, which are derived from the Maxwell equations (see, for example, Sec. I.5 of Ref. 68), are well known as

$$(\boldsymbol{D}_1 - \boldsymbol{D}_2) \cdot \boldsymbol{n} = \sigma_{\mathrm{S}}, \tag{1.52a}$$
$$(\boldsymbol{B}_1 - \boldsymbol{B}_2) \cdot \boldsymbol{n} = 0, \tag{1.52b}$$
$$(\boldsymbol{E}_1 - \boldsymbol{E}_2) \times \boldsymbol{n} = \boldsymbol{0}, \tag{1.52c}$$
$$(\boldsymbol{H}_1 - \boldsymbol{H}_2) \times \boldsymbol{n} = \boldsymbol{j}_{\mathrm{S}}, \tag{1.52d}$$

where $\boldsymbol{n}$ is the unit vector perpendicular to the interface, σ_{S} is the surface charge density, and $\boldsymbol{j}_{\mathrm{S}}$ is the surface current density. However, among these eight boundary conditions, some of them are necessary and sufficient, and the others are trivial because of the completeness of the Maxwell equations. This means that the number of unknown variables and that of the Maxwell boundary conditions are the same in usual boundary problems. For example, when we consider the reflection and refraction of s-polarized field in nonmagnetic and isotropic media as seen in Fig. 1.2, only two conditions in Eq. (1.52) are just sufficient in order to determine the unknown two fields, one reflection and one refraction fields (see, for

example, Sec. 7.3 of Ref. 68). However, when we consider that the refraction medium has the polariton dispersion [Eq. (1.49)] as seen in Fig. 1.3, for a given incident field, an ABC is required to uniquely determine the three unknown fields, reflection, polariton 1, and 2. This contradiction originates from considering the polariton dispersion relation [Eq. (1.49)] in the boundary condition, although it is derived for homogeneous media.

In order to solve this problem, Pekar [67] introduced the following ABC that gives no polarization at the boundary:

$$\chi(\boldsymbol{k}_1,\omega)E_1 + \chi(\boldsymbol{k}_2,\omega)E_2 = 0. \tag{1.53}$$

After the Pekar's study, subsequent studies have revealed that the ABC problems can be resolved by considering the microscopically determined boundary conditions of the exciton center-of-mass motion at the interfaces [69, 70, 71, 72]. Nowadays, in the semiclassical framework, some calculation methods independent from the notation of ABCs are established, which are called as ABC-free theory [29] or microscopic nonlocal theory [30, 31]. These theories consider the nonlocality of the susceptibility $\chi(\boldsymbol{r},\boldsymbol{r}',\omega)$ from the microscopic point of view, in contrast to the macroscopic consideration based on the phenomenological introduction of ABCs. In the next section, I explain the outline of the microscopic nonlocal theory [31].

1.4.3 Microscopic nonlocal theory

This theory is based on the motion equation of the polarization, and that of the electromagnetic field, i.e., the Maxwell equations. In this section, for simplicity, I consider the exciton-photon interaction as Eq. (1.39), which is valid for the linear response regime under weak excitation, although more general discussion has been performed in Ref. 31. From Eq. (1.39), we can derive the motion equation of the polarization as Eq. (1.38), and the other one is the wave equation for the electric field as

$$\boldsymbol{\nabla}\times\boldsymbol{\nabla}\times\boldsymbol{E}(\boldsymbol{r},\omega) - \frac{\omega^2}{c^2}\varepsilon_{\rm bg}(\boldsymbol{r},\omega)\boldsymbol{E}(\boldsymbol{r},\omega) = \mu_0\omega^2\boldsymbol{P}_{\rm ex}(\boldsymbol{r},\omega). \tag{1.54}$$

Substituting Eq. (1.38) into Eq. (1.54), we obtain an integro-differential equation as

$$\boldsymbol{\nabla}\times\boldsymbol{\nabla}\times\boldsymbol{E}(\boldsymbol{r},\omega) - \frac{\omega^2}{c^2}\varepsilon_{\rm bg}(\boldsymbol{r},\omega)\boldsymbol{E}(\boldsymbol{r},\omega) - \frac{\omega^2}{c^2}\int \mathrm{d}\boldsymbol{r}'\ \boldsymbol{\chi}_{\rm ex}(\boldsymbol{r},\boldsymbol{r}',\omega)\cdot\boldsymbol{E}(\boldsymbol{r}',\omega) = \boldsymbol{0}. \tag{1.55}$$

In principle, by solving this equation, we can uniquely determine the electric field for a particular initial condition, and no ABC is required. By assuming the nonlocal medium as being homogeneous, i.e., infinite system, it is easy to solve this equation and then we can obtain the dispersion relation [Eq. (1.47)]. However, it is difficult to solve this integro-differential equation in inhomogeneous systems. Instead, we can reduce this nonlocal problem into a linear equation set by using the fact that the nonlocal susceptibility [Eq. (1.42)] consists of the separable functions with respect to the two positions ($\boldsymbol{r}$ and $\boldsymbol{r}'$). This means that, by introducing a variable

$$X_\lambda(\omega) \equiv \frac{1}{\hbar\omega_\lambda - \hbar\omega - \mathrm{i}\delta}\int \mathrm{d}\boldsymbol{r}\ \langle\lambda|\hat{\boldsymbol{P}}_{\rm ex}(\boldsymbol{r})|0\rangle\cdot\boldsymbol{E}(\boldsymbol{r},\omega), \tag{1.56}$$

we can rewrite the motion equation [Eq. (1.38)] of the polarization as

$$\boldsymbol{P}_{\rm ex}(\boldsymbol{r},\omega) = \sum_\lambda\left[\langle 0|\hat{\boldsymbol{P}}_{\rm ex}(\boldsymbol{r})|\lambda\rangle\, X_\lambda(\omega) + \langle\lambda|\hat{\boldsymbol{P}}_{\rm ex}(\boldsymbol{r})|0\rangle\,\{X_\lambda(-\omega^*)\}^*\right], \tag{1.57}$$

where I use the relation originating from the fact that the electric field $\boldsymbol{E}(\boldsymbol{r},t)$ is a real function:

$$\boldsymbol{E}(\boldsymbol{r},\omega) = \{\boldsymbol{E}(\boldsymbol{r},-\omega^*)\}^*. \tag{1.58}$$

From Eq. (1.57), $X_\lambda(\omega)$ is considered as the exciton amplitude in state λ. On the other hand, by using the dyadic Green's function satisfying

$$\boldsymbol{\nabla}\times\boldsymbol{\nabla}\times\mathsf{G}_0(\boldsymbol{r},\boldsymbol{r}',\omega)-\frac{\omega^2}{c^2}\varepsilon(\boldsymbol{r},\omega)\mathsf{G}_0(\boldsymbol{r},\boldsymbol{r}',\omega)=\delta(\boldsymbol{r}-\boldsymbol{r}')\mathbf{1}, \tag{1.59}$$

the Maxwell wave equation (1.54) is rewritten as

$$\boldsymbol{E}(\boldsymbol{r},\omega)=\boldsymbol{E}_0(\boldsymbol{r},\omega)+\mu_0\omega^2\int \mathrm{d}\boldsymbol{r}'\ \mathsf{G}_0(\boldsymbol{r},\boldsymbol{r}',\omega)\cdot\boldsymbol{P}_{\mathrm{ex}}(\boldsymbol{r},\omega), \tag{1.60}$$

where $\boldsymbol{E}_0(\boldsymbol{r},\omega)$ is the background electric field, or the incident field for excitons. Substituting this equation into Eq. (1.56) and Eq. (1.57) into it, we obtain

$$(\hbar\omega_\lambda-\hbar\omega-\mathrm{i}\delta)X_\lambda(\omega)=F^0_\lambda(\omega)+\mu_0\omega^2\int\mathrm{d}\boldsymbol{r}\int\mathrm{d}\boldsymbol{r}'\ \langle\lambda|\hat{\boldsymbol{P}}_{\mathrm{ex}}(\boldsymbol{r})|0\rangle\cdot\mathsf{G}_0(\boldsymbol{r},\boldsymbol{r}',\omega)\cdot\boldsymbol{P}_{\mathrm{ex}}(\boldsymbol{r}',\omega) \tag{1.61}$$

$$=F^0_\lambda(\omega)-\sum_{\lambda'}\left[\Sigma_{\lambda,\lambda'}(\omega)X_{\lambda'}(\omega)+\Sigma'_{\lambda,\lambda'}(\omega)\{X_{\lambda'}(-\omega^*)\}^*\right], \tag{1.62}$$

Here, $F^0_\lambda(\omega)$ appearing on the right-hand side (RHS) is defined as

$$F^0_\lambda(\omega)\equiv\int\mathrm{d}\boldsymbol{r}\ \langle\lambda|\hat{\boldsymbol{P}}_{\mathrm{ex}}(\boldsymbol{r})|0\rangle\cdot\boldsymbol{E}_0(\boldsymbol{r},\omega), \tag{1.63}$$

and it represents the exciton component induced by the incident field $\boldsymbol{E}_0(\boldsymbol{r},\omega)$. On the other hand, the following terms represent the inter-polarization interaction via the electromagnetic fields:

$$\Sigma_{\lambda,\lambda'}(\omega)\equiv-\mu_0\omega^2\int\mathrm{d}\boldsymbol{r}\int\mathrm{d}\boldsymbol{r}'\ \langle\lambda|\hat{\boldsymbol{P}}_{\mathrm{ex}}(\boldsymbol{r})|0\rangle\cdot\mathsf{G}_0(\boldsymbol{r},\boldsymbol{r}',\omega)\cdot\langle0|\hat{\boldsymbol{P}}_{\mathrm{ex}}(\boldsymbol{r}')|\lambda'\rangle\,, \tag{1.64}$$

$$\Sigma'_{\lambda,\lambda'}(\omega)\equiv-\mu_0\omega^2\int\mathrm{d}\boldsymbol{r}\int\mathrm{d}\boldsymbol{r}'\ \langle\lambda|\hat{\boldsymbol{P}}_{\mathrm{ex}}(\boldsymbol{r})|0\rangle\cdot\mathsf{G}_0(\boldsymbol{r},\boldsymbol{r}',\omega)\cdot\langle\lambda'|\hat{\boldsymbol{P}}_{\mathrm{ex}}(\boldsymbol{r}')|0\rangle\,. \tag{1.65}$$

Together with the complex conjugate of Eq. (1.62), we obtain a linear equation set as

$$\sum_{\lambda'}\begin{bmatrix}(\hbar\omega_\lambda-\hbar\omega)\delta_{\lambda,\lambda'}+\Sigma_{\lambda,\lambda'}(\omega) & \Sigma'_{\lambda,\lambda'}(\omega)\\ \Sigma'^*_{\lambda,\lambda'}(-\omega) & (\hbar\omega_\lambda+\hbar\omega)\delta_{\lambda,\lambda'}+\Sigma^*_{\lambda,\lambda'}(-\omega)\end{bmatrix}\begin{bmatrix}X_{\lambda'}(\omega)\\ \{X_{\lambda'}(-\omega^*)\}^*\end{bmatrix}=\begin{bmatrix}F^0_\lambda(\omega)\\ \{F^0_\lambda(-\omega^*)\}^*\end{bmatrix}, \tag{1.66}$$

where I used the relation originating from that the dielectric function $\varepsilon_{\mathrm{bg}}(t)$ is real:

$$\mathsf{G}_0(\boldsymbol{r},\boldsymbol{r}',\omega)=\{\mathsf{G}_0(\boldsymbol{r},\boldsymbol{r}',-\omega^*)\}^*=\mathsf{G}^*_0(\boldsymbol{r},\boldsymbol{r}',-\omega). \tag{1.67}$$

Therefore, instead of solving integro-differential equation (1.55), the problem reduces to the linear equation set [Eq. (1.66)] with respect to $\{X_\lambda(\omega)\}$, and we can represent the polarization as Eq. (1.57) and also the electric field as Eq. (1.60) in terms of them.

On the other hand, under the rotating wave approximation (RWA), equation set (1.66) becomes more simple. This means that, under the RWA, the polarization [Eq. (1.57)] is approximated as

$$\boldsymbol{P}_{\mathrm{ex}}(\boldsymbol{r},\omega)=\sum_\lambda\langle0|\hat{\boldsymbol{P}}_{\mathrm{ex}}(\boldsymbol{r})|\lambda\rangle\,X_\lambda(\omega), \tag{1.68}$$

because of the denominator $(\omega_\lambda+\omega)^{-1}$ of $\{X_\lambda(-\omega^*)\}^*$ is negligible compared to $(\omega_\lambda-\omega)^{-1}$ of $X_\lambda(\omega)$ under the condition $\omega\simeq\omega_\lambda$. By using Eq. (1.68), we obtain a simple equation set as

$$\sum_{\lambda'}\left[(\hbar\omega_\lambda-\hbar\omega)\delta_{\lambda,\lambda'}+\Sigma_{\lambda,\lambda'}(\omega)\right]X_{\lambda'}(\omega)=F^0_\lambda(\omega). \tag{1.69}$$

Based on the microscopic theories, various linear and nonlinear phenomena in inhomogeneous materials have been discussed. In particular, for nano-structured materials where the coherence of the exciton

center-of-mass motion is maintained in whole material (weak confinement regime), the anomalous size dependence of their optical processes has been elucidated [32, 40, 34, 41, 37]. With regard to nanofilms, the nonlocal theory has successfully explained their peculiar spectral structures originating from the polariton interference [72, 73, 74]. Further, with the recent development of fabrication technologies for nano-structured samples, various peculiar effects due to the long-range coherence are appearing through the interplay between the spatial structures of electromagnetic and excitonic waves, such as the resonant enhancement of a nonlinear response [41], interchange of quantized states due to giant radiative shift [42], and ultrafast radiative decay with femtosecond order [43].

1.4.4 Self-sustaining modes

Based on the microscopic nonlocal theory explained in the previous section, self-sustaining modes in the inhomogeneous systems have been discussed for excitons confined in films [36, 38], multilayers [33], spheres [75, 35, 76, 77], and so on [31]. They have been recently observed in nonlinear experiments for semiconductor nano films [42, 43]. The self-sustaining condition in the microscopic nonlocal theory is given as

$$\det[\mathbf{S}(\tilde{\omega})] = 0, \tag{1.70}$$

where $\mathbf{S}(\omega)$ is the coefficient matrix in the self-consistent equation set [Eq. (1.66) or Eq. (1.69) under the RWA]. A self-sustaining mode is characterized by a complex frequency $\tilde{\omega}$ satisfying Eq. (1.70), and its real and imaginary parts respectively represent the resonance frequency $\omega_{\rm res}$ and radiative decay rate γ as $\tilde{\omega} = \omega_{\rm res} - {\rm i}\gamma$.

Fig. 1.4 shows the thickness dependence of (a) the radiative decay rate γ and (b) the resonance frequency $\omega_{\rm res}$ of self-sustaining modes in a CuCl film existing in vacuum. In this calculation, I consider the exciton center-of-mass wavefunction as

$$g_m(z) = \sqrt{\frac{2}{d}}\sin(q_m z), \tag{1.71}$$

where d is the film thickness, and $q_m = m\pi/d$ is the confinement wavenumber of excitons for $m = 1,\ 2,\ 3,\ \ldots$. The bare exciton eigenfrequency is given in line with the effective mass approximation as

$$\omega_m = \omega_{\rm T} + \frac{\hbar {q_m}^2}{2m_{\rm ex}}. \tag{1.72}$$

The other calculation parameters will be explained in Chap. 3. There are many self-sustaining modes at a particular thickness, and the number of modes is equal to that of exciton center-of-mass motion states, i.e., the number of atomic layers in the film. As seen in Fig. 1.4(a), the radiative decay rate γ of a self-sustaining mode has a maximum value at a particular thickness, and the maximum value gradually increases together with the maximizing thickness. On the other hand, as seen in Fig. 1.4(b), the resonance frequency $\omega_{\rm res}$ of a self-sustaining mode gradually decreases until its maximizing thickness, and it flips from lower to upper side around its thickness. After that, $\omega_{\rm res}$ decreases with increasing the thickness, and saturates to $\omega_{\rm T} + \omega_{\rm LT}$, the band edge frequency of upper branch polariton.

The above behavior of $\omega_{\rm res}$ and γ can be understood from the dispersion relation of exciton-polariton as seen in Fig. 1.5. Solid and dashed lines represent the polariton and bare exciton dispersion in bulk CuCl, respectively, and self-sustaining modes are plotted with vertical bars. The length of a bar represents the radiative decay width $\hbar\gamma$ of the mode, and the center is the resonance energy. As experimentally demonstrated by Tang et al. [74], in the case of a CuCl film with a thickness in the order of 10 nm, the

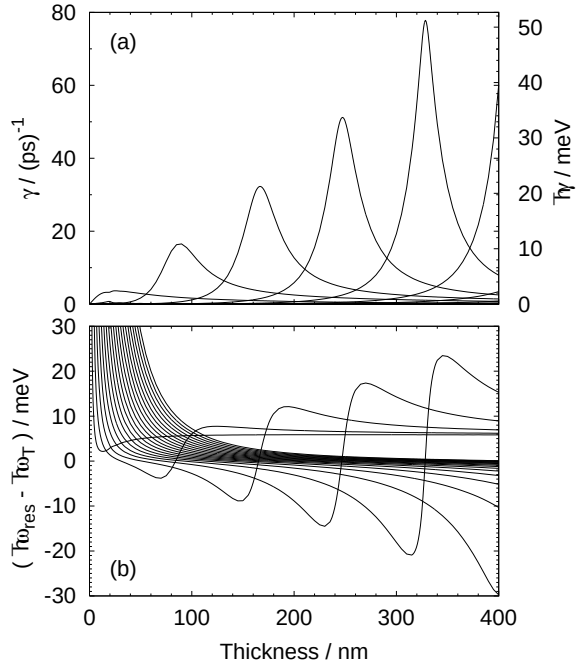

Figure 1.4: Thickness dependence of (a) radiative decay rate and (b) resonance frequency of self-sustaining modes in CuCl film existing in vacuum.

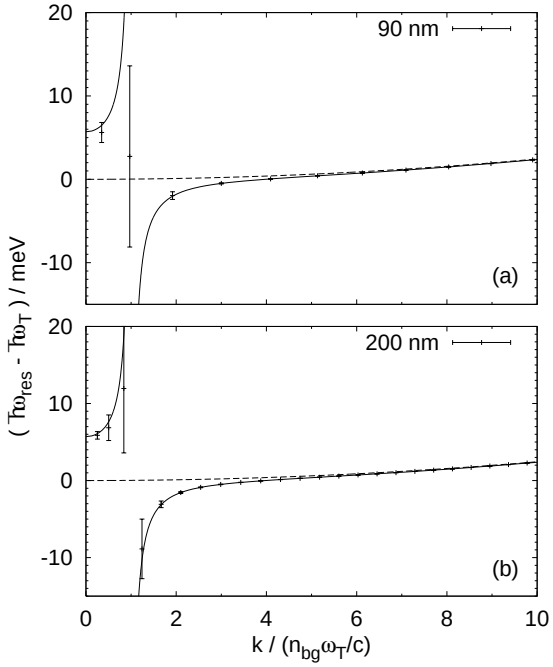

Figure 1.5: Dispersion relations of self-sustaining modes in CuCl film with thicknesses of (a) 90 nm and (b) 200 nm. The length of bar represents the radiative decay width, and the center is the resonance energy. Solid and dashed lines represent exciton-polariton and bare exciton dispersions, respectively.

quantized frequencies [Eq. (1.72)] of confined excitons are observed as dips in the reflection spectrum. However, even modes ($m = 2, 4, 6, \ldots$) can not be observed, because they are optically forbidden due to the parity of center-of-mass wavefunctions under the long wavelength approximation (LWA). On the other hand, for more than a few tens nanometer thickness, we must consider an energy shift of confined exciton modes due to the interaction with the electromagnetic fields (radiative shift). As seen in Fig. 1.5, if the confinement wavenumber $q_m = m\pi/d$ reaches the crossing wavenumber $n_{\rm bg}\omega_{\rm T}/c$ of the exciton and photon dispersion curves, the resonance frequency is strongly shifted from the bare exciton frequency, and the radiative decay rate increases due to the strong exciton-photon coupling. Since $q_m = m\pi/d$ decreases with increasing the thickness, $\omega_{\rm res}$ and γ of self-sustaining modes behave as seen in Fig. 1.4. Interestingly, the even modes are not optically forbidden and have finite radiative decay rate as seen in Fig. 1.5, because the LWA is broken in these film thicknesses, which are in the order of light wavelength in CuCl. Further, in contrast to the bulk polariton dispersion, one self-sustaining mode exists in the polariton band gap ($\omega_{\rm T} < \omega_{\rm res} < \omega_{\rm T} + \omega_{\rm LT}$) as seen in 1.5(a). Such modes deviate from the bulk polariton dispersion, and they are just in the transition from lower to upper frequency side and have a large radiative decay rate as see in Fig. 1.4(a).

The resonance frequency and radiative decay rate of the self-sustaining modes have been recently observed in experiments. Syouji et al. observed the large radiative shift of resonance frequency from the bare exciton one by means of the nondegenerate two-photon excitation scattering in CuCl film with thickness of 35.3 nm [42], where the first mode feels the positive radiative frequency shift and the second mode becomes the lowest energy state. On the other hand, Ichimiya et al. observed the quantized

resonance frequencies by the degenerate four-wave mixing in CuCl film with thicknesses of 187, 260, and 312 nm. Further, they observed a decay time of about 100 fs for 187 nm thickness, and its rapid decay is considered owing to the size-enhancement of the radiative decay rate as see in Fig. 1.4(a).

However, there remain some theoretical problems for understanding the thickness behavior of the self-sustaining modes. First, as seen in Fig. 1.4(a), the maximizing thickness for radiative decay rate does not obey the condition $q_m = m\pi/d = n_{\rm bg}\omega_{\rm T}/c$. This is because a self-sustaining mode consists of some exciton center-of-mass motion states especially under the strong exciton-photon coupling around the maximizing thickness, and then the confinement wavenumber cannot be strictly determined. Second, for more than 500 nm thickness, the maximization of γ becomes divergent, and the transition of $\omega_{\rm res}$ from lower to upper frequency side becomes discontinuous. The reason of this behavior has not been understood. Last, the crossover condition from the above radiative modification regime to bulk polariton one was not been completely clarified, although some prospects have been suggested by Ajiki [35].

1.5 Structure of this thesis

One of the main subjects of this thesis is the application of the calculation idea of the microscopic nonlocal theory into the QED theory of dispersive and absorptive media, or in other words, the redescription of the microscopic nonlocal theory in terms of the quantum electrodynamics. The present QED theory has good correspondences with these two underlying theories, and it will be discussed in Chap. 2.

Another subject is the comprehensive thickness dependence of the self-sustaining modes explained in Sec. 1.4.4. In the framework of the microscopic nonlocal theory, there remains a task to interpret the divergent thickness dependence of the self-sustaining modes appearing at the phase-matching thicknesses larger than, for example, 500 nm under the same condition as Fig. 1.4. This behavior has a close connection with the crossover of the radiative decay schemes of excitons, which has been discussed for more than 20 years, and Ajiki have provided an answer for this problem in the framework of the nonlocal theory. The novelty of the present work is deriving the crossover condition of the radiative decay schemes explicitly. This work has another subject to construct a calculation method for the resonance frequency and radiative decay rate of exciton-photon coupled modes in inhomogeneous systems, i.e., a calculation method for poles in the exciton-photon inhomogeneous systems, which is required to analytically express the retarded correlation functions of excitons. The details will be discussed in Chap. 3.

The other subject is providing the analytical expression of the retarded correlation functions of excitons in exciton-photon inhomogeneous systems by using the pole information obtained in Chap. 3. As will be explained in Chap. 2, the present QED theory or the semiclassical microscopic nonlocal theory provides the correlation functions. Therefore, for the future application of the present theory, their analytical expression should be obtained to derive the time-ordered and thermal correlation functions by the analytical continuation. I will show a good approximation of the analytical expression in Chap. 4.

In App. A.1, I explain general concepts of retarded correlation functions in relations to linear response theory, Kramers-Kronig relations, and Langevin equation. In App. B, I show a validity of the QED theory for dispersive and absorptive media by discussing the vacuum fluctuation of the electromagnetic fields in its framework. In App. C, I show a direct derivation technique of the Green's function for the integro-differential equation, and I show the Green's function for general multilayer system without the nonlocality in App. D. Further, I explain the numerical calculation method for poles in App. E, and show the definitions of Fourier transform, longitudinal and transverse fields in App. F.

Chapter 2

QED Theory of Excitons

In this chapter, I explain the main result of this thesis: the full quantum theory for the optical process of excitons (QED theory of excitons) with nonlocal susceptibility originating from their center-of-mass motion. As explained in Chap. 1, there is growing interest in the QED of elementary excitation in condensed matter, for example, the generation of entangled photons [1] and single photons [2] from semiconductors, and squeezing [4] and BEC [8, 9, 10] of polaritons in semiconductor microcavities. In order to systematically discuss these topics for actual materials with spatial structure, such as surfaces, substrates, and distributed Bragg reflectors (DBRs) with finite period, we require a QED theory of excitons applicable to arbitrary-structured 3D systems with considering their center-of-mass motion, radiative and nonradiative relaxations. While some papers have focused on the same subject previously, the novelty of the present theory is its practical calculation method applicable to arbitrary-structured 3D systems including exciton center-of-mass motion. This is owing to that the present theory adopts the calculation idea of the microscopic nonlocal theory by Kikuo Cho [31], which has been developed in the semiclassical framework as explained in Sec. 1.4.3. As the result, the present theory shows good correspondences with the nonlocal theory as well as the series of QED theories for dispersive and absorptive materials, which is explained in Sec. 1.3 for media with local susceptibility. The contents of this chapter was published in Ref. 78.

The previously discussed QED theories with the nonlocality is explained in Sec. 2.1. The Hamiltonian of the present theory is shown in Sec. 2.2, and two fundamental equations of it, the Maxwell wave equation and motion equations of excitons, are respectively shown in Secs. 2.3 and 2.4. The wave equation with the nonlocal susceptibility is explained in Sec. 2.5. The present QED theory is explained in Sec. 2.6, and the Green's function for the nonlocal wave equation is shown in Sec. 2.7. The validity and usefulness of the rotating wave approximation (RWA) in the present theory are shown in Sec. 2.8, and the practical calculation scheme is explained in Sec. 2.9. Finally, the comparison between the present QED theory and others is discussed in Sec. 2.10.

In this chapter, MKS units and Coulomb gauge are used.

2.1 Previous QED theories with nonlocal susceptibility

The series of QED theories [18] for dispersive and absorptive dielectrics, based on the pioneering work by Huttner and Barnett [21], enable us to discuss the optical process in arbitrary-structured 3D dielectrics characterized by a dielectric function $\varepsilon(\boldsymbol{r}, \omega)$. However, in order to discuss materials with the nonlocal susceptibility, we must consider more general elementary excitations that cannot be described by the

localized harmonic oscillators in the classical Hopfield model [19], which were adopted in the Huttner-Barnett theory.

As a pioneering study on such full quantum theory considering the nonlocality, Jenkins and Mukamel have discussed molecular crystals in d dimensions ($d = 1, 2, 3$) [79], where the relative motion of excitons is localized at a single molecule and the center-of-mass moves between molecules due to the dipole-dipole interaction. While their theory concentrates on treating the resonant polarization without nonradiative relaxation, recently, the nonlocality has been introduced into the field quantization in dispersive and absorptive media [23, 24, 25, 26, 27, 28], and some studies have demonstrated the application of their theories for specific structures [23, 28]. Stefano et al. discussed excitons with the nonlocality in media where the spatial translation symmetry is broken along one dimension, and they practically calculated the spatial and frequency dependences of the vacuum field fluctuation in a semiconductor quantum well structure [23]. Thereafter, they extended their theory to arbitrary-structured 3D media [24], and discussed the input-output relations in scattering systems [25]. On the other hand, Bechler performed the field quantization for homogeneous systems with the nonlocality by using the path-integral method [26], and Suttorp performed the same for nonlocal, inhomogeneous, and anisotropic systems by using the diagonalization method [27]. Most recently, Raabe et al. phenomenologically discussed the nonlocal systems with both dielectric and magnetic properties [28], and they proposed the use of the dielectric approximation with the surface impedance method for the practical application of their theory.

As seen in the above previous studies, it can be considered that a consistent framework for the field quantization in dielectrics with the nonlocal susceptibility has already been established. Thus, the issue of current importance is to establish a general and practical calculation method applicable to arbitrary-structured 3D systems; this is desired for the actual applications of the above framework, although interesting applications have already been demonstrated in specific situations by Stefano et al. and Raabe et al. The essential task for this purpose is the derivation of dyadic Green's function for the Maxwell wave equation with the nonlocal susceptibility, as seen in Eq. (1.55). However, it seems a hard task to solve such integro-differential equation for arbitrary structures.

On the other hand, in the semiclassical framework, such a calculation problem has been resolved by using the fact that the nonlocal susceptibility is represented as a summation of separable functions with respect to two positions [Eq. (2.51)], which is known as the ABC-free theory [29], or the microscopic nonlocal theory [30, 31] as explained in Sec. 1.4.3. I adopt the same calculation idea of them to provide a practical calculation method for the Green's function for arbitrary structures. Along the lines of this strategy, the present theory start from the Suttorp-Wubs Hamiltonian [63], which describes arbitrary-structured 3D isotropic linear media with local susceptibility, and consider the excitons with finite translational mass and nonradiative damping. In other words, this theory extends the microscopic nonlocal theory, previously discussed in the semiclassical framework, into the full quantum one. The present QED theory consists of two equations in ω-representation: the Maxwell wave equation with excitonic polarization and the motion equation of excitons. From these two equations, we can derive a linear equation set for exciton operators, which corresponds to the self-consistent equation set [Eq. (1.66)] in the semiclassical framework, instead of the Maxwell wave equation with nonlocal susceptibility [Eq. (1.55)].

2.2 Hamiltonian

The present theory describes the dielectric materials with resonant contributions from excitons with center-of-mass motion and nonresonant ones from the background with local dielectric function $\varepsilon_{\rm bg}(\boldsymbol{r},\omega)$. This treatment is useful for considering the modification of the background electromagnetic fields in the practical material structures (with absorption) such as substrate, dielectric multilayer cavity, photonic crystals, and so on, surrounding the excitonic active regions. The nonresonant background is treated by the Hamiltonian of Suttorp and Wubs [63], which describes inhomogeneous 3D dielectrics with local susceptibility, and the optical and nonradiative damping processes of excitons are discussed by considering the exciton-photon interaction and a reservoir of oscillators interacting with the excitons, respectively. The Hamiltonian in the whole system was derived in App. B of Ref. 78, and is written as

$$H = H_{\rm em} + H_{\rm int} + H_{\rm mat}, \tag{2.1}$$

where $H_{\rm em}$ describes the electromagnetic fields and the background dielectric medium, $H_{\rm mat}$ represents the excitons and the reservoir of oscillators, and $H_{\rm int}$ is the interaction between $H_{\rm em}$ and $H_{\rm mat}$. In the following discussion, the detailed representation of $H_{\rm em}$ is not important, and it is shown in Eq. (B9) of Ref. 78 or in Eq. (3) of Ref. 63.

On the other hand, the interaction Hamiltonian is represented as

$$H_{\rm int} = -\int {\rm d}\boldsymbol{r}\left[\boldsymbol{I}_{\rm ex}(\boldsymbol{r})\cdot\boldsymbol{A}(\boldsymbol{r}) - \frac{1}{2}N_{\rm ex}(\boldsymbol{r})\boldsymbol{A}^2(\boldsymbol{r})\right] + \int {\rm d}\boldsymbol{r}\ \phi_{\rm bg}(\boldsymbol{r})\rho_{\rm ex}(\boldsymbol{r}) + \frac{1}{2}\int {\rm d}\boldsymbol{r}\ \phi_{\rm ex}(\boldsymbol{r})\rho_{\rm ex}(\boldsymbol{r}). \tag{2.2}$$

Here, $\boldsymbol{A}(\boldsymbol{r},t)$ is the vector potential and $\phi_{\rm bg}(\boldsymbol{r},t)$ is the Coulomb potential induced in the background. $\boldsymbol{I}_{\rm ex}(\boldsymbol{r})$ is the excitonic current density without radiation contribution $-N_{\rm ex}(\boldsymbol{r})\boldsymbol{A}(\boldsymbol{r})$, i.e., the whole current density is written as $\boldsymbol{J}_{\rm ex}(\boldsymbol{r}) = \boldsymbol{I}_{\rm ex}(\boldsymbol{r}) - N_{\rm ex}(\boldsymbol{r})\boldsymbol{A}(\boldsymbol{r})$ (see App. A of Ref. 78 or Sec. 2.2 of Ref. 31). Further, $\rho_{\rm ex}(\boldsymbol{r})$ is the excitonic charge density and

$$\phi_{\rm ex}(\boldsymbol{r}) \equiv \int {\rm d}\boldsymbol{r}'\ \frac{\rho_{\rm ex}(\boldsymbol{r}')}{4\pi\varepsilon_0|\boldsymbol{r}-\boldsymbol{r}'|} \tag{2.3}$$

is the Coulomb potential. The first and second terms of Eq. (2.2) represent the interaction between the radiation field and excitons. The third term is the Coulomb interaction between the induced charges of the excitons and those of the background. The last term represents the interaction between the excitonic charges themselves, and it is also considered as the dipole-dipole interaction between excitonic polarizations, or the exchange interaction between electrons and holes [80, 75, 31] (or see App. B of Ref. 78). Although this term usually belongs to the matter Hamiltonian $H_{\rm mat}$, I displace it into $H_{\rm int}$ because it can also be considered as the interaction between the longitudinal component of the excitonic polarization and that of the electric field. This treatment will give us the motion equation of excitons in a simple form as seen in Eq. (2.37), and will eliminate the explicit consideration of the longitudinal-transverse (LT) splitting of the exciton eigenenergies, because the last term of Eq. (2.2) is just the origin of the LT splitting.

With regard to the excitons, they are, in principle, described in electron system with valence and conduction bands or in electron-hole system, and the Coulomb interactions between electrons and holes and between themselves are considered. However, as long as we consider the optical processes of excitons under weak excitation, it is valid to describe the electron system in terms of exciton eigenstates, and put the nonresonant (background) contributions into $H_{\rm em}$. In addition, in order to describe the nonradiative

damping process of excitons, I consider a reservoir of oscillators interacting with the excitons. In the present theory, the matter Hamiltonian is represented as

$$H_{\rm mat} = \sum_{\mu} \hbar\omega_{\mu} b_{\mu}^{\dagger} b_{\mu} + \sum_{\mu} \int_{0}^{\infty} {\rm d}\Omega \, \left\{ \hbar\Omega \, d_{\mu}^{\dagger}(\Omega) d_{\mu}(\Omega) + \left[b_{\mu} + b_{\mu}^{\dagger} \right] \left[g_{\mu}(\Omega) d_{\mu}(\Omega) + g_{\mu}^{*}(\Omega) d_{\mu}^{\dagger}(\Omega) \right] \right\}. \quad (2.4)$$

Here, b_{μ} is the annihilation operator of an exciton in eigenstate μ with eigenfrequency ω_{μ}, which does not include the LT splitting because I displace the exchange interaction between electrons and holes from $H_{\rm mat}$ to $H_{\rm int}$. The center-of-mass motion of excitons is confined in finite spaces, and index μ represents the degrees of freedom of not only the relative motion but also the translational one. Instead of evaluating the commutation relations of b_{μ} from the Fermi's commutation relations of electrons and holes, I consider the excitons as pure bosons satisfying

$$[b_{\mu}, b_{\mu'}^{\dagger}] = \delta_{\mu,\mu'}, \quad (2.5a)$$

$$[b_{\mu}, b_{\mu'}] = 0. \quad (2.5b)$$

On the other hand, in Eq. (2.4), $d_{\mu}(\Omega)$ is the annihilation operator of an reservoir oscillator with frequency Ω interacting with the excitons in state μ, and $g_{\mu}(\Omega)$ is its coupling parameter. The oscillators are independent of each other and satisfy the following commutation relations:

$$[d_{\mu}(\Omega), d_{\mu'}^{\dagger}(\Omega')] = \delta_{\mu,\mu'} \delta(\Omega - \Omega'), \quad (2.6a)$$

$$[d_{\mu}(\Omega), d_{\mu'}(\Omega')] = 0. \quad (2.6b)$$

The present theory consists of two equations in ω-representation: the motion equation of excitons and Maxwell wave equation, which are both derived from the Heisenberg equations. Because of the interaction with the reservoir oscillators, as seen in Sec. 2.4, the motion equation of excitons has fluctuation operators in the same manner as the Langevin equation (App. A.3). On the other hand, the Maxwell wave equation also has a fluctuation operator, the noise current density, which originates from the absorption in the background dielectrics as explained in Sec. 1.3. The quantum mechanical properties of electromagnetic fields are treated through the commutation relations of these fluctuation operators.

2.3 Maxwell wave equation

Since I consider the interaction Hamiltonian $H_{\rm int}$ between excitons and electromagnetic fields, the excitonic polarization is introduced into the Maxwell wave equation with the noise current density, which was explained in Sec. 1.3.3 for local dielectrics. In this section, I show that modified wave equation, whose derivation is shown in App. C of Ref. 78.

Since I consider the matter system as a combination of excitons and background medium, the electric field contains Coulomb potentials $\phi_{\rm ex}(\boldsymbol{r})$ and $\phi_{\rm bg}(\boldsymbol{r})$ induced by excitons and background, respectively, and it is represented as

$$\boldsymbol{E}(\boldsymbol{r}, t) = -\frac{\partial}{\partial t} \boldsymbol{A}(\boldsymbol{r}, t) - \boldsymbol{\nabla} \phi_{\rm bg}(\boldsymbol{r}, t) - \boldsymbol{\nabla} \phi_{\rm ex}(\boldsymbol{r}, t). \quad (2.7)$$

Because the Coulomb gauge is used in the present theory, the vector potential is a transverse field satisfying $\boldsymbol{\nabla} \cdot \boldsymbol{A}(\boldsymbol{r}) = 0$, and the second and third terms represent the longitudinal fields. The Maxwell wave equation for the electric field is written in ω-representation as

$$\boldsymbol{\nabla} \times \boldsymbol{\nabla} \times \hat{\boldsymbol{E}}^{+}(\boldsymbol{r}, \omega) - \frac{\omega^2}{c^2} \varepsilon_{\rm bg}(\boldsymbol{r}, \omega) \hat{\boldsymbol{E}}^{+}(\boldsymbol{r}, \omega) = {\rm i}\mu_0 \omega \hat{\boldsymbol{J}}_0(\boldsymbol{r}, \omega) + \mu_0 \omega^2 \hat{\boldsymbol{P}}_{\rm ex}^{+}(\boldsymbol{r}, \omega), \quad (2.8)$$

where $\hat{\boldsymbol{E}}^+(\boldsymbol{r},\omega)$ and $\hat{\boldsymbol{P}}^+_{\rm ex}(\boldsymbol{r},\omega)$ are the positive-frequency Fourier components of $\boldsymbol{E}(\boldsymbol{r},t)$ and the excitonic polarization density $\hat{\boldsymbol{P}}_{\rm ex}(\boldsymbol{r},t)$, respectively, and they are defined in the same manner as Eq. (1.5). I represent the Fourier transformed operators with a hat ($\hat{}$) in this chapter. Comparing to Eq. (1.30), the Maxwell wave equation for local media, Eq. (2.8) has the additional polarization $\hat{\boldsymbol{P}}^+_{\rm ex}(\boldsymbol{r},\omega)$, which reflects the matter information as well as the background dielectric function $\varepsilon_{\rm bg}(\boldsymbol{r},\omega)$. On the other hand, as compared to the classical electrodynamics, Eq. (2.8) has the noise current density operator $\hat{\boldsymbol{J}}_0(\boldsymbol{r},\omega)$ on the RHS, and it satisfies

$$\hat{\boldsymbol{J}}_0(\boldsymbol{r},\omega) = \{\hat{\boldsymbol{J}}_0(\boldsymbol{r},-\omega^*)\}^\dagger \tag{2.9}$$

as the vector potential satisfies Eq. (1.5), and also the electric field does. Furthermore, as the noise current density satisfies Eq. (1.31) in the Suttorp-Wubs theory, $\hat{\boldsymbol{J}}_0(\boldsymbol{r},\omega)$ should also satisfies

$$\Big[\hat{\boldsymbol{J}}_0(\boldsymbol{r},\omega),\{\hat{\boldsymbol{J}}_0(\boldsymbol{r}',\omega'^*)\}^\dagger\Big] = \Big[\hat{\boldsymbol{J}}_0(\boldsymbol{r},\omega),\hat{\boldsymbol{J}}_0(\boldsymbol{r}',-\omega')\Big] = \delta(\omega-\omega')\delta(\boldsymbol{r}-\boldsymbol{r}')\frac{\varepsilon_0\hbar\omega^2}{\pi}{\rm Im}[\varepsilon_{\rm bg}(\boldsymbol{r},\omega)]\mathbf{1}, \tag{2.10}$$

where $[\hat{\boldsymbol{J}}_0,\{\hat{\boldsymbol{J}}_0\}^\dagger]$ is a 3×3 tensor and its (ξ,ξ') element implies $[\{\hat{J}_0\}_\xi,\{\hat{J}_0^\dagger\}_{\xi'}]$ for $\xi = x,y,z$. Although Eq. (2.10) is phenomenologically introduced in the present theory, it can be derived through the Laplace transformation technique of Suttorp and Wubs [63]. However, the validity of Eq. (2.10) can be understood according to the series of QED theories for dispersive and absorptive media (Sec. 1.3), or the fluctuation dissipation theorem. In addition, we can verify that Eq. (2.10) provides reasonable commutation relations of excitons and electric field in the whole system as will discussed in Secs. 2.6 and 2.7.

By using the dyadic Green's function $\mathsf{G}_0(\boldsymbol{r},\boldsymbol{r}',\omega)$ satisfying Eq. (1.59), Eq. (2.8) can be rewritten as

$$\hat{\boldsymbol{E}}^+(\boldsymbol{r},\omega) = \hat{\boldsymbol{E}}^+_0(\boldsymbol{r},\omega) + \mu_0\omega^2\int {\rm d}\boldsymbol{r}'\ \mathsf{G}_0(\boldsymbol{r},\boldsymbol{r}',\omega)\cdot\hat{\boldsymbol{P}}^+_{\rm ex}(\boldsymbol{r}',\omega), \tag{2.11}$$

where $\hat{\boldsymbol{E}}^+_0(\boldsymbol{r},\omega)$ is considered as the background field, the electric field in $H_{\rm em}$ system, and defined as

$$\hat{\boldsymbol{E}}^+_0(\boldsymbol{r},\omega) \equiv {\rm i}\mu_0\omega\int {\rm d}\boldsymbol{r}'\ \mathsf{G}_0(\boldsymbol{r},\boldsymbol{r}',\omega)\cdot\hat{\boldsymbol{J}}_0(\boldsymbol{r}',\omega). \tag{2.12}$$

In the classical electrodynamics, this is usually introduced as a homogeneous solution satisfying

$$\boldsymbol{\nabla}\times\boldsymbol{\nabla}\times\Big\langle\hat{\boldsymbol{E}}^+_0(\boldsymbol{r},\omega)\Big\rangle - \frac{\omega^2}{c^2}\varepsilon_{\rm bg}(\boldsymbol{r},\omega)\Big\langle\hat{\boldsymbol{E}}^+_0(\boldsymbol{r},\omega)\Big\rangle = \mathbf{0}, \tag{2.13}$$

and is considered as an incident field for excitons. On the other hand, since the optical susceptibility is a response function connecting the electric field and matter polarization, according to Eq. (A.14), the background dielectric function $\varepsilon_{\rm bg} = 1+\chi_{\rm bg}$ satisfies

$$\varepsilon_{\rm bg}(\boldsymbol{r},\omega) = \{\varepsilon_{\rm bg}(\boldsymbol{r},-\omega^*)\}^* = \varepsilon^*_{\rm bg}(\boldsymbol{r},-\omega), \tag{2.14}$$

and also the Green's function satisfies

$$\mathsf{G}_0(\boldsymbol{r},\boldsymbol{r}',\omega) = \{\mathsf{G}_0(\boldsymbol{r},\boldsymbol{r}',-\omega^*)\}^* = \mathsf{G}^*_0(\boldsymbol{r},\boldsymbol{r}',-\omega). \tag{2.15}$$

Therefore, the negative-frequency Fourier component of the electric field is represented as

$$\hat{\boldsymbol{E}}^-(\boldsymbol{r},\omega) = \hat{\boldsymbol{E}}^+(\boldsymbol{r},-\omega) = \hat{\boldsymbol{E}}^-_0(\boldsymbol{r},\omega) + \mu_0\omega^2\int {\rm d}\boldsymbol{r}'\ \mathsf{G}^*_0(\boldsymbol{r},\boldsymbol{r}',\omega)\cdot\hat{\boldsymbol{P}}^-_{\rm ex}(\boldsymbol{r}',\omega), \tag{2.16}$$

and the background field is given as

$$\hat{\boldsymbol{E}}^-_0(\boldsymbol{r},\omega) \equiv -{\rm i}\mu_0\omega\int {\rm d}\boldsymbol{r}'\ \mathsf{G}^*_0(\boldsymbol{r},\boldsymbol{r}',\omega)\cdot\hat{\boldsymbol{J}}_0(\boldsymbol{r}',-\omega). \tag{2.17}$$

Since $\hat{\boldsymbol{J}}_0(\boldsymbol{r},\omega)$ satisfies Eq. (2.9), in the same manner as Eq. (1.5), $\hat{\boldsymbol{E}}_0^{\pm}(\boldsymbol{r},\omega)$ also satisfies

$$\hat{\boldsymbol{E}}_0^{\pm}(\boldsymbol{r},\omega) = \hat{\boldsymbol{E}}_0^{\mp}(\boldsymbol{r},-\omega) = \{\hat{\boldsymbol{E}}_0^{\pm}(\boldsymbol{r},-\omega^*)\}^{\dagger}. \tag{2.18}$$

Furthermore, from the commutation relation (2.10) of $\hat{\boldsymbol{J}}_0(\boldsymbol{r},\omega)$ with Eqs. (1.35) and (1.36), that of $\hat{\boldsymbol{E}}_0^{\pm}(\boldsymbol{r},\omega)$ can be derived as

$$\left[\hat{\boldsymbol{E}}_0^{+}(\boldsymbol{r},\omega), \hat{\boldsymbol{E}}_0^{-}(\boldsymbol{r}',\omega')\right] = \left[\hat{\boldsymbol{E}}_0^{+}(\boldsymbol{r},\omega), \hat{\boldsymbol{E}}_0^{+}(\boldsymbol{r}',-\omega')\right] = \delta(\omega-\omega')\frac{\mu_0\hbar\omega^2}{\mathrm{i}2\pi}[\mathsf{G}_0(\boldsymbol{r},\boldsymbol{r}',\omega) - \mathsf{G}_0^*(\boldsymbol{r},\boldsymbol{r}',\omega)]. \tag{2.19}$$

This has the same form as Eq. (1.34), and is also interpreted as that the Green's function $\mathsf{G}_0(\boldsymbol{r},\boldsymbol{r}',\omega)$ is the retarded correlation function of the electric field in the background system:

$$-\mu_0\omega^2\mathsf{G}_0(\boldsymbol{r},\boldsymbol{r}',\omega) = \frac{1}{\mathrm{i}\hbar}\int_{t'}^{\infty} \mathrm{d}t\ \mathrm{e}^{\mathrm{i}\omega(t-t')}\ \langle[\boldsymbol{E}_0(\boldsymbol{r},t), \boldsymbol{E}_0(\boldsymbol{r}',t')]\rangle\,. \tag{2.20}$$

This representation actually satisfies Eq. (2.19). Therefore, because of the causality seen in Eq. (2.20), $\mathsf{G}_0(\boldsymbol{r},\boldsymbol{r}',\omega)$ satisfies the Kramers-Kronig relation, and has no pole in the upper half of the complex ω-plane.

2.4 Motion equation of excitons

The motion equation of the electric field has been obtained as the Maxwell wave equation [Eq. (2.8)] or Eq. (2.11). On the other hand, there remains a task to derive the motion equation of excitons or the excitonic polarization $\hat{\boldsymbol{P}}_{\mathrm{ex}}^{+}(\boldsymbol{r},\omega)$ appearing in the Maxwell equations. As seen in App. A of Ref. 78, the second-quantized form of the excitonic polarization is represented in terms of the exciton operator set $\{b_\mu\}$ as

$$\boldsymbol{P}_{\mathrm{ex}}(\boldsymbol{r}) = \sum_{\mu}\left[\boldsymbol{\mathcal{P}}_\mu(\boldsymbol{r})\ b_\mu + \boldsymbol{\mathcal{P}}_\mu^*(\boldsymbol{r})\ b_\mu^\dagger\right], \tag{2.21}$$

where the expansion coefficient $\boldsymbol{\mathcal{P}}_\mu(\boldsymbol{r})$ is written as

$$\boldsymbol{\mathcal{P}}_\mu(\boldsymbol{r}) = \mathcal{P}_\mu\boldsymbol{e}_\mu G_\mu(\boldsymbol{r}). \tag{2.22}$$

$\mathcal{P}_\mu$ is the transition dipole moment, $\boldsymbol{e}_\mu$ is a unit vector in the polarization direction, and $G_\mu(\boldsymbol{r})$ is the center-of-mass wavefunction in exciton state μ. Under the weak (center-of-mass) confinement regime of excitons, their relative motion is approximated as that in bulk system, and $\mathcal{P}_\mu$ is related to the LT splitting energy as $\Delta_{\mathrm{LT}}^{\mu} = |\mathcal{P}_\mu|^2/\varepsilon_0\varepsilon_{\mathrm{bg}}$.

From the matter Hamiltonian [Eq. (2.4)] and the interaction one [Eq. (2.2)], neglecting the radiation contribution of the current density $N_{\mathrm{ex}}(\boldsymbol{r})\boldsymbol{A}^2(\boldsymbol{r})/2$ under the assumption of weak excitation, the Heisenberg equation of exciton operator is derived as

$$\begin{aligned}\mathrm{i}\hbar\frac{\partial}{\partial t}b_\mu(t) = \hbar\omega_\mu b_\mu(t) - \int \mathrm{d}\boldsymbol{r}\left[\boldsymbol{\mathcal{I}}_\mu^*(\boldsymbol{r})\cdot\boldsymbol{A}(\boldsymbol{r},t) - \rho_\mu^*(\boldsymbol{r})\phi_{\mathrm{bg}}(\boldsymbol{r},t) - \rho_\mu^*(\boldsymbol{r})\phi_{\mathrm{ex}}(\boldsymbol{r},t)\right] \\ + \int_0^{\infty}\mathrm{d}\Omega\left[g_\mu(\Omega)d_\mu(\Omega,t) + g_\mu^*(\Omega)d_\mu^\dagger(\Omega,t)\right].\end{aligned} \tag{2.23}$$

Here, $\boldsymbol{\mathcal{I}}_\mu(\boldsymbol{r})$ and $\rho_\mu(\boldsymbol{r})$ are, respectively, the expansion coefficients of $\boldsymbol{I}_{\mathrm{ex}}(\boldsymbol{r})$ and $\rho_{\mathrm{ex}}(\boldsymbol{r})$ as

$$\boldsymbol{I}_{\mathrm{ex}}(\boldsymbol{r}) = \sum_{\mu}\left[\boldsymbol{\mathcal{I}}_\mu(\boldsymbol{r})\ b_\mu + \boldsymbol{\mathcal{I}}_\mu^*(\boldsymbol{r})\ b_\mu^\dagger\right], \tag{2.24}$$

$$\rho_{\mathrm{ex}}(\boldsymbol{r}) = \sum_{\mu}\left[\rho_\mu(\boldsymbol{r})\ b_\mu + \rho_\mu^*(\boldsymbol{r})\ b_\mu^\dagger\right]. \tag{2.25}$$

Further, from the relations of excitonic polarization under weak excitation

$$\boldsymbol{I}_{\rm ex}(\boldsymbol{r}) = \frac{\partial}{\partial t}\boldsymbol{P}_{\rm ex}(\boldsymbol{r}) = \frac{1}{\mathrm{i}\hbar}\left[\boldsymbol{P}_{\rm ex}(\boldsymbol{r}), H\right] \simeq \frac{1}{\mathrm{i}\hbar}\left[\boldsymbol{P}_{\rm ex}(\boldsymbol{r}), H_{\rm ex}\right], \tag{2.26}$$

$$\rho_{\rm ex}(\boldsymbol{r}) = -\boldsymbol{\nabla}\cdot\boldsymbol{P}_{\rm ex}(\boldsymbol{r}), \tag{2.27}$$

the coefficients can be rewritten as

$$\boldsymbol{\mathcal{I}}_\mu(\boldsymbol{r}) = -\mathrm{i}\omega_\mu\boldsymbol{\mathcal{P}}_\mu(\boldsymbol{r}), \tag{2.28}$$

$$\rho_\mu = -\boldsymbol{\nabla}\cdot\boldsymbol{\mathcal{P}}_\mu(\boldsymbol{r}). \tag{2.29}$$

On the other hand, the Heisenberg equation of reservoir operator is derived as

$$\mathrm{i}\hbar\frac{\partial}{\partial t}d_\mu(\Omega,t) = \hbar\Omega\ d_\mu(\Omega,t) + g_\mu^*(\Omega)\left[b_\mu(t) + b_\mu^\dagger(t)\right]. \tag{2.30}$$

By the same procedure as deriving the Langevin equation (App. A.3), the motion equation (2.23) of excitons is rewritten by substituting Eq. (2.30) as

$$\mathrm{i}\hbar\frac{\partial}{\partial t}b_\mu(t) = \hbar\omega_\mu b_\mu(t) - \int \mathrm{d}\boldsymbol{r}\left[\boldsymbol{\mathcal{I}}_\mu^*(\boldsymbol{r})\cdot\boldsymbol{A}(\boldsymbol{r},t) - \rho_\mu^*(\boldsymbol{r})\phi_{\rm bg}(\boldsymbol{r},t) - \rho_\mu^*(\boldsymbol{r})\phi_{\rm ex}(\boldsymbol{r},t)\right] - \int_{-\infty}^{t}\mathrm{d}t'\ \frac{\mathrm{i}\Gamma_\mu(t-t')}{2}\left[b(t') + b^\dagger(t')\right] + \mathcal{D}_\mu(t), \tag{2.31}$$

where the coefficient function is defined as

$$\frac{\Gamma_\mu(t-t')}{2} \equiv \int_0^\infty \mathrm{d}\Omega\ \frac{|g_\mu(\Omega)|^2}{\hbar}\left[\mathrm{e}^{-\mathrm{i}\Omega(t-t')} - \mathrm{e}^{\mathrm{i}\Omega(t-t')}\right] = \frac{\Gamma_\mu^*(t'-t)}{2}. \tag{2.32}$$

Further, the fluctuation operator $\mathcal{D}_\mu(t)$ is defined as

$$\mathcal{D}_\mu(t) \equiv \int_0^\infty \mathrm{d}\Omega\left[g_\mu(\Omega)\mathrm{e}^{-\mathrm{i}\Omega(t-t_0)}d_\mu(t_0) + g_\mu^*(\Omega)\mathrm{e}^{\mathrm{i}\Omega(t-t_0)}d_\mu^\dagger(t_0)\right] = \mathcal{D}_\mu^\dagger(t), \tag{2.33}$$

where $t_0 \to \infty$ is the time that the exciton-reservoir interaction is switched on. This operator satisfies

$$\left[\mathcal{D}_\mu(t), \mathcal{D}_{\mu'}^\dagger(t')\right] = \left[\mathcal{D}_\mu(t), \mathcal{D}_{\mu'}(t')\right] = \frac{\hbar\Gamma_\mu(t-t')}{2}. \tag{2.34}$$

In the present theory, the noise current density $\hat{\boldsymbol{J}}_0(\boldsymbol{r},\omega)$ and $\mathcal{D}_\mu(t)$ [or its Fourier transform $\hat{\mathcal{D}}_\mu(\omega)$] are the fundamental fluctuation operators, whose commutation relations are already known.

Next, I show the ω-Fourier transform of the exciton motion equation. The Fourier transform of exciton operator is defined as

$$\hat{b}_\mu(\omega) \equiv \frac{1}{2\pi}\int_{-\infty}^{\infty}\mathrm{d}t\ \mathrm{e}^{\mathrm{i}\omega t}b_\mu(t), \tag{2.35a}$$

$$\hat{b}_\mu^\dagger(\omega) \equiv \frac{1}{2\pi}\int_{-\infty}^{\infty}\mathrm{d}t\ \mathrm{e}^{\mathrm{i}\omega t}b_\mu^\dagger(t) = \{\hat{b}_\mu(-\omega^*)\}^\dagger. \tag{2.35b}$$

Since the electric field [Eq. (2.7)] is transformed into

$$\hat{\boldsymbol{E}}(\boldsymbol{r},\omega) = \mathrm{i}\omega\hat{\boldsymbol{A}}(\boldsymbol{r},\omega) - \boldsymbol{\nabla}\hat{\phi}_{\rm bg}(\boldsymbol{r},\omega) - \boldsymbol{\nabla}\hat{\phi}_{\rm ex}(\boldsymbol{r},\omega), \tag{2.36}$$

By using Eqs. (2.28) and (2.29) with the partial integration, Eq. (2.31) is rewritten under the resonant condition $\omega \simeq \omega_\mu$ as

$$\left[\hbar\omega_\mu - \hbar\omega - \mathrm{i}\Gamma_\mu(\omega)/2\right]\hat{b}_\mu(\omega) + \left[-\mathrm{i}\Gamma_\mu(\omega)/2\right]\{\hat{b}_\mu(-\omega^*)\}^\dagger = \int\mathrm{d}\boldsymbol{r}\ \boldsymbol{\mathcal{P}}_\mu^*(\boldsymbol{r})\cdot\hat{\boldsymbol{E}}^+(\boldsymbol{r},\omega) + \hat{\mathcal{D}}_\mu(\omega), \tag{2.37}$$

where $\varGamma_\mu(\omega)$ is the nonradiative damping width defined as

$$\frac{\varGamma_\mu(\omega)}{2} \equiv \int_0^\infty \mathrm{d}t\ \mathrm{e}^{\mathrm{i}\omega t}\frac{\varGamma_\mu(t)}{2} = \int_0^\infty \mathrm{d}\varOmega\ \frac{|g_\mu(\varOmega)|^2}{\mathrm{i}\hbar}\left[\frac{1}{\varOmega-\omega-\mathrm{i}\delta}+\frac{1}{\varOmega+\omega+\mathrm{i}\delta}\right], \tag{2.38}$$

and it satisfies

$$\varGamma_\mu(\omega) = -\{\varGamma_\mu(-\omega^*)\}^* = -\varGamma_\mu^*(-\omega). \tag{2.39}$$

In the calculation for analyzing practical materials, we usually give real values $\{\varGamma_\mu(\omega)\}$ as fitting parameters, rather than estimating them from their definition [Eq. (2.38)] for given coefficients $\{g_\mu(\varOmega)\}$, which reflect into the present theory only through $\{\varGamma_\mu(\omega)\}$. On the other hand, the fluctuation operator $\hat{\mathcal{D}}_\mu(\omega)$ is written in ω-representation as

$$\hat{\mathcal{D}}_\mu(\omega) \equiv \frac{1}{2\pi}\int_{-\infty}^\infty \mathrm{d}t\ \mathrm{e}^{\mathrm{i}\omega t}\mathcal{D}_\mu(t) = \{\hat{\mathcal{D}}_\mu(-\omega^*)\}^\dagger, \tag{2.40}$$

and, by the same procedure as App. A.3, its commutation relation is obtained as

$$\left[\hat{\mathcal{D}}_\mu(\omega), \{\hat{\mathcal{D}}_{\mu'}(\omega'^*)\}^\dagger\right] = \left[\hat{\mathcal{D}}_\mu(\omega), \hat{\mathcal{D}}_{\mu'}(-\omega')\right] = \delta_{\mu,\mu'}\delta(\omega-\omega')\frac{\hbar}{\mathrm{i}2\pi}\frac{\mathrm{i}\varGamma_\mu(\omega)+\mathrm{i}\varGamma_\mu^*(\omega)}{2}. \tag{2.41}$$

Since the origins of $\hat{\mathcal{D}}_\mu(\omega)$ and $\hat{\boldsymbol{J}}_0(\boldsymbol{r},\omega)$ are independent with each other, they should be commutable as

$$\left[\hat{\mathcal{D}}_\mu(\omega), \hat{\boldsymbol{J}}_0(\boldsymbol{r},\omega')\right] = \left[\hat{\mathcal{D}}_\mu(\omega), \{\hat{\boldsymbol{J}}_0(\boldsymbol{r},\omega'^*)\}^\dagger\right] = \boldsymbol{0}. \tag{2.42}$$

We can verify the validity of this relation from the fact that the fundamental commutation relations, Eqs. (2.10), (2.41), and (2.42), provides those of excitons and electric field with reasonable representation as will seen in Secs. 2.6 and 2.7.

Motion equation (2.37) of excitons is rewritten with its Hermite conjugate as

$$\underline{\mathbf{S}}_\mu(\omega)\begin{bmatrix}\hat{b}_\mu(\omega)\\ \{\hat{b}_\mu(-\omega^*)\}^\dagger\end{bmatrix} = \int \mathrm{d}\boldsymbol{r}\begin{bmatrix}\boldsymbol{\mathcal{P}}_\mu^*(\boldsymbol{r})\\ \boldsymbol{\mathcal{P}}_\mu(\boldsymbol{r})\end{bmatrix}\cdot\hat{\boldsymbol{E}}^+(\boldsymbol{r},\omega) + \begin{bmatrix}1\\1\end{bmatrix}\hat{\mathcal{D}}_\mu(\omega), \tag{2.43}$$

where the coefficient matrix is defined as

$$\underline{\mathbf{S}}_\mu(\omega) = \begin{bmatrix}\hbar\omega_\mu-\hbar\omega-\mathrm{i}\varGamma_\mu(\omega)/2 & -\mathrm{i}\varGamma_\mu(\omega)/2\\ -\mathrm{i}\varGamma_\mu(\omega)/2 & \hbar\omega_\mu+\hbar\omega-\mathrm{i}\varGamma_\mu(\omega)/2\end{bmatrix}. \tag{2.44}$$

By introducing the inverse matrix $\underline{\mathbf{W}}_\mu(\omega) \equiv [\underline{\mathbf{S}}_\mu(\omega)]^{-1}$, Eq. (2.43) becomes

$$\begin{bmatrix}\hat{b}_\mu(\omega)\\ \{\hat{b}_\mu(-\omega^*)\}^\dagger\end{bmatrix} = \underline{\mathbf{W}}_\mu(\omega)\int \mathrm{d}\boldsymbol{r}\ \begin{bmatrix}\boldsymbol{\mathcal{P}}_\mu^*(\boldsymbol{r})\\ \boldsymbol{\mathcal{P}}_\mu(\boldsymbol{r})\end{bmatrix}\cdot\hat{\boldsymbol{E}}^+(\boldsymbol{r},\omega) + \underline{\mathbf{W}}_\mu(\omega)\begin{bmatrix}1\\1\end{bmatrix}\hat{\mathcal{D}}_\mu(\omega). \tag{2.45}$$

Here, it is worth to note that $\underline{\mathbf{W}}_\mu(\omega)$ can be interpreted as the retarded correlation function of excitons in H_{ex} system:

$$-\underline{W}_\mu^{11}(\omega) = \frac{1}{\mathrm{i}\hbar}\int_{t'}^\infty \mathrm{d}t\ \mathrm{e}^{\mathrm{i}\omega(t-t')}\left\langle[\underline{b}_\mu(t), \underline{b}_\mu^\dagger(t')]\right\rangle, \tag{2.46a}$$

$$-\underline{W}_\mu^{12}(\omega) = \frac{1}{\mathrm{i}\hbar}\int_{t'}^\infty \mathrm{d}t\ \mathrm{e}^{\mathrm{i}\omega(t-t')}\left\langle\left[\underline{b}_\mu(t), \underline{b}_\mu(t')\right]\right\rangle, \tag{2.46b}$$

where the exciton operators in the interaction representation is defined as

$$\underline{b}_\mu(t) \equiv \mathrm{e}^{\mathrm{i}H_{\mathrm{ex}}t/\hbar}\ b_\mu\ \mathrm{e}^{-\mathrm{i}H_{\mathrm{ex}}t/\hbar}, \tag{2.47a}$$

$$\underline{b}_\mu^\dagger(t) \equiv \mathrm{e}^{\mathrm{i}H_{\mathrm{ex}}t/\hbar}\ b_\mu^\dagger\ \mathrm{e}^{-\mathrm{i}H_{\mathrm{ex}}t/\hbar}. \tag{2.47b}$$

This is because, as seen in Eq. (2.37), the interaction Hamiltonian $H_{\rm int}$ [Eq. (2.2)] can be approximated under the linear optical process with weak excitation as

$$H_{\rm int} \simeq -\int {\rm d}\boldsymbol{r}\ \boldsymbol{P}_{\rm ex}(\boldsymbol{r})\cdot\boldsymbol{E}(\boldsymbol{r}) = \sum_{\mu}\int {\rm d}\boldsymbol{r}\left[\boldsymbol{\mathcal{P}}_{\mu}(\boldsymbol{r})\ b_{\mu} + \boldsymbol{\mathcal{P}}^{*}_{\mu}(\boldsymbol{r})\ b^{\dagger}_{\mu}\right]\cdot\boldsymbol{E}(\boldsymbol{r}), \tag{2.48}$$

and then, according to the linear response theory, $\underline{\mathsf{W}}_{\mu}(\omega)$ is interpreted as the correlation function from Eq. (2.45).

On the other hand, the ω-representation of the polarization density [Eq. (2.21)] is written as

$$\hat{\boldsymbol{P}}^{+}_{\rm ex}(\boldsymbol{r},\omega) = \sum_{\mu}\left[\boldsymbol{\mathcal{P}}_{\mu}(\boldsymbol{r})\hat{b}_{\mu}(\omega) + \boldsymbol{\mathcal{P}}^{*}_{\mu}(\boldsymbol{r})\{\hat{b}_{\mu}(-\omega^{*})\}^{\dagger}\right], \tag{2.49}$$

$$= \varepsilon_0\int {\rm d}\boldsymbol{r}'\ \boldsymbol{\chi}_{\rm ex}(\boldsymbol{r},\boldsymbol{r}',\omega)\cdot\hat{\boldsymbol{E}}^{+}(\boldsymbol{r},\omega) + \sum_{\mu}\begin{bmatrix}\boldsymbol{\mathcal{P}}_{\mu}(\boldsymbol{r})\\ \boldsymbol{\mathcal{P}}^{*}_{\mu}(\boldsymbol{r})\end{bmatrix}^{\rm t}\underline{\mathsf{W}}_{\mu}(\omega)\begin{bmatrix}1\\1\end{bmatrix}\hat{\mathcal{D}}_{\mu}(\omega), \tag{2.50}$$

where the dyadic susceptibility has a nonlocal form as

$$\boldsymbol{\chi}_{\rm ex}(\boldsymbol{r},\boldsymbol{r}',\omega) = \frac{1}{\varepsilon_0}\sum_{\mu}\begin{bmatrix}\boldsymbol{\mathcal{P}}_{\mu}(\boldsymbol{r})\\ \boldsymbol{\mathcal{P}}^{*}_{\mu}(\boldsymbol{r})\end{bmatrix}^{\rm t}\underline{\mathsf{W}}_{\mu}(\omega)\begin{bmatrix}\boldsymbol{\mathcal{P}}^{*}_{\mu}(\boldsymbol{r}')\\ \boldsymbol{\mathcal{P}}_{\mu}(\boldsymbol{r}')\end{bmatrix}. \tag{2.51}$$

Since this function can be directly derived from the motion equation (2.23) of excitons and that (2.30) of reserver oscillators with maintaining the causality, $\boldsymbol{\chi}_{\rm ex}(\boldsymbol{r},\boldsymbol{r}',\omega)$ satisfies the Kramers-Kronig relations and has no pole in the upper half of the ω-plane. Further, it also satisfies

$$\boldsymbol{\chi}_{\rm ex}(\boldsymbol{r},\boldsymbol{r}',\omega) = \{\boldsymbol{\chi}_{\rm ex}(\boldsymbol{r},\boldsymbol{r}',-\omega^{*})\}^{*}, \tag{2.52}$$

but does not have the reciprocity relation $\boldsymbol{\chi}_{\rm ex}(\boldsymbol{r},\boldsymbol{r}',\omega) \neq \{\boldsymbol{\chi}_{\rm ex}(\boldsymbol{r}',\boldsymbol{r},\omega)\}^{\rm t}$ because of the anisotropy of excitons in general. The spatial spreading of the exciton center-of-mass motion, the origin of the nonlocality, is reflected through the polarization coefficient $\boldsymbol{\mathcal{P}}_{\mu}(\boldsymbol{r})$ or the center-of-mass wave function $G_{\mu}(\boldsymbol{r})$. On the other hand, the spatial structure of the background dielectrics is characterized by the dielectric function $\varepsilon_{\rm bg}(\boldsymbol{r},\omega)$ in the Maxwell wave equation [Eq. (2.8)] and in commutation relation (2.10). Through these position-dependent functions, the present theoretical framework can be applied to arbitrary-structured exciton motions and background dielectrics.

2.5 Maxwell wave equation with nonlocal susceptibility

In order to discuss the optical processes of excitons, we must simultaneously solve the Maxwell wave equation [Eq. (2.8)] and the motion equation of the excitonic polarization [Eq. (2.50)] for describing the unknown physical operators $\hat{\boldsymbol{E}}^{+}(\boldsymbol{r},\omega)$ and $\hat{\boldsymbol{P}}^{+}_{\rm ex}(\boldsymbol{r},\omega)$ in terms of the fluctuation operators $\hat{\boldsymbol{J}}_0(\boldsymbol{r},\omega)$ and $\hat{\mathcal{D}}_{\mu}(\omega)$, whose commutation relations are already known. Substituting Eq. (2.50) into Eq. (2.8), a wave equation with the nonlocal susceptibility is obtained as

$$\boldsymbol{\nabla}\times\boldsymbol{\nabla}\times\hat{\boldsymbol{E}}^{+}(\boldsymbol{r},\omega) - \frac{\omega^2}{c^2}\varepsilon_{\rm bg}(\boldsymbol{r},\omega)\hat{\boldsymbol{E}}^{+}(\boldsymbol{r},\omega) - \frac{\omega^2}{c^2}\int {\rm d}\boldsymbol{r}'\ \boldsymbol{\chi}_{\rm ex}(\boldsymbol{r},\boldsymbol{r}',\omega)\cdot\hat{\boldsymbol{E}}^{+}(\boldsymbol{r}',\omega) = {\rm i}\mu_0\omega\hat{\boldsymbol{J}}'_0(\boldsymbol{r},\omega), \tag{2.53}$$

where the new noise operator $\hat{\boldsymbol{J}}'_0(\boldsymbol{r},\omega)$ consists of $\hat{\boldsymbol{J}}_0(\boldsymbol{r},\omega)$ and the second term of Eq. (2.50) as

$$\hat{\boldsymbol{J}}'_0(\boldsymbol{r},\omega) = \hat{\boldsymbol{J}}_0(\boldsymbol{r},\omega) - {\rm i}\omega\sum_{\mu}\begin{bmatrix}\boldsymbol{\mathcal{P}}_{\mu}(\boldsymbol{r})\\ \boldsymbol{\mathcal{P}}^{*}_{\mu}(\boldsymbol{r})\end{bmatrix}^{\rm t}\underline{\mathsf{W}}_{\mu}(\omega)\begin{bmatrix}1\\1\end{bmatrix}\hat{\mathcal{D}}_{\mu}(\omega). \tag{2.54}$$

From Eqs. (2.9), (2.39), and (2.40), this operator also satisfies

$$\hat{\boldsymbol{J}}'_0(\boldsymbol{r},\omega) = \{\hat{\boldsymbol{J}}'_0(\boldsymbol{r},-\omega^{*})\}^{\dagger}. \tag{2.55}$$

From commutation relations (2.10), (2.41), and (2.42), that of $\hat{\boldsymbol{J}}'_0(\boldsymbol{r},\omega)$ is obtained [derivation is shown in App. E of Ref. 78] as

$$\left[\hat{\boldsymbol{J}}'_0(\boldsymbol{r},\omega),\{\hat{\boldsymbol{J}}'_0(\boldsymbol{r}',\omega'^*)\}^\dagger\right] = \delta(\omega-\omega')\frac{\varepsilon_0\hbar\omega^2}{\mathrm{i}2\pi}\left[\boldsymbol{\varepsilon}(\boldsymbol{r},\boldsymbol{r}',\omega)-\boldsymbol{\varepsilon}^{*\mathrm{t}}(\boldsymbol{r}',\boldsymbol{r},\omega)\right], \tag{2.56}$$

where $\boldsymbol{\varepsilon}(\boldsymbol{r},\boldsymbol{r}',\omega)$ is the dyadic dielectric function defined as

$$\boldsymbol{\varepsilon}(\boldsymbol{r},\boldsymbol{r}',\omega) = \delta(\boldsymbol{r}-\boldsymbol{r}')\varepsilon_{\mathrm{bg}}(\boldsymbol{r},\omega)\mathbf{1} + \boldsymbol{\chi}_{\mathrm{ex}}(\boldsymbol{r},\boldsymbol{r}',\omega). \tag{2.57}$$

Wave equation (2.53) and commutation relation (2.56) are just the ones discussed by Savasta et al. [24, 25], and they also have the same forms as those of Raabe et al. [28]. Further, Eq. (2.56) can be understood as a natural result from the fluctuation dissipation theorem as discussed in Refs. 24, 25, and 28 (or see Sec. 1.3.2). Along the lines of those works, the problem reduces to finding the dyadic Green's function $\mathsf{G}(\boldsymbol{r},\boldsymbol{r}',\omega)$ satisfying

$$\boldsymbol{\nabla}\times\boldsymbol{\nabla}\times\mathsf{G}(\boldsymbol{r},\boldsymbol{r}',\omega) - \frac{\omega^2}{c^2}\varepsilon_{\mathrm{bg}}(\boldsymbol{r},\omega)\mathsf{G}(\boldsymbol{r},\boldsymbol{r}',\omega) - \frac{\omega^2}{c^2}\int \mathrm{d}\boldsymbol{r}''\ \boldsymbol{\chi}_{\mathrm{ex}}(\boldsymbol{r},\boldsymbol{r}'',\omega)\cdot\mathsf{G}(\boldsymbol{r}'',\boldsymbol{r}',\omega) = \delta(\boldsymbol{r}-\boldsymbol{r}')\mathbf{1}. \tag{2.58}$$

This function renormalizes the linear optical process of excitons with the nonlocality, and enables us to rewrite Eq. (2.53) as

$$\hat{\boldsymbol{E}}^+(\boldsymbol{r},\omega) = \mathrm{i}\mu_0\omega\int \mathrm{d}\boldsymbol{r}'\ \mathsf{G}(\boldsymbol{r},\boldsymbol{r}',\omega)\cdot\hat{\boldsymbol{J}}'_0(\boldsymbol{r}',\omega). \tag{2.59}$$

However, it seems very difficult to solve this nonlocal equation in practical problems. However, this difficulty becomes avoidable by using the fact that the nonlocal susceptibility [Eq. (2.51)] is represented as a summation of separable functions with respect to $\boldsymbol{r}$ and $\boldsymbol{r}'$. One scheme is to directly derive $\mathsf{G}(\boldsymbol{r},\boldsymbol{r}',\omega)$ as discussed in Ref. 81 (or see App. C), and the other is to reduce this integro-differential equation into a simultaneous linear equation set along the lines of the microscopic nonlocal theory [31] (or see Sec. 1.4.3). The present QED theory adopts the latter scheme because it provides not only the dyadic Green's function of the former but also the retarded correlation function of excitons in inhomogeneous exciton-photon systems as discussed in the following sections.

2.6 Simultaneous linear equation set for exciton operators

Instead of solving the integro-differential equation [Eq. (2.58)], I reduce the problem into a linear equation set by using the same technique as the microscopic nonlocal theory developed in the semiclassical framework [31]. Substituting Eq. (2.11), the electric field represented with Green's function $\mathsf{G}_0(\boldsymbol{r},\boldsymbol{r}',\omega)$, into Eq. (2.37), the motion equation of excitons, with expanding $\hat{\boldsymbol{P}}^+_{\mathrm{ex}}(\boldsymbol{r},\omega)$ as Eq. (2.49), a linear equation for exciton operators $\{\hat{b}_\mu(\omega),\{\hat{b}_\mu(-\omega^*)\}^\dagger\}$ is obtained as

$$\sum_{\mu'}\left[S^{11}_{\mu,\mu'}(\omega)\hat{b}_{\mu'}(\omega) + S^{12}_{\mu,\mu'}(\omega)\{\hat{b}_{\mu'}(-\omega^*)\}^\dagger\right] = \int \mathrm{d}\boldsymbol{r}\ \boldsymbol{\mathcal{P}}^*_\mu(\boldsymbol{r})\cdot\hat{\boldsymbol{E}}^+_0(\boldsymbol{r},\omega) + \hat{\mathcal{D}}_\mu(\omega), \tag{2.60}$$

where the coefficients are defined as

$$S^{11}_{\mu,\mu'}(\omega) \equiv \left[\hbar\omega_\mu - \hbar\omega - \mathrm{i}\Gamma_\mu(\omega)/2\right]\delta_{\mu,\mu'} + \Sigma_{\mu,\mu'}(\omega), \tag{2.61a}$$

$$S^{12}_{\mu,\mu'}(\omega) \equiv \left[-\mathrm{i}\Gamma_\mu(\omega)/2\right]\delta_{\mu,\mu'} + \Sigma'_{\mu,\mu'}(\omega). \tag{2.61b}$$

The first term on the RHS of Eq. (2.60) can be interpreted as the exciton amplitude directly induced by the background electric field. Here, the word "directly" means that this term does not include the

diffusion of the exciton amplitude via the electromagnetic fields. Instead, such an effect is reflected through the correction terms appearing in Eqs. (2.61):

$$\Sigma_{\mu,\mu'}(\omega) = -\mu_0\omega^2 \int \mathrm{d}\boldsymbol{r} \int \mathrm{d}\boldsymbol{r}'\ \boldsymbol{\mathcal{P}}^*_{\mu}(\boldsymbol{r}) \cdot \mathbf{G}_0(\boldsymbol{r},\boldsymbol{r}',\omega) \cdot \boldsymbol{\mathcal{P}}_{\mu'}(\boldsymbol{r}'), \tag{2.62a}$$

$$\Sigma'_{\mu,\mu'}(\omega) = -\mu_0\omega^2 \int \mathrm{d}\boldsymbol{r} \int \mathrm{d}\boldsymbol{r}'\ \boldsymbol{\mathcal{P}}^*_{\mu}(\boldsymbol{r}) \cdot \mathbf{G}_0(\boldsymbol{r},\boldsymbol{r}',\omega) \cdot \boldsymbol{\mathcal{P}}^*_{\mu'}(\boldsymbol{r}'). \tag{2.62b}$$

These can be interpreted as that the polarization at $\boldsymbol{r}'$ induces an electric field, and then it induces another polarization at $\boldsymbol{r}$ later. The interaction between the transverse fields is the retarded interaction, and the one between the longitudinal fields is interpreted as the Coulomb interaction between induced charges. The latter is just the exchange interaction between electrons and holes, which is displaced from H_{mat} to H_{int}, and gives the LT splitting as a correction to exciton eigenenergies.

From Eq. (2.60) and its Hermite conjugate, a simultaneous linear equation set for $\{\hat{b}_\mu(\omega), \{\hat{b}_\mu(-\omega^*)\}^\dagger\}$ is obtained as

$$\sum_{\mu'} \begin{bmatrix} S^{11}_{\mu,\mu'}(\omega) & S^{12}_{\mu,\mu'}(\omega) \\ S^{12*}_{\mu,\mu'}(-\omega) & S^{11*}_{\mu,\mu'}(-\omega) \end{bmatrix} \begin{bmatrix} \hat{b}_{\mu'}(\omega) \\ \{\hat{b}_{\mu'}(-\omega^*)\}^\dagger \end{bmatrix} = \int \mathrm{d}\boldsymbol{r} \begin{bmatrix} \boldsymbol{\mathcal{P}}^*_{\mu}(\boldsymbol{r}) \\ \boldsymbol{\mathcal{P}}_{\mu}(\boldsymbol{r}) \end{bmatrix} \cdot \hat{\boldsymbol{E}}^+_0(\boldsymbol{r},\omega) + \begin{bmatrix} 1 \\ 1 \end{bmatrix} \hat{\mathcal{D}}_\mu(\omega). \tag{2.63}$$

This equation has the same form as Eq. (1.66) in the semiclassical microscopic nonlocal theory, except for the fluctuation operator $\hat{\mathcal{D}}_\mu(\omega)$ on the RHS of Eq. (2.63). Further, the background field $\hat{\boldsymbol{E}}^+_0(\boldsymbol{r},\omega)$ satisfies commutation relation (2.19), and then we can discuss the vacuum fluctuation of electromagnetic fields. By calculating the inverse of the coefficient matrix as $\mathbf{W}(\omega) = [\mathbf{S}(\omega)]^{-1}$, Eq. (2.63) is rewritten as

$$\begin{bmatrix} \hat{b}_\mu(\omega) \\ \{\hat{b}_\mu(-\omega^*)\}^\dagger \end{bmatrix} = \sum_{\mu'} \begin{bmatrix} W^{11}_{\mu,\mu'}(\omega) & W^{12}_{\mu,\mu'}(\omega) \\ W^{12*}_{\mu,\mu'}(-\omega) & W^{11*}_{\mu,\mu'}(-\omega) \end{bmatrix} \left\{ \int \mathrm{d}\boldsymbol{r} \begin{bmatrix} \boldsymbol{\mathcal{P}}^*_{\mu'}(\boldsymbol{r}) \\ \boldsymbol{\mathcal{P}}_{\mu'}(\boldsymbol{r}) \end{bmatrix} \cdot \hat{\boldsymbol{E}}^+_0(\boldsymbol{r},\omega) + \begin{bmatrix} 1 \\ 1 \end{bmatrix} \hat{\mathcal{D}}_{\mu'}(\omega) \right\}, \tag{2.64}$$

where I consider that the inverse matrix should have the same symmetry as the original one. In the same manner as the exciton correlation function in H_{ex} system appearing in Eq. (2.45), $\mathbf{W}(\omega)$ is interpreted as the Fourier transform of the retarded correlation functions of excitons in the whole system:

$$-W^{11}_{\mu,\mu'}(\omega) = \frac{1}{\mathrm{i}\hbar} \int_{t'}^{\infty} \mathrm{d}t\ \mathrm{e}^{\mathrm{i}\omega(t-t')} \left\langle [b_\mu(t), b^\dagger_{\mu'}(t')] \right\rangle, \tag{2.65a}$$

$$-W^{12}_{\mu,\mu'}(\omega) = \frac{1}{\mathrm{i}\hbar} \int_{t'}^{\infty} \mathrm{d}t\ \mathrm{e}^{\mathrm{i}\omega(t-t')} \left\langle [b_\mu(t), b_{\mu'}(t')] \right\rangle. \tag{2.65b}$$

Therefore, from the calculation scheme of the microscopic nonlocal theory [31], the exciton retarded correlation functions renormalizing the exciton-photon interaction can be obtained by the matrix inversion. On the other hand, in App. E of Ref. 78, the commutation relations of excitons were calculated from those of $\hat{\boldsymbol{E}}^\pm_0(\boldsymbol{r},\omega)$ and $\hat{\mathcal{D}}_\mu(\omega)$ [Eqs. (2.19), (2.41), and (2.42)]. As the result, they are represented by the elements of $\mathbf{W}(\omega)$ as

$$\left[\hat{b}_\mu(\omega), \{\hat{b}_{\mu'}(\omega'^*)\}^\dagger\right] = \delta(\omega-\omega') \frac{\hbar}{\mathrm{i}2\pi} \left[W^{11}_{\mu,\mu'}(\omega) - W^{11*}_{\mu',\mu}(\omega)\right], \tag{2.66a}$$

$$\left[\hat{b}_\mu(\omega), \hat{b}_{\mu'}(-\omega')\right] = \delta(\omega-\omega') \frac{\hbar}{\mathrm{i}2\pi} \left[W^{12}_{\mu,\mu'}(\omega) - W^{12}_{\mu',\mu}(-\omega)\right]. \tag{2.66b}$$

These are reasonable results that can be derived from Eq. (2.65).

2.7 Green's function for nonlocal wave equation

Since the exciton operators are represented in terms of fluctuation operators as seen in Eq. (2.64), the other physical variables can also be described in terms of them and $\hat{\boldsymbol{E}}^\pm_0(\boldsymbol{r},\omega)$ in the present theory. For

example, the excitonic polarization is written as Eq. (2.49), and the electric field [Eq. (2.11)] as

$$\hat{\boldsymbol{E}}^{+}(\boldsymbol{r},\omega)=\hat{\boldsymbol{E}}_{0}^{+}(\boldsymbol{r},\omega)+\sum_{\mu}[\boldsymbol{\mathcal{E}}_{\mu}(\boldsymbol{r},\omega)\hat{b}_{\mu}(\omega)-\boldsymbol{\mathcal{E}}_{\mu}^{*}(\boldsymbol{r},-\omega)\{\hat{b}_{\mu}(-\omega^{*})\}^{\dagger}], \tag{2.67}$$

where the coefficients are defined as

$$\boldsymbol{\mathcal{E}}_{\mu}(\boldsymbol{r},\omega)\equiv\mu_{0}\omega^{2}\int \mathrm{d}\boldsymbol{r}'\ \mathsf{G}_{0}(\boldsymbol{r},\boldsymbol{r}',\omega)\cdot\boldsymbol{\mathcal{P}}_{\mu}(\boldsymbol{r}'), \tag{2.68a}$$

$$\boldsymbol{\mathcal{F}}_{\mu}(\boldsymbol{r},\omega)\equiv\mu_{0}\omega^{2}\int \mathrm{d}\boldsymbol{r}'\ \mathsf{G}_{0}(\boldsymbol{r},\boldsymbol{r}',\omega)\cdot\boldsymbol{\mathcal{P}}_{\mu}^{*}(\boldsymbol{r}'), \tag{2.68b}$$

and, from Eq. (2.15), they have the relation as

$$\boldsymbol{\mathcal{E}}_{\mu}(\boldsymbol{r},\omega)=\boldsymbol{\mathcal{F}}_{\mu}^{*}(\boldsymbol{r},-\omega)=\{\boldsymbol{\mathcal{F}}_{\mu}(\boldsymbol{r},-\omega^{*})\}^{*}. \tag{2.69}$$

Here, from Eq. (2.67), the commutation relation of the electric field operator is obtained (derivation is shown in App. E of Ref. 78) as

$$\left[\hat{\boldsymbol{E}}^{+}(\boldsymbol{r},\omega),\hat{\boldsymbol{E}}^{-}(\boldsymbol{r}',\omega')\right]=\left[\hat{\boldsymbol{E}}^{+}(\boldsymbol{r},\omega),\hat{\boldsymbol{E}}^{+}(\boldsymbol{r}',-\omega')\right]=\delta(\omega-\omega')\frac{\mu_{0}\hbar\omega^{2}}{\mathrm{i}2\pi}\left[\mathsf{G}(\boldsymbol{r},\boldsymbol{r}',\omega)-\mathsf{G}^{*\mathrm{t}}(\boldsymbol{r}',\boldsymbol{r},\omega)\right], \tag{2.70}$$

where the dyadic function $\mathsf{G}(\boldsymbol{r},\boldsymbol{r}',\omega)$ is defined as

$$\begin{aligned}\mathsf{G}(\boldsymbol{r},\boldsymbol{r}',\omega)=\mathsf{G}_{0}(\boldsymbol{r},\boldsymbol{r}',\omega)+\frac{1}{\mu_{0}\omega^{2}}\sum_{\mu,\mu'}\big\{&\boldsymbol{\mathcal{E}}_{\mu}(\boldsymbol{r},\omega)W_{\mu,\mu'}^{11}(\omega)\boldsymbol{\mathcal{F}}_{\mu'}(\boldsymbol{r}',\omega)+\boldsymbol{\mathcal{E}}_{\mu}(\boldsymbol{r},\omega)W_{\mu,\mu'}^{12}(\omega)\boldsymbol{\mathcal{E}}_{\mu'}(\boldsymbol{r}',\omega)\\&+\boldsymbol{\mathcal{E}}_{\mu}^{*}(\boldsymbol{r},-\omega)W_{\mu,\mu'}^{11*}(-\omega)\boldsymbol{\mathcal{F}}_{\mu'}^{*}(\boldsymbol{r}',-\omega)+\boldsymbol{\mathcal{E}}_{\mu}^{*}(\boldsymbol{r},-\omega)W_{\mu,\mu'}^{12*}(-\omega)\boldsymbol{\mathcal{E}}_{\mu'}^{*}(\boldsymbol{r}',-\omega)\big\}.\end{aligned} \tag{2.71}$$

In the same manner as the discussion in Sec. 1.3.2, this function corresponds to the Fourier transform of the retarded correlation function of the electric field in the whole system as

$$-\mu_{0}\omega^{2}\mathsf{G}(\boldsymbol{r},\boldsymbol{r}',\omega)=\frac{1}{\mathrm{i}\hbar}\int_{t'}^{\infty}\mathrm{d}t\ \mathrm{e}^{\mathrm{i}\omega(t-t')}\left\langle[\boldsymbol{E}(\boldsymbol{r},t),\boldsymbol{E}(\boldsymbol{r}',t')]\right\rangle. \tag{2.72}$$

Actually, as verified in App. F of Ref. 78, $\mathsf{G}(\boldsymbol{r},\boldsymbol{r}',\omega)$ satisfies Eq. (2.58), the wave equation with nonlocal susceptibility. On the other hand, this function satisfies

$$\mathsf{G}(\boldsymbol{r},\boldsymbol{r}',\omega)=\{\mathsf{G}(\boldsymbol{r},\boldsymbol{r}',-\omega^{*})\}^{*}=\mathsf{G}^{*}(\boldsymbol{r},\boldsymbol{r}',-\omega), \tag{2.73}$$

but does not satisfy the reciprocity relation $\mathsf{G}(\boldsymbol{r},\boldsymbol{r}',\omega)\neq\{\mathsf{G}(\boldsymbol{r}',\boldsymbol{r},\omega)\}^{\mathrm{t}}$ because of the anisotropic susceptibility tensor (2.51) of the excitonic polarization. In this way, the dyadic Green's function satisfying Eq. (2.58), the nonlocal wave equation, is obtained for arbitrary-structured 3D systems in the present theory.

2.8 Under rotating-wave approximation

In the semiclassical framework, the microscopic nonlocal theory has mostly been discussed under the rotating wave approximation (RWA) for its practical applications. The RWA is valid for most of the excitonic systems, and also the self-consistent equation set [Eq. (2.63)] becomes simple under the RWA. In this section, I show the validity and usefulness of the RWA in the present QED theory.

The RWA means that nonresonant terms proportional to $(\omega+\omega_{\mu})^{-1}$ are negligible as compared to resonant terms $(\omega-\omega_{\mu})^{-1}$. In discussing the resonant optical processes of elementary excitations in

condensed matter and also in atoms and molecules, the RWA is usually considered to be a valid approximation, because the width of the energy range of interest is usually sufficiently small as compared to the eigenenergies of the elementary excitations. In particular, in the case of excitons, the width is of the order of LT splitting, center-of-mass kinetic energy, or radiative and nonradiative relaxation widths, which are usually more than three orders of magnitude smaller than the excitons' eigenenergies. Since the nonlocality becomes essential only under resonance conditions, the RWA does not impose any significant restriction on the present theory for discussing nonlocal systems. In the following paragraphs, the RWA will be applied to the excitons' motion, and simplified equations and commutation relations will be derived.

Under the RWA, i.e., $\omega \sim \omega_\mu$, the excitons' motion equation, Eq. (2.37), can be approximated as

$$[\hbar\omega_\mu - \hbar\omega - \mathrm{i}\Gamma_\mu(\omega)/2]\,\hat{b}_\mu(\omega) = \int \mathrm{d}\boldsymbol{r}\ \boldsymbol{\mathcal{P}}_\mu^*(\boldsymbol{r}) \cdot \hat{\boldsymbol{E}}^+(\boldsymbol{r},\omega) + \hat{\mathcal{D}}_\mu(\omega), \tag{2.74}$$

because the contribution from $\{\hat{b}_\mu(-\omega^*)\}^\dagger = \hat{b}_\mu^\dagger(\omega)$ is negligible as compared to that of $\hat{b}_\mu(\omega)$. For the same reason, the excitonic polarization [Eq. (2.49)] is also rewritten as

$$\hat{\boldsymbol{P}}_{\mathrm{ex}}^+(\boldsymbol{r},\omega) = \sum_\mu \boldsymbol{\mathcal{P}}_\mu(\boldsymbol{r})\hat{b}_\mu(\omega). \tag{2.75}$$

Substituting Eq. (2.74) into this equation, the excitonic polarization is written, instead of Eq. (2.50), as

$$\hat{\boldsymbol{P}}_{\mathrm{ex}}^+(\boldsymbol{r},\omega) = \varepsilon_0 \int \mathrm{d}\boldsymbol{r}'\ \widetilde{\boldsymbol{\chi}}_{\mathrm{ex}}(\boldsymbol{r},\boldsymbol{r}',\omega) \cdot \hat{\boldsymbol{E}}^+(\boldsymbol{r},\omega) + \sum_\mu \frac{\boldsymbol{\mathcal{P}}_\mu(\boldsymbol{r})\hat{\mathcal{D}}_\mu(\omega)}{\hbar\omega_\mu - \hbar\omega - \mathrm{i}\Gamma_\mu(\omega)/2}, \tag{2.76}$$

where the susceptibility tensor, Eq. (2.51), is simplified as

$$\widetilde{\boldsymbol{\chi}}_{\mathrm{ex}}(\boldsymbol{r},\boldsymbol{r}',\omega) = \frac{1}{\varepsilon_0}\sum_\mu \frac{\boldsymbol{\mathcal{P}}_\mu(\boldsymbol{r})\boldsymbol{\mathcal{P}}_\mu^*(\boldsymbol{r}')}{\hbar\omega_\mu - \hbar\omega - \mathrm{i}\Gamma_\mu(\omega)/2}. \tag{2.77}$$

This function also satisfies the Kramers-Kronig relation and has no pole in the upper of the complex ω-plane, because it is also derived from Eqs. (2.23) and (2.30), the motion equations of excitons and of reservoir oscillators under the RWA. However, while the susceptibility (2.51) satisfies Eq. (2.52) without the RWA, Eq. (2.77) obeys $\widetilde{\boldsymbol{\chi}}_{\mathrm{ex}}(\boldsymbol{r},\boldsymbol{r}',\omega) \neq \{\widetilde{\boldsymbol{\chi}}_{\mathrm{ex}}(\boldsymbol{r},\boldsymbol{r}'-\omega^*)\}^*$ because the focusing frequency is only under $\omega \sim \omega_\mu$.

Substituting Eq. (2.76) into the Maxwell wave equation [Eq. (2.8)], a new wave equation is obtained, instead of Eq. (2.53), as

$$\boldsymbol{\nabla}\times\boldsymbol{\nabla}\times\hat{\boldsymbol{E}}^+(\boldsymbol{r},\omega) - \frac{\omega^2}{c^2}\varepsilon_{\mathrm{bg}}(\boldsymbol{r},\omega)\hat{\boldsymbol{E}}^+(\boldsymbol{r},\omega) - \frac{\omega^2}{c^2}\int \mathrm{d}\boldsymbol{r}'\ \widetilde{\boldsymbol{\chi}}_{\mathrm{ex}}(\boldsymbol{r},\boldsymbol{r}',\omega)\cdot\hat{\boldsymbol{E}}^+(\boldsymbol{r}',\omega) = \mathrm{i}\mu_0\omega\hat{\boldsymbol{J}}_0''(\boldsymbol{r},\omega), \tag{2.78}$$

where the noise current density [Eq. (2.54)] is rewritten as

$$\hat{\boldsymbol{J}}_0''(\boldsymbol{r},\omega) = \hat{\boldsymbol{J}}_0(\boldsymbol{r},\omega) - \mathrm{i}\omega\sum_\mu \frac{\boldsymbol{\mathcal{P}}_\mu(\boldsymbol{r})\hat{\mathcal{D}}_\mu(\omega)}{\hbar\omega_\mu - \hbar\omega - \mathrm{i}\Gamma_\mu(\omega)/2}. \tag{2.79}$$

From commutation relations (2.10), (2.41), and (2.42), that of $\hat{\boldsymbol{J}}_0''(\boldsymbol{r},\omega)$ is obtained as

$$\left[\hat{\boldsymbol{J}}_0''(\boldsymbol{r},\omega), \{\hat{\boldsymbol{J}}_0''(\boldsymbol{r}',\omega'^*)\}^\dagger\right] = \delta(\omega-\omega')\frac{\varepsilon_0\hbar\omega^2}{\mathrm{i}2\pi}\left[\widetilde{\boldsymbol{\varepsilon}}(\boldsymbol{r},\boldsymbol{r}',\omega) - \widetilde{\boldsymbol{\varepsilon}}^{*\mathrm{t}}(\boldsymbol{r}',\boldsymbol{r},\omega)\right], \tag{2.80}$$

where the nonlocal dielectric tensor is represented as

$$\widetilde{\boldsymbol{\varepsilon}}(\boldsymbol{r},\boldsymbol{r}',\omega) = \delta(\boldsymbol{r}-\boldsymbol{r}')\varepsilon_{\mathrm{bg}}(\boldsymbol{r},\omega)\mathbf{1} + \widetilde{\boldsymbol{\chi}}_{\mathrm{ex}}(\boldsymbol{r},\boldsymbol{r}',\omega). \tag{2.81}$$

In this way, even under the RWA, the commutation relation has the the same form as the original one [Eq. (2.56)], which is represented by the nonlocal dielectric tensor $\boldsymbol{\varepsilon}(\boldsymbol{r},\boldsymbol{r}',\omega)$ [Eq. (2.57)].

On the other hand, substituting Eq. (2.11), the representation of the electric field, into Eq. (2.74), the approximated motion equation of excitons, with expanding $\hat{\boldsymbol{P}}^{+}_{\rm ex}(\boldsymbol{r},\omega)$ as the approximated form (2.75), a linear equation set with respect to only $\{\hat{b}_{\mu}(\omega)\}$ is obtained, instead of Eq. (2.60), as

$$\sum_{\mu'} S^{11}_{\mu,\mu'}(\omega)\hat{b}_{\mu'}(\omega) = \int {\rm d}\boldsymbol{r}\ \boldsymbol{\mathcal{P}}^{*}_{\mu}(\boldsymbol{r})\cdot\hat{\boldsymbol{E}}^{+}_{0}(\boldsymbol{r},\omega) + \hat{\mathcal{D}}_{\mu}(\omega). \tag{2.82}$$

By calculating the inverse matrix $\widetilde{\mathbf{W}}(\omega) = [\mathbf{S}^{11}(\omega)]^{-1}$, on the basis of the exciton eigenstates, the exciton operators are represented as

$$\hat{b}_{\mu}(\omega) = \sum_{\mu'}\widetilde{W}_{\mu,\mu'}(\omega)\left[\int {\rm d}\boldsymbol{r}\ \boldsymbol{\mathcal{P}}^{*}_{\mu'}(\boldsymbol{r})\cdot\hat{\boldsymbol{E}}^{+}_{0}(\boldsymbol{r},\omega) + \hat{\mathcal{D}}_{\mu'}(\omega)\right]. \tag{2.83}$$

From commutation relations (2.19), (2.41), and (2.42), those of excitons are derived under the RWA as

$$\left[\hat{b}_{\mu}(\omega),\{\hat{b}_{\mu'}(\omega'^{*})\}^{\dagger}\right] = \delta(\omega-\omega')\frac{\hbar}{{\rm i}2\pi}\left[\widetilde{W}_{\mu,\mu'}(\omega) - \widetilde{W}^{*}_{\mu',\mu}(\omega)\right], \tag{2.84a}$$

$$\left[\hat{b}_{\mu}(\omega),\hat{b}_{\mu'}(-\omega')\right] = 0. \tag{2.84b}$$

Here, from the relation $\widetilde{W}_{\mu,\mu'}(-\omega) \ll \widetilde{W}_{\mu,\mu'}(\omega)$ obtained under $\omega\sim\omega'\sim\omega_{\mu}>0$, Eq. (2.84b) can be approximated to be zero. In addition, the relations $W^{11}_{\mu,\mu'}(\omega) \gg W^{12}_{\mu,\mu'}(\omega)$ and $W^{11}_{\mu,\mu'}(\omega) \simeq \widetilde{W}_{\mu,\mu'}(\omega)$ are obtained under the RWA. Therefore, commutation relations (2.84) can be considered as approximations of Eqs. (2.66), which are derived without the RWA.

On the other hand, instead of Eq. (2.67), the electric field is written under the RWA as

$$\hat{\boldsymbol{E}}^{+}(\boldsymbol{r},\omega) = \hat{\boldsymbol{E}}^{+}_{0}(\boldsymbol{r},\omega) + \sum_{\mu}\boldsymbol{\mathcal{E}}_{\mu}(\boldsymbol{r},\omega)\hat{b}_{\mu}(\omega). \tag{2.85}$$

From commutation relations (2.19) and (2.84), those of the electric field are obtained in the same form as Eq. (2.70) as

$$\left[\hat{\boldsymbol{E}}^{+}(\boldsymbol{r},\omega),\hat{\boldsymbol{E}}^{-}(\boldsymbol{r}',\omega')\right] = \delta(\omega-\omega')\frac{\mu_0\hbar\omega^2}{{\rm i}2\pi}\left[\widetilde{\mathbf{G}}(\boldsymbol{r},\boldsymbol{r}',\omega) - \widetilde{\mathbf{G}}^{*{\rm t}}(\boldsymbol{r}',\boldsymbol{r},\omega)\right], \tag{2.86}$$

where the dyadic Green's function $\widetilde{\mathbf{G}}(\boldsymbol{r},\boldsymbol{r}',\omega)$ is represented, instead of Eq. (2.71), as

$$\widetilde{\mathbf{G}}(\boldsymbol{r},\boldsymbol{r}',\omega) = \mathbf{G}_0(\boldsymbol{r},\boldsymbol{r}',\omega) + \frac{1}{\mu_0\omega^2}\sum_{\mu,\mu'}\boldsymbol{\mathcal{E}}_{\mu}(\boldsymbol{r},\omega)\widetilde{W}_{\mu,\mu'}(\omega)\boldsymbol{\mathcal{F}}_{\mu'}(\boldsymbol{r}',\omega). \tag{2.87}$$

Since $W^{11}_{\mu,\mu'}(\omega) \gg W^{12}_{\mu,\mu'}(\omega)$ and $W^{11}_{\mu,\mu'}(\omega) \gg W^{11*}_{\mu,\mu'}(-\omega)$, $\widetilde{\mathbf{G}}(\boldsymbol{r},\boldsymbol{r}',\omega)$ can be considered as an approximation of Eq. (2.71). Further, instead of Eq. (2.58), this function also satisfies

$$\boldsymbol{\nabla}\times\boldsymbol{\nabla}\times\widetilde{\mathbf{G}}(\boldsymbol{r},\boldsymbol{r}',\omega) - \frac{\omega^2}{c^2}\varepsilon_{\rm bg}(\boldsymbol{r},\omega)\widetilde{\mathbf{G}}(\boldsymbol{r},\boldsymbol{r}',\omega) - \frac{\omega^2}{c^2}\int {\rm d}\boldsymbol{r}''\ \widetilde{\boldsymbol{\chi}}_{\rm ex}(\boldsymbol{r},\boldsymbol{r}'',\omega)\cdot\widetilde{\mathbf{G}}(\boldsymbol{r}'',\boldsymbol{r}',\omega) = \delta(\boldsymbol{r}-\boldsymbol{r}')\mathbf{1}. \tag{2.88}$$

However, Eq. (2.73) is not maintained under the RWA as $\widetilde{\mathbf{G}}(\boldsymbol{r},\boldsymbol{r}',\omega) \neq \{\widetilde{\mathbf{G}}(\boldsymbol{r},\boldsymbol{r}',-\omega^{*})\}^{*}$.

From Eqs. (2.83) and (2.88), under the RWA, $\widetilde{W}_{\mu,\mu'}(\omega)$ and $\widetilde{\mathbf{G}}(\boldsymbol{r},\boldsymbol{r}',\omega)$ can also be considered as retarded correlation functions of excitons and electric field, respectively. This can also be verified from the fact that the commutation relations of them, Eqs. (2.84) and (2.86), maintain their forms from the general ones. Furthermore, since those correlation functions functions are considered as approximations of the general ones, it is safe to say that the RWA is valid in the present QED theory, and it is useful in the practical application from the viewpoint of the simplicity of the self-consistent equation set [Eq. (2.82)] and the dyadic Green's function [Eq. (2.87)].

2.9 For practical calculations

In this section, I explicitly show a calculation scheme for practical applications of the present theory.

First, the practical materials should be described in terms of the parameters of the present theory, i.e., background dielectric function $\varepsilon_{\rm bg}(\boldsymbol{r},\omega)$, excitons' eigenfrequencies $\{\omega_\mu\}$, transition dipole moments $\{\mathcal{P}_\mu\}$, polarization direction $\{\boldsymbol{e}_\mu\}$, center-of-mass wave functions $\{G_\mu(\boldsymbol{r})\}$, and nonradiative relaxation widths $\{\Gamma_\mu\}$. Usually, $\{\omega_\mu\}$ and $\{G_\mu(\boldsymbol{r})\}$ are determined from boundary conditions for the exciton center-of-mass motion. The absolute value of $\mathcal{P}_\mu$ is determined by the LT splitting energy $\Delta_{\rm LT}^\mu = |\mathcal{P}_\mu|^2/\varepsilon_0\varepsilon_{\rm bg}$ in bulk system, and $\{\Gamma_\mu\}$ and the phase differences of $\{\mathcal{P}_\mu\}$ between different relative-motion states are treated as fitting parameters for experimental results. However, it is sufficient to consider only the lowest relative motion of excitons, when the eigenfrequencies of higher states are far from the frequency region of interest. In such a case, the phase of $\mathcal{P}_\mu$ does not appear in the calculation of observables under the RWA, and only $\{\Gamma_\mu\}$ remain as fitting parameters.

Next, the dyadic Green's function $\mathbf{G}_0(\boldsymbol{r},\boldsymbol{r}',\omega)$, which satisfies Eq. (1.59) and is uniquely determined for given $\varepsilon_{\rm bg}(\boldsymbol{r},\omega)$, should be derived. The form of $\mathbf{G}_0(\boldsymbol{r},\boldsymbol{r}',\omega)$ has already been known for various structures with high symmetry [65], and it can also be numerically calculated for arbitrary 3D structures [66]. Therefore, the integrations appearing in $\Sigma_{\mu,\mu'}(\omega)$, $\Sigma'_{\mu,\mu'}(\omega)$, $\boldsymbol{\mathcal{E}}_\mu(\boldsymbol{r},\omega)$, and $\boldsymbol{\mathcal{F}}_\mu(\boldsymbol{r},\omega)$ [Eqs. (2.62a), (2.62b), (2.68a), and (2.68b)] can be performed, and then the inverse of the coefficient matrix of the self-consistent equation set [Eq. (2.63) or Eq. (2.82) under the RWA] is numerically calculated. The dyadic Green's function $\mathbf{G}(\boldsymbol{r},\boldsymbol{r}',\omega)$ satisfying Eq. (2.58) is obtained as Eq. (2.71) [or $\widetilde{\mathbf{G}}(\boldsymbol{r},\boldsymbol{r}',\omega)$ as Eq. (2.87) under the RWA].

The size of the coefficient matrix is $2N \times 2N$ (or $N \times N$ under the RWA), where N is the number of exciton states to be considered in the calculation. The above numerical calculation has been performed for semiconductor quantum dots, films, multilayers, and so on in the semiclassical framework [31]. Furthermore, the present QED theory with the RWA has already been applied to the analysis of the entangled-photon generation from a semiconductor film with thickness of a few hundreds nanometers [46]. In this numerical calculation, 200 exciton center-of-mass motion states were considered. In this way, the present QED theory is definitely feasible for practical applications.

2.10 Discussion

In this chapter, based on the framework of QED for dispersive and absorptive media [21, 18, 63] and the calculation idea of the microscopic nonlocal theory [31], a QED theory for excitons in arbitrary-structured 3D dielectrics has been constructed with considering the nonlocal susceptibility and the nonradiative damping of excitons. This theory maintains good correspondences with both the two underlying theories. On the other hand, as mentioned in Sec. 2.1, the QED of nonlocal media has already been discussed in a few studies. From the viewpoint of practical applications, I compare the present theory with the studies of Stefano et al. [23, 24, 25] and Raabe et al. [28].

Stefano et al. have discussed the quantum-well structures of dispersive and absorptive dielectrics with the nonlocality in Ref. 23, and their theory is generalized to enable the consideration of arbitrary structures in Refs. 24 and 25. However, there still remains a problem in deriving the dyadic Green's function for the generalized wave equation, as shown in Eq. (2.58) in this thesis. On the other hand, the present

theory gives a solution to this problem by providing a definite calculation method based on a linear equation set, which is derived in the same line as the microscopic nonlocal theory [31], i.e., by using the Green's function $\mathbf{G}_0(\boldsymbol{r}, \boldsymbol{r}', \omega)$ and the fact that the nonlocal susceptibility is represented as a summation of separable functions with respect to two positions, as seen in Eq. (2.51). In the present theory, the Green's function required in Ref. 25 can be obtained as Eq. (2.71), which can be applied to arbitrary-structured excitonic polarization and background dielectrics.

On the other hand, Raabe et al. proposed the use of the dielectric approximation with the surface impedance method for the practical calculation of the dyadic Green's function for the wave equation with nonlocal susceptibility. In the dielectric approximation, the characteristic length of spatial dispersion (the spatial spreading of the excitons' center-of-mass motion) is assumed to be small as compared to the spatial length of materials, and the information outside of a focusing region is compressed to integrations of the electromagnetic fields at the interfaces. The Green's function can be derived using the surface impedance method for a given surface impedance or admittance, which includes the outside information. In contrast, the present theory provides the Green's function, without any significant approximations, for given $\varepsilon_{\rm bg}(\boldsymbol{r}, \omega)$ and microscopic information of excitons.

As mentioned in Chap. 1, there is a growing interest in the QED of elementary excitations in condensed matters. For example, theoretical studies on entangled-photon generation via biexcitons have already been performed by Savasta et al. [44, 45] (although the nonlocality was not sufficiently considered in these calculations). Further, by extending the present QED theory, the same kind of study has also been performed for the excitonic system weakly confined in nano-structures [46], which are known to exhibit anomalous nonlinear optical phenomena [32, 40, 34, 41, 37]. In addition, Scheel and Welsch have discussed the QED of nonlinear media with absorption and dispersion (but without the nonlocality) [59, 60]. When we discuss the nonlinear processes of excitons with the nonlocality, we must self-consistently treat their nonlinear motion equation and the Maxwell equations. Based on the self-consistent equation set [Eq. (2.63) or (2.82)], as discussed in this thesis, the new objective is to solve the equation set with nonlinear terms originating from nonlinear processes, as performed in Ref. 46. On the other hand, based on the Maxwell wave equation [Eq. (2.53)] with the nonlocal susceptibility as discussed in the previously discussed QED theories [23, 24, 25, 26, 27, 28], we must solve the wave equation with nonlinear and nonlocal susceptibility. Both approaches can be performed by applying some techniques such as successive approximation, and the expectation values of observables are calculated based on commutation relations (2.66) of excitons and that (2.70) of the electric field [Eqs. (2.84) and (2.86) under the RWA] that are described in terms of $W^{11}_{\mu,\mu'}(\omega)$, $W^{12}_{\mu,\mu'}(\omega)$, and $\mathbf{G}(\boldsymbol{r}, \boldsymbol{r}', \omega)$ derived in this thesis. However, such calculations are usually difficult, and then more detailed and systematic calculations should be performed by using the Feynman diagram technique with the time-ordered correlation functions, which identifies with the retarded correlation functions under the RWA and also derived by the analytic continuation from the retarded ones. In this sense, the present scheme will be a powerful tool to discuss the nonlinear processes of elementary excitations in condensed matter with the nonlocality, and also nonclassical light emitted from such processes.

Chapter 3

Crossover of Radiative Relaxation of Excitons

According to Fermi's golden rule, the radiative decay rate of excitons increases together with the crystal size because of the increment of the interaction volume between the excitons and the radiation field. This is called exciton superradiance. On the other hand, in thick film where the exciton-polariton picture is valid, the radiative decay time should be proportional to the time of flight (film thickness divided by polariton group velocity). Therefore, the radiative decay rate is inversely proportional to the film thickness in contrast to the exciton superradiance scheme. The subject of this chapter is to elucidate the crossover condition between the two radiative decay schemes based on the theoretical framework of the microscopic nonlocal theory, which continuously describes weakly confined excitons to bulk-like system and can connect the two decay schemes.

3.1 Background

In order to obtain a strong and coherent response from nonlinear optical process in condensed matter, the radiative decay of elementary excitations should generally be rapid as compared to dephasing processes at their resonance conditions. The dephasings can usually be suppressed in low dimensional systems owing to the quantization of the excitation and phonon states. Especially in quantum-dot systems, very long dephasing times of subnanosecond [82, 83] and more [84, 85] have been experimentally observed. On the other hand, there is an attempt to enhance the radiative decay due to the strong coupling between the elementally excitation and the radiation field. In particular, the exciton superradiance, a size enhancement of the radiative decay rate of excitons, has been studied theoretically and experimentally for more than 20 years [86, 87, 88, 89, 90, 91, 92, 93, 94, 95, 35, 77]. In a crystal where the exciton center-of-mass motion is confined, their radiative decay rate gets larger with increasing the crystal size because of the expansion of interaction volume between the exciton and the radiation field [86, 87, 88, 89, 90, 91, 92, 93]. The same kind of enhancement occurs with respect to the oscillator strength and nonlinearity of excitons [87, 88, 89, 96]. In the case of a semiconductor film, the radiative decay rate of the lowest exciton center-of-mass motion state gets larger with increasing thickness until about a half light wavelength at the resonance frequency, but after that it reversely decreases. The origin of this superradiance suppression is the phase mismatch between the center-of-mass motion and the radiation field [92, 93, 95]. In the same manner, the decay rate of the higher center-of-mass motion state is maximized at each phase-matching thickness, and the maximum value becomes larger with increasing thickness [94, 97, 35, 36, 77] in line with the exciton superradiance. Further, the resonance frequency of the exciton state is also shifted due to the exciton-photon interaction [94, 95, 97, 35, 36, 77], and its anomalous frequency shift has

been experimentally observed in the nondegenerate two-photon excitation scattering in a CuCl film with thickness of several tens nanometers [42]. On the other hand, in addition to the frequency shift, a rapid decay time about 100 fs has recently been observed in the degenerate four-wave mixing in a CuCl film with thickness of a few hundred nanometers [43], and it is considered as a radiative decay enhanced by the exciton superradiance. Although it is usually considered that the size enhancement of the radiative decay rate is suppressed due to the dephasing processes of excitons, its suppression picture is broken if the radiative decay rate is enhanced beyond any dephasing processes in a single crystal with little impurities and defects as the samples used in Ref. 43. Therefore, there should be another mechanism to suppress the exciton superradiance without considering any dephasing processes.

As an answer for this question, Knoester [92] predicted and Björk et al. [94] theoretically demonstrated that the exciton superradiance is only maintained until a particular film thickness, and thereafter the radiative decay rate of the phase-matching exciton is inversely proportional to the thickness in the same manner as the radiative decay scheme of polaritons, where the decay time is proportional to the time of flight (thickness divided by group velocity) [98, 95, 99]. Further, Björk et al. also showed that the superradiance suppression can be interpreted as a crossover of the exciton-photon coupled modes from exciton-like (superradiant) and photon-like modes to the upper and lower branch polaritons. This is similar to the case of the cavity quantum electrodynamics (QED) [100]. In the weak coupling regime between an excitation and a cavity mode, the spontaneous emission rate is larger than the coupling strength, and these modes are slightly modified from the bare states and almost independent. On the other hand, in the strong coupling regime, the coupling strength is larger than the emission rate, and the energies of the coupled modes split into upper and lower sides (Rabi splitting). In the discussion of the exciton superradiance, the exciton- and photon-like modes are considered in the weak-coupling regime, and a photon created by the exciton-photon recombination can go outside of the film without the reabsorption, and then the radiative decay rate is enhanced obeying Fermi's golden rule. On the other hand, the polariton modes are in the strong coupling regime, and the photon is reabsorbed in the material because of the strong coupling. Therefore, the exciton and photon behave as a polariton, and the radiative decay rate is inversely proportional to the film thickness.

However, in the calculation by Björk et al. [94], they considered the retarded interaction (interaction via electromagnetic fields) between the same exciton states but not between the different states. Therefore, their crossover thickness may be different from the correct one, because the inter-state retarded interaction must be considered under the strong exciton-photon coupling at the crossover. On the other hand, the inter-state retarded interaction has been considered in works by Agranovich et al. [95] and by Ajiki [35]. Agranovich et al. properly considered the wavenumber uncertainty originating from the translational symmetry breaking perpendicular to the surface, and demonstrated the smooth thickness dependence of radiative decay rate after the phase-matching thickness instead of the oscillating behavior, which is a result of neglecting the inter-state retarded interaction [94, 97]. Further, the authors showed a correct expression of the radiative decay rate in the polariton scheme as seen in Eqs. (3.48) and (3.45) of the present thesis. On the other hand, Ajiki discussed the crossover in a spherical semiconductor with a size of from quantum dot to bulk limit, and showed that the radiative decay rate decreases with increasing the crystal size if the crystal becomes larger than a particular size. However, in these two studies, the crossover condition from exciton-/photon-like modes to polariton ones has not been completely clarified. The subject of this chapter is to elucidate the crossover condition by means of a rigorous calculation method connecting the two radiative decay schemes.

3.2 Calculation method

I consider a material where the translational symmetry is broken in the z direction, and discuss the radiative decay of s-polarized exciton whose center-of-mass is confined in a finite region. I suppose a background system characterized by dielectric function $\varepsilon_{\rm bg}(z,\omega)$, and a resonant contribution from excitons inducing a polarization $P(z,\omega)$. The Maxwell wave equation for the electric field $E(z,\omega)$ is represented as

$$\left[(\partial^2/\partial z^2) + q^2(z,\omega)\right] E(z,\omega) = -\mu_0\omega^2 P(z,\omega), \tag{3.1}$$

where $q^2(z,\omega) = \varepsilon_{\rm bg}(z,\omega)\omega^2/c^2 - {k_\parallel}^2$ and $k_\parallel$ is the in-plane wavenumber. This wave equation can be rewritten as

$$E(z,\omega) = E_0(z,\omega) - \mu_0\omega^2 \int {\rm d}z'\ G(z,z',\omega)\ P(z',\omega), \tag{3.2}$$

where $E_0(z,\omega)$ is the homogeneous solution of Eq. (3.1), and $G(z,z',\omega)$ is the Green's function satisfying

$$\left[(\partial^2/\partial z^2) + q^2(z,\omega)\right] G(z,z',\omega) = \delta(z-z'). \tag{3.3}$$

On the other hand, I consider the Hamiltonian of the whole system as

$$\hat{H} = \hat{H}_{\rm rad} + \hat{H}_{\rm ex} + \hat{H}_{\rm int}. \tag{3.4}$$

Here, $\hat{H}_{\rm rad}$ represents the radiation field and the background dielectric medium, and it provides the Maxwell wave equation with quantum fluctuation as discussed in the QED of dispersive and absorptive media [21, 18] (or see Sec. 1.3). On the other hand, $\hat{H}_{\rm ex}$ describes the resonant contribution from excitons, and $\hat{H}_{\rm int}$ represents the interaction between the exciton and the radiation field as

$$\hat{H}_{\rm int} = -\int {\rm d}z\ \hat{E}(z)\hat{P}(z). \tag{3.5}$$

Since the expectation value $E = \langle\hat{E}\rangle$ of the vector potential is given in the same form as Eq. (3.2) according to the linear response theory, $G(z,z',\omega)$ is interpreted as the retarded correlation function of $\hat{E}$ in $\hat{H}_{\rm rad}$ system as discussed in chap. 6 of Ref. 53:

$$\mu_0\omega^2 G(z,z',\omega) = \frac{1}{{\rm i}\hbar}\int_0^\infty {\rm d}t\ {\rm e}^{{\rm i}\omega t}\,\langle[\hat{E}_0(z,t),\hat{E}_0(z',0)]\rangle_{\rm rad}\,, \tag{3.6}$$

where the time representation of the electric field is defined as

$$\hat{E}_0(z,t) \equiv {\rm e}^{{\rm i}\hat{H}_{\rm rad}t/\hbar}\hat{E}(z){\rm e}^{-{\rm i}\hat{H}_{\rm rad}t/\hbar}. \tag{3.7}$$

Furthermore, under the rotating wave approximation (RWA), $G(z,z',\omega)$ also corresponds to the time-ordered correlation function of $\hat{A}$:

$$\mu_0\omega^2 G(z,z',\omega) \simeq \frac{1}{{\rm i}\hbar}\int_{-\infty}^\infty {\rm d}t\ {\rm e}^{{\rm i}\omega t}\,\langle{\rm T}\hat{E}_0(z,t)\hat{E}_0(z',0)\rangle_{\rm rad}\,, \tag{3.8}$$

where T is the time-ordering operator. Therefore, under the RWA, the correlation function of $\hat{E}$ in the background system can be obtained by finding the Green function satisfying Eq. (3.3), which has already been known for general multilayer systems [65].

Next, I discuss the time-ordered correlation functions of exciton. For simplicity, I consider only one relative exciton motion with eigenfrequency $\omega_{\rm T}$, and denote the center-of-mass motion by index m, its

annihilation operator by $\hat{b}_m$, and its eigenfrequency by Ω_m, which includes the center-of-mass kinetic energy. In this chapter, I simply consider that the exciton is a pure boson, and the system is linear as

$$\hat{H}_{\rm ex} = \sum_m \hbar\Omega_m \hat{b}_m^\dagger \hat{b}_m. \tag{3.9}$$

In this situation, the exciton correlation function in $\hat{H}_{\rm ex}$ system is derived as

$$\mathfrak{G}^{(0)}_{m,m'}(\omega) = -\mathrm{i}\int_{-\infty}^{\infty} \mathrm{d}t\ \mathrm{e}^{\mathrm{i}\omega t} \left\langle \mathrm{T}\hat{b}^{(0)}_m(t)\hat{b}^{(0)\dagger}_{m'}(0)\right\rangle_{\rm ex} = \frac{\delta_{m,m'}}{\omega - \Omega_m + \mathrm{i}\delta}, \tag{3.10}$$

where the time representation is defined as

$$\hat{b}^{(0)}_m(t) \equiv \mathrm{e}^{\mathrm{i}\hat{H}_{\rm ex}t/\hbar}\hat{b}_m \mathrm{e}^{-\mathrm{i}\hat{H}_{\rm ex}t/\hbar}, \tag{3.11a}$$

$$\hat{b}^{(0)\dagger}_m(t) \equiv \mathrm{e}^{\mathrm{i}\hat{H}_{\rm ex}t/\hbar}\hat{b}^\dagger_m \mathrm{e}^{-\mathrm{i}\hat{H}_{\rm ex}t/\hbar}. \tag{3.11b}$$

On the other hand, the excitonic polarization appearing in Eq. (3.5), the interaction Hamiltonian, is quantized as

$$\hat{P}(z) = \mathcal{P}\sum_m g_m(z)\ \hat{b}_m + \mathrm{H.c.}, \tag{3.12}$$

where $g_m(z)$ is the exciton center-of-mass wavefunction in state m, and the absolute value of the coefficient $\mathcal{P}$ can be estimated by the longitudinal-transverse (LT) splitting energy of excitons as $\hbar\omega_{\rm LT} = |\mathcal{P}|^2/\varepsilon_{\rm bg}\varepsilon_0$. Under the RWA, according to the linear response theory, the excitonic component of the optical susceptibility is obtained as a nonlocal from [31, 78]:

$$\chi(z,z',\omega) = \frac{-1}{\mathrm{i}\hbar\varepsilon_0}\int_0^\infty \mathrm{d}t\ \mathrm{e}^{\mathrm{i}\omega t}\left\langle[\hat{P}_0(z,t),\hat{P}_0(z',0)]\right\rangle_{\rm ex} \simeq \varepsilon_{\rm bg}\omega_{\rm LT}\sum_m \frac{g_m(z)g^*_m(z')}{\Omega_m - \omega - \mathrm{i}\delta}, \tag{3.13}$$

which characterizes $\hat{P}(z,\omega)$ at position z induced by $\hat{E}(z',\omega)$ at the other position z' as

$$\hat{P}(z,\omega) = \varepsilon_0\int_{-\infty}^{\infty}\mathrm{d}z'\ \chi(z,z',\omega)\hat{E}(z',\omega). \tag{3.14}$$

Here, in the case of bulk system, we can consider the exciton center-of-mass wavefunction as $g_m = \mathrm{e}^{\mathrm{i}k_m z}/\sqrt{L}$, where L is the normalization length and $k_m = 2\pi m/L$ for $m = 0,\ \pm1,\ \pm2,\ \ldots$ In this situation, the nonlocal susceptibility, Eq. (3.13), is diagonal in the k-space, but it depends not only on ω but also on k due to the nonlocality as

$$\chi(k,k',\omega) = \frac{1}{L}\int_{-\infty}^{\infty}\mathrm{d}z\int_{-\infty}^{\infty}\mathrm{d}z'\ \mathrm{e}^{-\mathrm{i}kz}\chi(z,z',\omega)\mathrm{e}^{\mathrm{i}k'z'} = \delta_{k,k'}\frac{\varepsilon_{\rm bg}\omega_{\rm LT}}{\Omega(k) - \omega - \mathrm{i}\delta} = \delta_{k,k'}\chi(k,\omega). \tag{3.15}$$

Substituting Eqs. (3.14) and (3.15) into the Maxwell wave equation, Eq. (3.1), the polariton dispersion relation in bulk system is obtained as

$$\frac{c^2({k_\parallel}^2 + k^2)}{\omega^2} = \varepsilon_{\rm bg}(\omega) + \chi(k,\omega). \tag{3.16}$$

On the other hand, in the general case, the self-energy tensor $\mathbf{\Sigma}(\omega)$ of exciton states is derived from the interaction Hamiltonian [Eq. (3.5)] as

$$\Sigma_{m,m'}(\omega) = \varepsilon_{\rm bg}\omega_{\rm LT}(\omega/c)^2\int_{-\infty}^{\infty}\mathrm{d}z\int_{-\infty}^{\infty}\mathrm{d}z'\ g^*_m(z)G(z,z',\omega)g_{m'}(z'), \tag{3.17}$$

which describes the retarded interaction not only between the same exciton states ($m = m'$) but also between the different states ($m \neq m'$). Further, the time-ordered correlation function tensor $\mathbf{\mathfrak{G}}(\omega)$ of

exciton states in the whole system is derived from the Dyson equation, i.e., it is obtained as the inverse of the matrix whose elements are given as

$$[\mathfrak{G}^{-1}(\omega)]_{m,m'} = (\omega - \Omega_m)\delta_{m,m'} - \Sigma_{m,m'}(\omega). \tag{3.18}$$

The resonance frequency $\omega_{\rm res}$ and the radiative decay rate γ of exciton-photon coupled modes are respectively obtained from the real and imaginary parts of poles $\tilde{\omega} = \omega_{\rm res} - {\rm i}\gamma$ of the exciton correlation function tensor. The calculation of these poles is just identical to that of the self-sustaining modes discussed under the microscopic nonlocal theory in the semiclassical framework [35, 36, 77, 31, 38] (or see Sec. 1.4.4).

The above calculation method can consider the inter-state retarded interaction through the self-energy tensor, Eq. (3.17). Further, in this chapter, I numerically calculate the poles without any pole approximations in contrast to Ref. 35. With regard to the RWA, it can be considered as a good approximation, because neither the frequency shift nor the radiative decay rate reaches only a few percent of the bare exciton frequency $\omega_{\rm T}$ even at the maximum in the calculation.

I consider a CuCl film with thickness d, and suppose the background dielectric constant $\varepsilon_{\rm bg} = {n_{\rm bg}}^2 = 5.59$ inside of the film. In the case that the background is a homogeneous medium [$\varepsilon_{\rm bg}(z) = \varepsilon_{\rm bg}$], the Green function satisfying Eq. (3.3) is derived as

$$G(z, z', \omega) = \frac{{\rm e}^{{\rm i}q|z-z'|}}{{\rm i}2q}. \tag{3.19}$$

On the other hand, as shown in Ref. 65 (or see App. D), in general multilayer systems, the Green function from a focusing layer to the same one is written as

$$\begin{aligned} &{\rm i}2qG(z, z', \omega) \\ &= {\rm e}^{{\rm i}q|z-z'|} + {\rm e}^{{\rm i}qz}\tilde{R}_L\left[{\rm e}^{{\rm i}qz'} + {\rm e}^{{\rm i}qd}\tilde{R}_R{\rm e}^{{\rm i}q(d-z')}\right]\tilde{M} \\ &\quad + {\rm e}^{-{\rm i}q(z-d)}\tilde{R}_R\left[{\rm e}^{{\rm i}q(d-z')} + {\rm e}^{{\rm i}qd}\tilde{R}_L{\rm e}^{{\rm i}qz'}\right]\tilde{M}, \end{aligned} \tag{3.20}$$

where I consider that the left-hand interface of the focusing layer is at $z = 0$, and the right-hand at $z = d$. In Eq. (3.20), $\tilde{R}_{L/R}$ is the generalized reflection coefficient [65] (App. D) from the focusing layer to the left-/right-hand interface, and $\tilde{M} = [1 - \tilde{R}_L\tilde{R}_R{\rm e}^{{\rm i}2qd}]^{-1}$. In the case of a three-layer system where the background dielectric constants are respectively given as ε_L, $\varepsilon_{\rm bg}$, and ε_R, when we focus on the middle layer, $\tilde{R}_{L/R}$ is simply represented as the Fresnel reflection coefficient:

$$\tilde{R}_{L/R} = \frac{q - k_{L/R}}{q + k_{L/R}}, \tag{3.21}$$

where $k_{L/R}$ is the wavenumber in the left-/right-hand region:

$$k_{L/R} = \left[\varepsilon_{L/R}\omega^2/c^2 - {k_\parallel}^2\right]^{1/2}. \tag{3.22}$$

In this chapter, I discuss only the modes perpendicular to the layers, i.e., $k_\parallel = 0$, and I consider the wavefunctions of the exciton center-of-mass motion as sinusoidal functions whose amplitudes are zero at the interfaces of the focusing layer:

$$g_m(z) = \begin{cases} \sqrt{2/d}\sin(k_m z) & 0 < z < d \\ 0 & \text{otherwise} \end{cases} \tag{3.23}$$

where $k_m = m\pi/d$ and $m = 1, 2, \ldots$. The exciton translational mass is $m_{\rm ex} = 2.3m_0$, where m_0 is the free electron mass. The bare exciton frequencies are given as $\hbar\omega_{\rm T} = 3.2022$ eV and $\Omega_m = \omega_{\rm T} + \hbar{k_m}^2/2m_{\rm ex}$. The LT splitting energy is $\hbar\omega_{\rm LT} = 5.7$ meV.

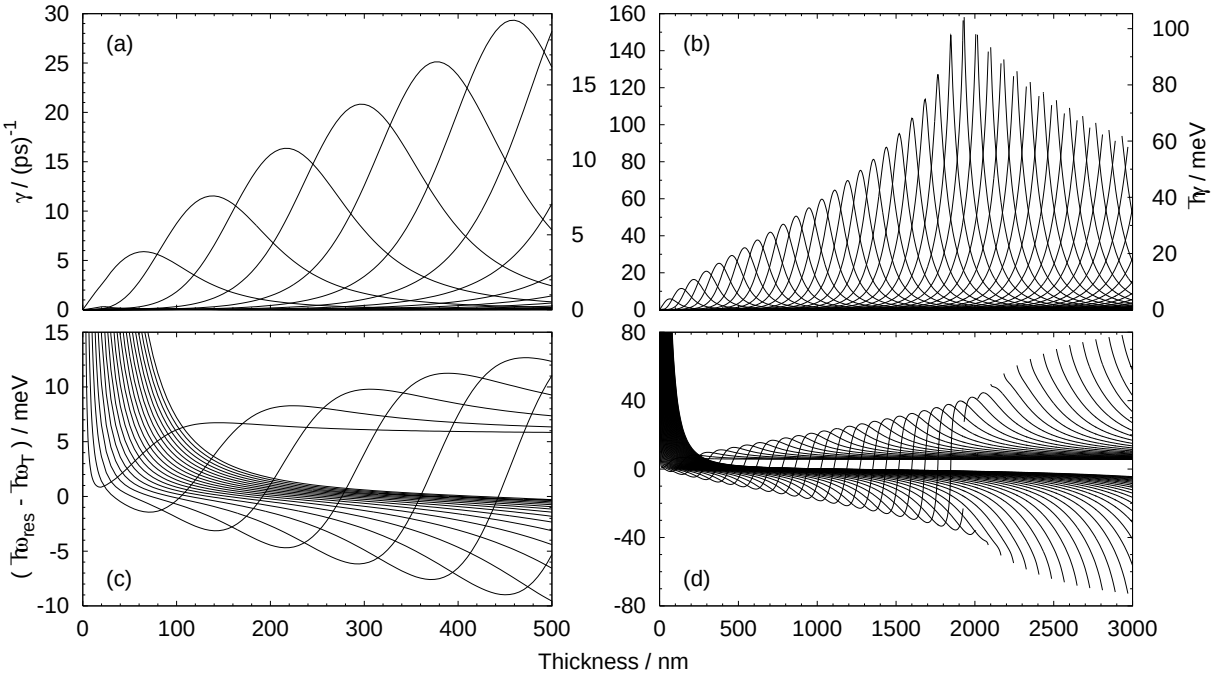

Figure 3.1: Thickness dependence of (a) (b) radiative decay rates and (c) (d) resonance frequencies of exciton-photon coupled modes in a CuCl film. Outside of the film is $\varepsilon_L = \varepsilon_R = \varepsilon_{\rm bg}$. 200 states of exciton center-of-mass motion are considered.

3.3 Thickness dependence

First I discuss the thickness dependence of the exciton-photon coupled modes in the case of homogeneous background, $\varepsilon_L = \varepsilon_R = \varepsilon_{\rm bg}$. The calculation algorithm is explained in App. E. In Fig. 3.1, I plot the radiative decay rate γ and resonance frequency $\omega_{\rm res}$ of the exciton-photon coupled modes with continuously changing thickness d. As seen in Fig. 3.1(a), γ of the lowest mode is maximized at thickness about 50 nm. Although this thickness should be approximately equal to $\lambda/2 = \pi c/n_{\rm bg}\omega_{\rm T} \simeq 80$ nm, a half light wavelength at frequency $\omega_{\rm T}$ in the background medium, there is a mismatch due to the deviation of the lowest exciton center-of-mass motion from a continuous wave. On the other hand, in the case of the higher modes, the phase-matching condition, $k_m = m\pi/d = n_{\rm bg}\omega_{\rm T}/c$ or $d = m\lambda/2 \simeq m \times 80$ nm, is gradually satisfied with increasing the mode number because of increasing the wavefunction continuity. Further, increasing the mode number, the maximum value of γ also increases in line with the exciton superradiance. As theoretically demonstrated by Agranovich et al. [95], we can find no oscillation in the thickness dependence of γ after the phase-matching thickness owing to the consideration of the inter-state retarded interaction. With regard to the resonance frequency $\omega_{\rm res}$ as seen in Fig. 3.1(c), when we focus on a particular mode, $\omega_{\rm res}$ gradually decreases with increasing d until the phase-matching thickness, but it flips to the higher side around its thickness. After that, $\omega_{\rm res}$ gradually decreases and saturate to $\omega_{\rm T} + \omega_{\rm LT}$, the band edge of the upper polariton. This behavior can be understood by considering the polariton dispersion relation [95, 42] and the decrease of wavenumber $k_m = m\pi/d$ with increasing thickness as will seen in Fig. 3.3(a).

On the other hand, as seen in Fig. 3.1(b), the exciton superradiance is suppressed at thickness over

about 2 μm, although any dephasing processes are not considered in the calculation. Further, the behavior becomes discontinuous at the peak, and the peak value cannot be found in this numerical calculation. As seen in Fig. 3.1(d), the thickness dependence of $\omega_{\rm res}$ also becomes discontinuous after the crossover thickness, so that $\omega_{\rm res}$ suddenly flips to the higher frequency side at the phase-matching thickness. According to the work by Björk et al. [94], this behavior just reflects the crossover from exciton-/photon-like modes to polariton ones. In other words, the discontinuity reflects the frequency splitting of upper and lower polaritons at the phase-matching wavenumber $k = n_{\rm bg}\omega_{\rm T}/c$ in bulk system as will seen in Fig. 3.4(a). In order to elucidate this crossover condition, I calculate γ and $\omega_{\rm res}$ by another calculation method discussed in the next two sections.

3.4 Dispersion relation

The calculation of the previous section is based on the exciton correlation function tensor renormalizing the exciton-photon interaction. However, this method is relatively complicated to analyze the superradiance suppression. In this section, I approximate the self-energy tensor, Eq. (3.17), and try to derive a simplified equation for the complex frequency of the exciton-photon coupled modes by introducing a complex wavenumber, whose imaginary part represents the wavenumber uncertainty in finite systems.

In the homogeneous background medium, $\varepsilon_{\rm bg}(z,\omega) = \varepsilon_{\rm bg}(\omega)$, the Green's function satisfying Eq. (3.3) is diagonal with respect to the wavenumber as

$$\begin{aligned} G_{k,k'}(\omega) &= \frac{1}{L}\int_{-\infty}^{\infty}{\rm d}z\int_{-\infty}^{\infty}{\rm d}z'\ {\rm e}^{-{\rm i}kz}\ G(z,z',\omega)\ {\rm e}^{{\rm i}k'z'} \\ &= \frac{\delta_{k,k'}}{(q+{\rm i}\delta)^2-k^2}, \end{aligned} \tag{3.24}$$

where L is the normalization length. Eq. (3.19) can be obtained by transforming this equation into the real space. Substituting Eq. (3.24) into Eq. (3.17), the self-energy tensor, I obtain

$$\Sigma_{m,m'}(\omega) = \omega_{\rm LT}\ {q_0}^2\sum_k \frac{g^*_{m,k}\ g_{m',k}}{(q+{\rm i}\delta)^2-k^2}, \tag{3.25}$$

where ${q_0}^2 \equiv \varepsilon_{\rm bg}\omega^2/c^2$, and $g_{m,k}$ is the Fourier transform of the exciton center-of-mass wavefunction:

$$g_{m,k} = \frac{1}{\sqrt{L}}\int_{-\infty}^{\infty}{\rm d}z\ {\rm e}^{-{\rm i}kz}g_m(z). \tag{3.26}$$

In contrast to the infinitesimal interval $2\pi/L$ between the neighboring k, the interval of q_m is much large as π/d. Therefore, the base-transformation between m and k is not unitary in the case of a film with finite thickness. This means that the transform coefficient set $\{g_{m,k}\}$ satisfies the orthogonality as

$$\sum_k g^*_{m,k}\ g_{m',k} = \int_{-\infty}^{\infty}{\rm d}z\ g_m(z)\ g^*_{m'}(z) = \delta_{m,m'}, \tag{3.27}$$

but it does not satisfy the completeness:

$$\sum_m g^*_{m,k}g_{m,k'} = \frac{1}{L}\int_{-d/2}^{d/2}{\rm d}z\ {\rm e}^{{\rm i}(k-k')z} = \frac{d}{L}\frac{\sin[(k-k')d/2]}{(k-k')d/2}, \tag{3.28}$$

where I consider that the exciton center-of-mass motion is confined in $-d/2 < z < d/2$. Therefore, the self-energy, Eq. (3.25), becomes diagonal with respect to k only in infinite systems.

In order to obtain a simple equation for a smooth analysis of the crossover condition, I consider the following approximation to quasi-diagonalize the self-energy, Eq. (3.25). The function $\sin(x)/x$ appearing in Eq. (3.28) can be approximated as $\sin(x)/x \simeq 1$ under the condition $|x| \ll 1$. Therefore, by relaxing the identical condition of k as $|k - k'| \ll d^{-1}$, Eq. (3.28) can be approximated as

$$(L/d) \sum_m g^*_{m,k} g_{m,k} \simeq \delta_{k,k'}, \tag{3.29}$$

and then $\{g_{m,k}\}$ has a quasi-completeness. Here, since I admit an uncertainty of k in the order of d^{-1}, the wavenumber should have an imaginary part as $k \to k - \mathrm{i}\alpha/d$, and the summation becomes $\sum_k \to (L/d)\sum_k$. The physical meaning of the nondimensional value α will be discussed later. As the result of the above approximation, the self-energy, Eq. (3.25), becomes quasi-diagonal as

$$\Sigma_{k,k'}(\omega) = \sum_{m,m'} g_{m,k}\ \Sigma_{m,m'}(\omega)\ g^*_{m',k'} \simeq \frac{d}{L}\delta_{k,k'} \frac{\omega_{\mathrm{LT}}\ {q_0}^2}{(q + \mathrm{i}\delta)^2 - (k - \mathrm{i}\alpha/d)^2}. \tag{3.30}$$

In the same manner, the diagonal part of the correlation function, Eq. (3.18), is rewritten as

$$\sum_m g_{m,k}(\Omega_m - \omega) g^*_{m,k'} \simeq \delta_{k,k'} \frac{d}{L} \left[\Omega(k - \mathrm{i}\alpha/d) - \omega\right], \tag{3.31}$$

where the bare exciton frequency is written as

$$\Omega(k - \mathrm{i}\alpha/d) = \omega_{\mathrm{T}} + \frac{\hbar}{2m_{\mathrm{ex}}} \left[{k_\parallel}^2 + \left(k - \mathrm{i}\frac{\alpha}{d}\right)^2\right]. \tag{3.32}$$

Therefore, the exciton correlation function can be obtained as a diagonal form as

$$[\mathfrak{G}^{-1}(\omega)]_{k,k'} = \sum_{m,m'} g_{m,k}[\mathfrak{G}^{-1}(\omega)]_{m,m'} g^*_{m',k'} \simeq \delta_{k,k'} \frac{d}{L} \left[\omega - \Omega(k - \mathrm{i}\alpha/d) - \frac{\omega_{\mathrm{LT}}\ {q_0}^2}{(q + \mathrm{i}\delta)^2 - (k - \mathrm{i}\alpha/d)^2}\right], \tag{3.33}$$

and the pole $\tilde{\omega} = \omega_{\mathrm{res}} - \mathrm{i}\gamma$ is obtained for a given complex wavenumber $\tilde{k} = k - \mathrm{i}\alpha/d$ from

$$\tilde{\omega} = \Omega(\tilde{k}) + \frac{\omega_{\mathrm{LT}}\varepsilon_{\mathrm{bg}}(\tilde{\omega}/c)^2}{\varepsilon_{\mathrm{bg}}(\tilde{\omega}/c)^2 - {k_\parallel}^2 - \tilde{k}^2}. \tag{3.34}$$

Here, we can rewrite this into the dispersion relation

$$\frac{c^2({k_\parallel}^2 + \tilde{k}^2)}{\tilde{\omega}^2} = \varepsilon_{\mathrm{bg}} + \frac{\varepsilon_{\mathrm{bg}}\omega_{\mathrm{LT}}}{\Omega(\tilde{k}) - \tilde{\omega}} = \varepsilon_{\mathrm{bg}} + \chi(\tilde{k}, \tilde{\omega}), \tag{3.35}$$

which has the same form as Eq. (3.16) obtained in the bulk system. However, there remains a task to determine the nondimensional value α and the k-selection rule that governs the discrete k values for a finite thickness.

3.5 Self-sustaining condition

In order to determine the complex wavenumber $\tilde{k} = k - \mathrm{i}\alpha/d$, I consider a self-sustaining condition of exciton-photon coupled modes in a film with polariton dispersion. If the translational mass of exciton is assumed to be infinite, there is only a single polariton mode satisfying dispersion relation (3.34) for a given frequency $\tilde{\omega}$, and the self-sustaining condition is simply considered as

$$r_L\ r_R\ \mathrm{e}^{\mathrm{i}2\tilde{k}d} = 1, \tag{3.36}$$

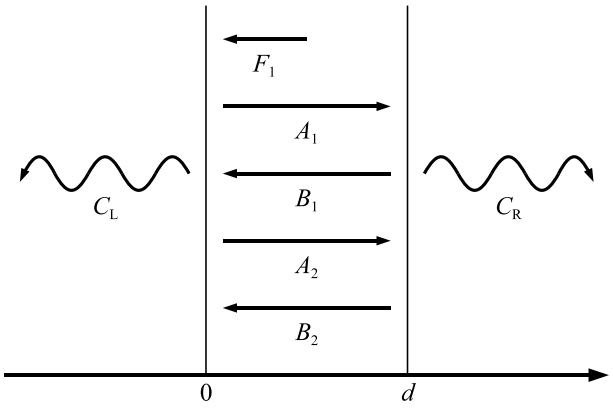

Figure 3.2: Schematic view of polariton and photon fields to calculate the reflection coefficients from inside of the film.

where $r_{L/R}$ is the Fresnel reflection coefficient at the left-/right-hand interface:

$$r_{L/R} = \frac{\tilde{k} - \tilde{k}_{L/R}}{\tilde{k} + \tilde{k}_{L/R}}, \tag{3.37}$$

and $\tilde{k}_{L/R}$ is the outside wavenumber defined in Eq. (3.22) by replacing ω with $\tilde{\omega} = \omega_{\rm res} - \mathrm{i}\gamma$. The self-sustaining condition, Eq. (3.36), means that there is neither amplitude decay nor phase shift after a round trip inside of the film. Actually, this intuitive method consisting the dispersion and self-sustaining condition provides the complex wavenumber set $\{\tilde{\omega}_\lambda\}$ obtained in the matrix method. However, if we consider the exciton center-of-mass kinetic energy with finite translational mass, we must consider an additional boundary condition (ABC) [67] besides the Maxwell boundary conditions, because there are two wavenumbers $\tilde{k}_1$ and $\tilde{k}_2$ satisfying dispersion relation (3.34) for a given $\tilde{\omega}$.

As seen in Fig. 3.2, I consider forward (A_1 and A_2) and backward fields (B_1 and B_2) for each polariton, and two outward fields (C_L and C_R) from the film. In order to derive the reflection coefficients for polariton 1 from inside of the film, I consider an incident field F_1 from inside to the left interface. The electric fields in the left-hand side, polariton 1, 2, and right-hand side are respectively written as follows:

$$E_L(z) = C_L \mathrm{e}^{-\mathrm{i}\tilde{k}_L z}, \tag{3.38a}$$
$$E_1(z) = A_1 \mathrm{e}^{\mathrm{i}\tilde{k}_1 (z-d)} + B_1 \mathrm{e}^{-\mathrm{i}\tilde{k}_1 z} (+F_1 \mathrm{e}^{-\mathrm{i}\tilde{k}_1 z} \text{ only at } z = 0), \tag{3.38b}$$
$$E_2(z) = A_2 \mathrm{e}^{\mathrm{i}\tilde{k}_2 (z-d)} + B_2 \mathrm{e}^{-\mathrm{i}\tilde{k}_2 z}, \tag{3.38c}$$
$$E_R(z) = C_R \mathrm{e}^{\mathrm{i}\tilde{k}_R z}. \tag{3.38d}$$

Here, I define the phase origins of the polariton modes as opposite as usual in order to avoid a numerical divergence caused by $\mathrm{Im}[\tilde{k}_i] < 0$. From Eqs. (3.38), I obtain four Maxwell boundary conditions at $z = 0$ and $z = d$ as

$$F_1 + A_1 \mathrm{e}^{-\mathrm{i}\tilde{k}_1 d} + B_1 + A_2 \mathrm{e}^{-\mathrm{i}\tilde{k}_2 d} + B_2 = C_L, \tag{3.39a}$$
$$A_1 + B_1 \mathrm{e}^{-\mathrm{i}\tilde{k}_1 d} + A_2 + B_2 \mathrm{e}^{-\mathrm{i}\tilde{k}_2 d} = C_R, \tag{3.39b}$$
$$-k_1(-F_1 + A_1 \mathrm{e}^{-\mathrm{i}\tilde{k}_1 d} - B_1) - k_2(A_2 \mathrm{e}^{-\mathrm{i}\tilde{k}_2 d} - B_2) = \tilde{k}_L C_L, \tag{3.39c}$$
$$k_1(A_1 - B_1 \mathrm{e}^{-\mathrm{i}\tilde{k}1 d}) + k_2(A_2 - B_2 \mathrm{e}^{-\mathrm{i}\tilde{k}_2 d}) = \tilde{k}_R C_R. \tag{3.39d}$$

In addition, since I consider the exciton center-of-mass wavefunction, Eq. (3.23), whose amplitudes are zero at the interfaces, the following Pekar's ABCs are required [67, 70]:

$$\chi_1(F_1 + A_1 \mathrm{e}^{-\mathrm{i}\tilde{k}_1 d} + B_1) + \chi_2(A_2 \mathrm{e}^{-\mathrm{i}\tilde{k}_2 d} + B_2) = 0, \tag{3.39e}$$

$$\chi_1(A_1 + B_1 \mathrm{e}^{-\mathrm{i}\tilde{k}_1 d}) + \chi_2(A_2 + B_2 \mathrm{e}^{-\mathrm{i}\tilde{k}_2 d}) = 0, \tag{3.39f}$$

where the susceptibilities χ_1 and χ_2 are written as

$$\chi_i = \frac{(c\tilde{k}_i)^2 + (ck_\parallel)^2}{\tilde{\omega}^2} - \varepsilon_{\mathrm{bg}}. \tag{3.40}$$

Usually, we cannot define the reflectance from inside of the film with multiple polariton modes, because the amplitude of one mode is also transferred to the other modes after the reflection, and it also go back to the original mode after another reflection. In order to derive the appropriate self-sustaining condition, I consider that, as a result of the multiple reflections inside of the film, B_1/F_1 should be represented by a product of the two reflection coefficients, r'_L and r'_R, as

$$B_1/F_1 = \sum_{n=1}^{\infty} (r'_L r'_R \ \mathrm{e}^{\mathrm{i}2\tilde{k}_1 d})^n. \tag{3.41}$$

From this relation, by solving the boundary problem [Eq. (3.39)], $r'_L r'_R$ should be represented as

$$r'_L r'_R = \frac{(B_1/F_1)\mathrm{e}^{-\mathrm{i}2\tilde{k}_1 d}}{1 + (B_1/F_1)}, \tag{3.42}$$

and, comparing with Eq. (3.36), the self-sustaining condition for the multimode system is obtained as

$$r'_L r'_R \ \mathrm{e}^{\mathrm{i}2\tilde{k}_1 d} = \frac{(B_1/F_1)}{1 + (B_1/F_1)} = 1. \tag{3.43}$$

Although this equation is satisfied only in the limit of $|B_1/F_1| \to \infty$, I renew $\tilde{k}_1$ as

$$\tilde{k}_1 := \frac{-1}{\mathrm{i}2d} \ln(r'_L \ r'_R) = \frac{-1}{\mathrm{i}2d} \ln \frac{(B_1/F_1)\mathrm{e}^{-\mathrm{i}2\tilde{k}_1 d}}{1 + (B_1/F_1)}. \tag{3.44}$$

in the numerical successive calculation. Actually, by simultaneously solving Eqs. (3.34) and (3.44), I can reproduce $\{\omega_{\mathrm{res}} - \mathrm{i}\gamma\}$ obtained by the correlation function method in Sec. 3.2. The calculation algorithm is explained in App. E.

3.6 Polariton scheme

In Fig. 3.3, I show (a) dispersion relation and (b) frequency dependence of γ at thicknesses of 50, 200, and 500 nm. The poles of the exciton correlation function tensor are plotted with symbols, and $\tilde{k} = k - \mathrm{i}\alpha$ is calculated from dispersion relation (3.34) for each $\tilde{\omega} = \omega_{\mathrm{res}} - \mathrm{i}\gamma$. On the other hand, the lines are calculated by the intuitive method discussed in the previous two sections. However, the ABC and k-selection rule are not considered in the self-sustaining condition [Eq. (3.43)] in order to show the continuous k-dependence. This means that, instead of Eq. (3.44), I consider only the relation between α and $\tilde{\omega}$ for a given real k as

$$\alpha = \frac{1}{4} \ln \frac{1}{|r_L r_R|^2}, \tag{3.45}$$

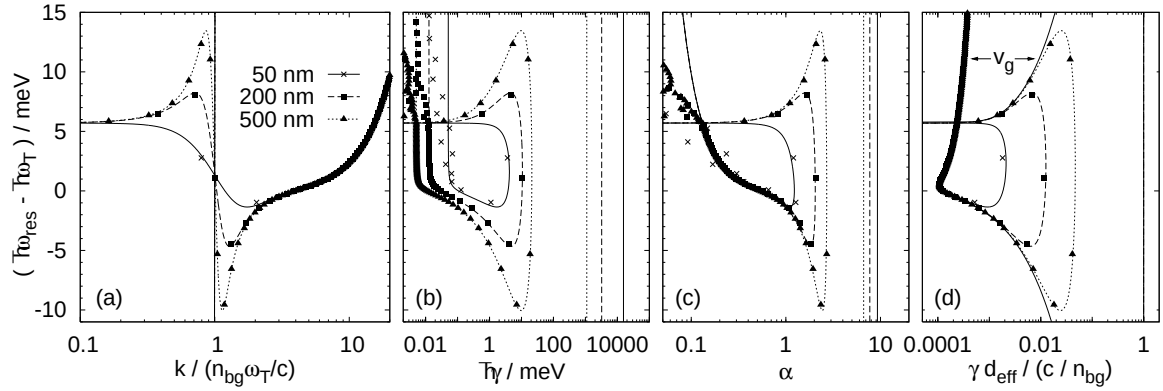

Figure 3.3: (a) Dispersion relation and frequency dependence of (b) radiative decay rate γ, (c) α, and (d) apparent propagation speed $\gamma d_{\rm eff}$ at thicknesses of 50, 200, and 500 nm. The lines are calculated by solving Eqs. (3.34) and (3.45) for a given real wavenumber k. The symbols are the poles of the exciton correlation functions. $\varepsilon_L = \varepsilon_R = \varepsilon_{\rm bg}$.

where $r_{L/R}$ is the reflection coefficient without the ABC, i.e., the Fresnel coefficient [Eq. (3.37)]. Eqs. (3.34) and (3.45) give solutions for arbitrary k as seen in Fig. 3.3. However, if the ABC is considered, the solutions are obtained only for particular k satisfying self-sustaining condition (3.43).

Since dispersion relation (3.34) is rewritten as a third-order polynomial equation for $\tilde{\omega}$ as

$$[\tilde{\omega} - \Omega(\tilde{k})][\varepsilon_{\rm bg}(\tilde{\omega}/c)^2 - {k_\parallel}^2 - \tilde{k}^2] = \omega_{\rm LT}\varepsilon_{\rm bg}(\tilde{\omega}/c)^2, \tag{3.46}$$

there are three solutions for a given $\tilde{k}$. One is an unphysical solution with negative frequency, and the other two satisfying Eq. (3.45) are plotted in Fig. 3.3 for a given real k. One solution has an exciton-like frequency $\omega_{\rm res} \simeq \omega_{\rm T}$ with small γ, and the other has a photon-like frequency $\omega_{\rm res} \simeq ck/n_{\rm bg}$ with large γ. These exciton-like and photon-like modes are slightly modified from the bare exciton and photon states, respectively, because of the relatively weak exciton-photon coupling. As seen in Figs. 3.3(a) and (b), increasing the thickness, the deviation of $\omega_{\rm res}$ of the exciton-like mode from $\omega_{\rm T}$ increases at the phase-matching condition $k \simeq n_{\rm bg}\omega_{\rm T}/c$, and γ also increases in line with the exciton superradiance. By using the correlation function method, only the exciton-like modes are numerically obtained, because the photon-like modes are divergent solutions for finding the poles of the exciton correlation function tensor [Eq. (3.18)]. This can be understood by rewriting dispersion relation (3.34) as

$$\tilde{\omega} - \Omega(\tilde{k}) - \frac{\omega_{\rm LT}\varepsilon_{\rm bg}(\tilde{\omega}/c)^2}{\varepsilon_{\rm bg}(\tilde{\omega}/c)^2 - {k_\parallel}^2 - \tilde{k}^2} = f(\tilde{\omega}, \tilde{k}) = 0. \tag{3.47}$$

It is difficult to numerically find the zero points of function $f(\tilde{\omega}, \tilde{k})$ for the photon-like solutions ($k \simeq n_{\rm bg}\omega_{\rm res}/c$), because the last term of the left-hand side (LHS) is divergent. This is the reason of the discontinuity in Figs. 3.1(b) and (d). On the other hand, although we can find good agreements between symbols and lines in the dispersion relation [Fig. 3.3(a)], there are some deviations of γ in Fig. 3.3(b), especially for thickness of 50 nm and for k larger than $10 \times n_{\rm bg}\omega_{\rm T}/c$. This is because of the neglect of ABC in the intuitive calculation method. By considering the ABC, I can obtain the exact agreement between the two calculations under the numerical precision.

As discussed by Agranovich et al. [95], Eq. (3.45), the representation of α, is also obtained along the calculation of radiative decay rate in the polariton scheme, which provides the radiative decay rate as

$$\gamma = \alpha v_{\rm g}/d. \tag{3.48}$$

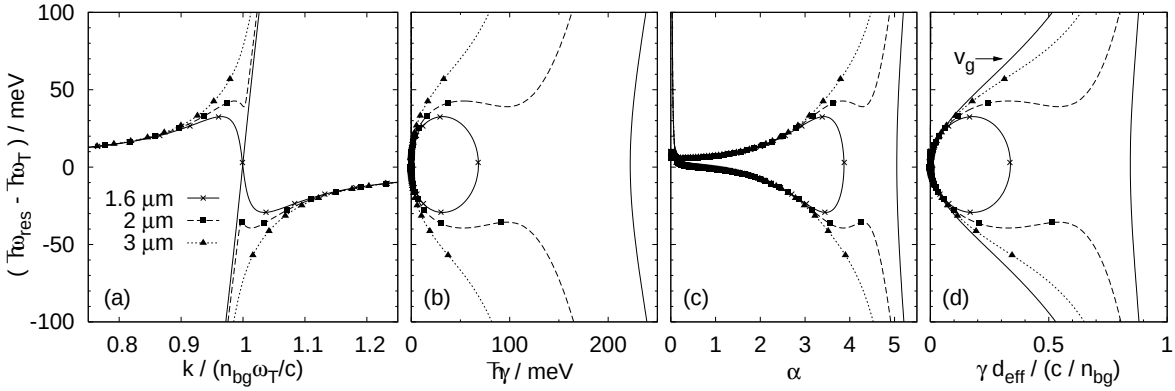

Figure 3.4: (a) Dispersion relation and frequency dependence of (b) radiative decay rateγ, (c) α, and (d) apparent propagation speed $\gamma d_{\rm eff}$ at thicknesses of 1.6, 2, and 3 μm. The lines are calculated by solving Eqs. (3.34) and (3.45) for a given real wavenumber k. The symbols are the poles of the exciton correlation functions, where 400 states of exciton center-of-mass motion are considered. $\varepsilon_L = \varepsilon_R = \varepsilon_{\rm bg}$.

On the other hand, in the present intuitive calculation method, Eq. (3.45) is obtained from the self-sustaining condition, and Eq. (3.48) can be obtained from dispersion relation (3.34) in particular situations. When the radiative decay rate is much smaller than the resonance frequency as $\gamma \ll \omega_{\rm res}$, and the uncertainty of the wavenumber is much small as $\alpha/d \ll k$, Eq. (3.34) can be approximated as

$$\omega = \omega_{\rm T} + \frac{\hbar k^2}{2m_{\rm ex}} + \frac{\omega_{\rm LT}\ {q_0}^2}{{q_0}^2 - {k_\parallel}^2 - k^2}, \tag{3.49}$$

$$\gamma = \frac{\hbar k}{m_{\rm ex}}\frac{\alpha}{d} + \frac{2\omega_{\rm LT}{q_0}^2[k\alpha/d - ({k_\parallel}^2 + k^2)\gamma/\omega]}{({q_0}^2 - {k_\parallel}^2 - k^2)^2}. \tag{3.50}$$

Here, Eq. (3.49) is just the dispersion relation in bulk system [Eq. (3.16)] under the RWA, and it gives the group velocity as

$$v_{\rm g} = \frac{{\rm d}\omega}{{\rm d}k} = \frac{({q_0}^2 - {k_\parallel}^2 - k^2)^2\hbar k/m_{\rm ex} + 2\omega_{\rm LT}{q_0}^2 k}{({q_0}^2 - {k_\parallel}^2 - k^2)^2 + 2\varepsilon_{\rm bg}\omega_{\rm LT}\omega({k_\parallel}^2 + k^2)/c^2}. \tag{3.51}$$

From this representation of $v_{\rm g}$, Eq. (3.48) can be obtained by rewriting Eq. (3.50) without any information outside of the excitonic medium, which is described by self-sustaining condition (3.36) or (3.43). Although Eq. (3.48) cannot be applied to superradiant excitons, I define an effective thickness of an exciton-photon coupled mode as

$$d_{\rm eff} = \alpha/d = -{\rm Im}[\tilde{k}]^{-1}, \tag{3.52}$$

which gives $\gamma = v_{\rm g}/d_{\rm eff}$ in the polariton scheme. Further, I define an apparent propagation speed of the coupled modes as $\gamma d_{\rm eff}$, the effective thickness divided by the radiative decay time, and it agrees with $v_{\rm g}$ in the polariton scheme.

In Fig. 3.3(c) and (d), I respectively plot the frequency dependence of α and $\gamma d_{\rm eff}$, and also I plot the polariton group velocity $v_{\rm g}$ with bold solid lines in Fig. 3.3(d). Although $\gamma d_{\rm eff}$ of superradiant excitons ($k \simeq n_{\rm bg}\omega_{\rm T}/c$ and $\omega_{\rm res} \simeq \omega_{\rm T}$) gets larger with increasing thickness, we can find that $\gamma d_{\rm eff}$ of the other exciton-like modes agree with $v_{\rm g}$. In other words, all the exciton-like modes without the phase-matching condition obey the polariton scheme even at small thickness where the exciton superradiance is maintained. This is because that the above conditions $\gamma \ll \omega_{\rm res}$ and $\alpha/d \ll k$, which are used to derive

Eq. (3.50), are satisfied even for those phase-mismatching modes. On the other hand, we can find that $\gamma d_{\rm eff}$ of photon-like modes agree with $c/n_{\rm bg}$, the light speed in the background medium because of the relatively weak exciton-photon coupling at the small thickness. As seen in Fig. 3.3(c), there are some deviations of α between the two calculation methods for large wavenumber and for small thickness. This is because α is determined by self-sustaining condition (3.36) or (3.44) as discussed above. On the other hand, $\gamma d_{\rm eff}$ of the two are well agreed even for large wavenumber, because Eq. (3.48) is obtained only from dispersion relation (3.34).

Fig. 3.4 shows the dispersion relation and frequency dependence of γ, α, and $\gamma d_{\rm eff}$ at large thicknesses of 1.6, 2, and 3 μm. For thickness of 1.6 μm, where the exciton superradiance is maintained, γ and $\gamma d_{\rm eff}$ of the superradiant modes are much larger than those of Fig. 3.3 obeying the exciton superradiance. On the other hand, $\gamma d_{\rm eff}$ of photon-like modes decrease from $c/n_{\rm bg}$ because of the relatively strong exciton-photon coupling. In this thickness region near the crossover, increasing the thickness, $\gamma d_{\rm eff}$ of the superradiant and photon-like modes gradually close to each other, and after the crossover of exciton-photon coupled modes, the two solutions of the intuitive method split into the upper and lower branches as seen in Fig. 3.4(a). After that, the phase-matching modes disappear from the polariton band gap, and then the exciton superradiance is suppressed. On the other hand, the frequency dependence of γ also splits into upper and lower branches, and $\gamma d_{\rm eff}$ gradually saturates to the polariton group velocity $v_{\rm g}$ even at the phase-matching condition. Therefore, all the modes obey the polariton scheme after the crossover. This is the suppression mechanism of the exciton superradiance as discussed by Björk et al. [94].

3.7 Crossover condition

The crossover condition between the exciton/photon-like modes and the polariton ones can be obtained from dispersion relation (3.34). At the phase-matching condition ${k_\parallel}^2 + k^2 = \varepsilon_{\rm bg}{\omega_{\rm T}}^2/c^2$, the real part of Eq. (3.46) is written as

$$(\omega - \omega_{\rm T})(\omega^2 - \gamma^2 - {\omega_{\rm T}}^2 + \beta^2) - 2\gamma\left[\omega\gamma - (ck/n_{\rm bg})\beta\right] = \omega_{\rm LT}\omega^2, \tag{3.53}$$

where $\beta = c\alpha/n_{\rm bg}d$. Further, at small thickness where the exciton superradiance is maintained, the resonance frequency obeys $\omega_{\rm res} \simeq \omega_{\rm T}$ as seen in Fig. 3.3(a), and the first bracket in the LHS of Eq. (3.53) is negligible:

$$\gamma^2 - \eta(c\alpha/n_{\rm bg}d)\gamma + \omega_{\rm T}\omega_{\rm LT}/2 = 0, \tag{3.54}$$

where $\eta = ck/n_{\rm bg}\omega_{\rm T}$ is the perpendicular component of the propagation direction. When the film is thin enough compared to the crossover thickness, the two solutions of Eq. (3.54) are obtained as

$$\gamma = (n_{\rm bg}\omega_{\rm T}\omega_{\rm LT}/2\eta c)d_{\rm eff} \tag{3.55}$$

for the exciton-like (superradiant) mode, and

$$\gamma = \eta(c/n_{\rm bg})/d_{\rm eff} \tag{3.56}$$

for the photon-like mode. Here, we can find that the propagation speed of the latter is the light speed $\eta(c/n_{\rm bg})$ perpendicular to the layer in the background medium, and it is verified in Fig. 3.3(d), where $k_\parallel = 0$ and then $\eta = ck/n_{\rm bg}\omega_{\rm T} = 1$. Since Eq. (3.55) is proportional to d and Eq. (3.56) is to d^{-1}, these values gradually close to each other with increasing the thickness, and they finally reach to

$$\gamma d_{\rm eff} = \eta c/2n_{\rm bg}, \tag{3.57}$$

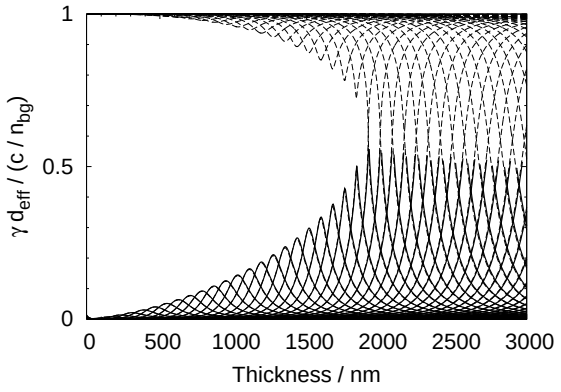

Figure 3.5: Thickness dependence of apparent propagation speed $\gamma d_{\rm eff}$. Dashed lines are calculated by the intuitive method with ABC, and solid lines are by the correlation function method. 200 exciton states are considered and $\varepsilon_L = \varepsilon_R = \varepsilon_{\rm bg}$.

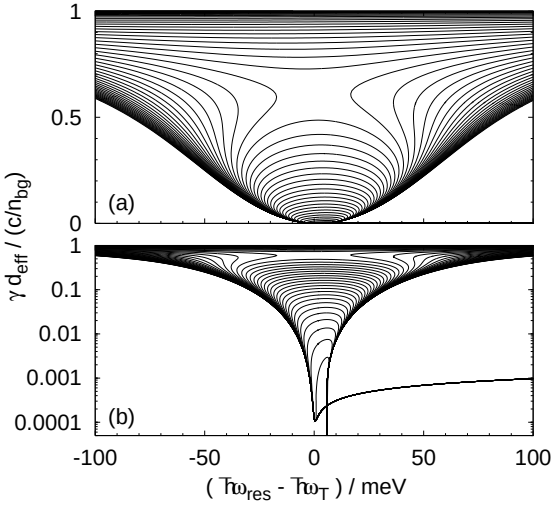

Figure 3.6: Frequency dependence of apparent propagation speed $\gamma d_{\rm eff}$. This is calculated by the intuitive method with ABC. 200 exciton states are considered and $\varepsilon_L = \varepsilon_R = \varepsilon_{\rm bg}$.

which is the degenerate solution of Eq. (3.54). This is the crossover condition between exciton-/photon-like modes and polariton ones, and it is roughly verified in Fig. 3.4(d). Since $c/2n_{\rm bg}$ is the polariton group velocity at the phase-matching condition, Eq. (3.57) means that the crossover occurs when the apparent propagation speed $\gamma d_{\rm eff}$ of superradiant exciton reaches the group velocity $c/2n_{\rm bg}$ of polariton. Therefore, the photon created by the electron-hole recombination cannot go outside of the film without reabsorption, when its propagation speed looks beyond the group velocity.

Fig. 3.5 shows the thickness dependence of $\gamma d_{\rm eff}$. The solid lines are calculated by the correlation function method, and the effective thickness $d_{\rm eff}$ is derived from dispersion relation (3.34) for each $\tilde{\omega} = \omega - {\rm i}\gamma$. On the other hand, dashed lines are calculated by the intuitive method with ABC, i.e., by simultaneously solving dispersion relation (3.34) and self-sustaining condition (3.44). We can verify that the crossover occurs when $\gamma d_{\rm eff}$ of superradiant exciton reaches $c/2n_{\rm bg}$. On the other hand, Fig. 3.6 shows the frequency dependence of $\gamma d_{\rm eff}$ with continuously changing the thickness, which is calculated by simultaneously solving Eqs. (3.34) and (3.44). When we focus on a particular mode with relatively small mode number, $\omega_{\rm res}$ shifts to the lower side and γ gets larger with increasing d until its phase-matching thickness, and around its thickness, $\omega_{\rm res}$ flips to the higher side with maximizing γ. After that, $\omega_{\rm res}$ decreases to the band edge $\omega_{\rm T} + \omega_{\rm LT}$ of the upper branch, and γ monotonally decreases. Although the maximum value of γ gradually increases together with d in line with the exciton superradiance, it is suppressed when $\gamma d_{\rm eff}$ reaches $c/2n_{\rm bg}$ as discussed above. After the crossover, the exciton-photon coupled modes split into upper and lower branches, and $\gamma d_{\rm eff}$ gradually decreases and saturate to the polariton group velocity $v_{\rm g}$ when we focus on a particular frequency. On the other hand, as seen in Fig. 3.6(b), $\gamma d_{\rm eff}$ of the phase-mismatching modes agree with $v_{\rm g}$ even at small thickness where the exciton superradiance is maintained.

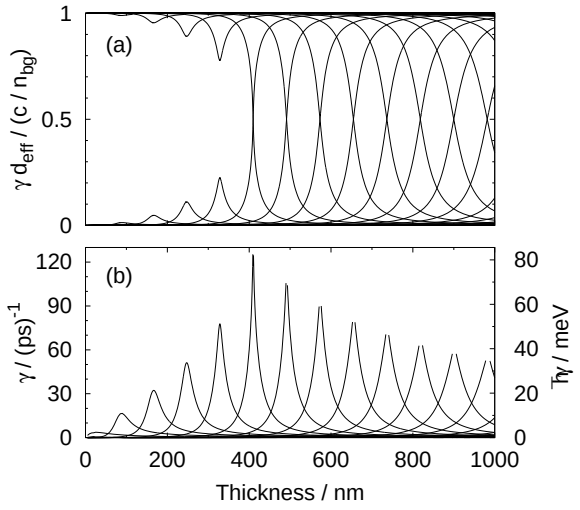

Figure 3.7: Thickness dependence of (a) apparent propagation speed and (b) radiative decay rate in the case of $\varepsilon_L = \varepsilon_R = 1$. (a) is calculated by the intuitive method with the ABC, and (b) is by the correlation function method.

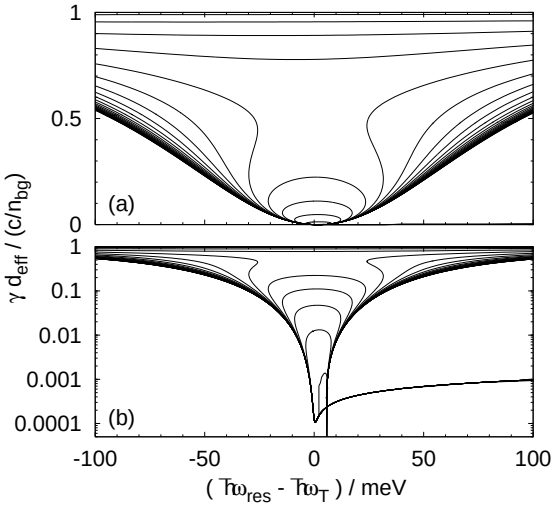

Figure 3.8: Frequency dependence of apparent propagation speed $\gamma d_{\rm eff}$ in the case of $\varepsilon_L = \varepsilon_R = 1$. This is calculated by the intuitive method with ABC.

3.8 General properties

It is worth to note that the breakdown condition, Eq. (3.57), may be applied to general situations, for example, a excitonic layer in cavity, multiple layers separated by a transparent layer, a sphere as discussed by Ajiki [35], and photonic crystal structures. This is because Eq. (3.57) is simply derived from the dispersion relation, Eq. (3.34), which includes no information outside of the excitonic medium. For a demonstration of the generality, I verify the breakdown condition for a CuCl film in vacuum, i.e., $\varepsilon_L = \varepsilon_R = 1$. Fig. 3.7 shows the thickness dependence of (a) $\gamma d_{\rm eff}$ and (b) γ. The former is calculated by the intuitive method with ABC, and the latter is by the correlation function method. As the result of the multiple reflections inside of the film, the size enhancement of γ becomes more rapid and the crossover thickness becomes smaller compared to Fig. 3.1, where the outside dielectric constant is $\varepsilon_L = \varepsilon_R = \varepsilon_{\rm bg}$. In other words, $d_{\rm eff} = d/\alpha$ is enhanced by the multiple reflections obeying Eq. (3.45). However, we can find that the breakdown also occurs when $\gamma d_{\rm eff}$ reaches $c/2n_{\rm bg}$ as seen in Fig. 3.7(a). On the other hand, Fig. 3.8 shows the frequency dependence of $\gamma d_{\rm eff}$, and it also reflects the crossover from the exciton-/photon-like modes to polariton ones as discussed above.

For a large thickness where the polariton scheme is valid, at the phase-matching condition $k = n_{\rm bg}\omega_{\rm T}/c$, the resonance frequency has the same value as bulk polariton as

$$\omega \simeq \omega_{\rm T} \pm \omega_{\rm T}\sqrt{\frac{\omega_{\rm LT}}{2\omega_{\rm T}}}, \tag{3.58}$$

which is approximately obtained from Eq. (3.49). On the other hand, the crossover thickness is obtained from the condition that Eq. (3.54) has the degenerate solution:

$$d/\alpha = \frac{c}{n_{\rm bg}\sqrt{2\omega_{\rm T}\omega_{\rm LT}}} = \frac{\lambda}{2\pi}\sqrt{\frac{\omega_{\rm T}}{2\omega_{\rm LT}}}, \tag{3.59}$$

where $\lambda = 2\pi c/n_{\rm bg}\omega_{\rm T}$. Therefore, the maximum value of γ of the superradiant mode is derived as

$$\gamma = \frac{c/2n_{\rm bg}}{d/\alpha} = \omega_{\rm T}\sqrt{\frac{\omega_{\rm LT}}{2\omega_{\rm T}}}. \tag{3.60}$$

This is just the frequency shift of bulk polariton at $k = n_{\rm bg}\omega_{\rm T}/c$ as seen in Eq. (3.58). For the CuCl crystal, the frequency shift is about 80 meV as seen in Fig. 3.4(a), and Eq. (3.60) can be verified in Fig. 3.1(b) and Fig. 3.7(b), although more large γ is obtained for polariton modes just after the crossover, and also much larger γ is obtained for photon-like modes at small thickness. However, in order to obtain a strong and rapid nonlinear optical response, we must also consider the ratio of exciton component in these exciton-photon coupled modes, and discuss the most suitable thickness that gives both the large exciton nonlinearity and the rapid radiative decay.

3.9 Summary

I calculate the resonance frequency and radiative decay rate of exciton-photon coupled modes in a film with finite thickness from weak- to strong-coupling scheme or from the exciton superradiance to the polariton regime. One of the calculation methods is based on the exciton correlation function tensor renormalizing the exciton-photon interaction in finite system, and I show that the exciton superradiance is suppressed after a particular thickness, which reflects the crossover of exciton-photon coupled modes from exciton-/photon-like to polariton ones as indicated by Björk et al. [94]. In order to elucidate the crossover condition, I use another calculation method based on the dispersion relation in excitonic medium and the self-sustaining condition for the complex frequency and wavenumber. In addition to reproducing the calculation results of the former method, this method also provides the photon-like modes for all thickness from weak- to strong-coupling scheme. By analyzing the dispersion relation, I obtain the crossover condition, Eq. (3.57), of the exciton-photon coupled modes. This condition means that the crossover occurs when the apparent propagation speed of superradiant exciton reaches the group velocity of polariton. In other words, the photon emitted by electron-hole recombination cannot propagate beyond the group velocity without the reabsorption. Further, this crossover condition may be a general condition because its derivation needs no information outside of the excitonic medium.

Chapter 4

Correlation Functions in Exciton-Photon Inhomogeneous System

One of the main achievements of the QED theory for excitons explained in Chap. 2 (or the semiclassical microscopic nonlocal theory [31]) is providing the retarded correlation functions of excitons in exciton-photon inhomogeneous system. While it is a powerful tool for discussing nano-structured materials where exciton center-of-mass motion is confined, its calculation method is not suited for macroscopic materials because we must consider much number of center-of-mass motion states of excitons. On the other hand, in the traditional calculation method connecting the electromagnetic fields in different media by the Maxwell boundary conditions and some additional boundary conditions (ABCs), there are usually only a few variables to be determined, and the number of unknowns is fixed regardless of the material size. The subject of this chapter is to derive the analytical expression of the exciton correlation functions from the information of the exciton-photon coupled modes discussed in Chap. 3, whose complex frequencies and wavenumbers are calculated from the dispersion relation and the resonance condition described by a boundary problem with ABCs.

4.1 Introduction

It is well known that the classical electromagnetism is completely described by the Maxwell equations together with the Lorentz force law. However, in boundary problems for connecting the electromagnetic fields between different media, we sometimes require additional boundary conditions (ABCs; see Ref. 22 or Sec. 1.4.2 in this thesis) in addition to the Maxwell boundary conditions, which are derived from the Maxwell equations. This ABC problem emerges when we consider the materials that have multiple light modes for a given frequency. The ABC problem was first pointed out by Pekar [67] for exciton-polariton systems with exciton center-of-mass kinetic energy, and the subsequent studies have elucidated that ABCs are uniquely obtained for the exciton center-of-mass wavefunctions that microscopically determined in finite system with interfaces [70, 71, 72, 101], although ABCs are frequently introduced for analyzing experimental results by phenomenological calculations. However, only a few ABCs have been derived by such first-principle calculations, and a calculation method for deriving ABCs for general boundary problems has not been established. On the other hand, some calculation methods without deriving ABCs have already been established, and they are called ABC-Free theory [29] or microscopic nonlocal theory [30, 31]. Based on the same idea of these theories, I have constructed a quantum electrodynamics (QED) theory for excitons in inhomogeneous systems (see Ref. 78 or Chap. 2). These nonlocal theories can

be applied to general problems for given set of elementary excitations in finite system, and a boundary problem is reduced to a simultaneous linear equation set.

However, in other words, the present QED theory and the semiclassical microscopic nonlocal theory require the complete set of elementary excitations in excitonic materials in principle, and, in order to derive exciton correlation functions renormalizing the interaction with the electromagnetic fields, we must calculate the inverse of a large matrix whose size is the number of all excitation states. One method for reducing the matrix size is describing the contribution from non-resonant excitations, such as phonons and higher excitons, by the background dielectric function in the Maxwell equations as $\varepsilon = \varepsilon_{\rm bg} + \chi_{\rm ex}$. However, even by using this technique, we must consider large number of exciton center-of-mass motion states in order to discuss macroscopic materials in contrast to the ABC method, where only a few unknowns are considered regardless of the material size. Here, we should pay attention to the fact that, in Chap. 3, the exciton-photon coupled modes could be calculated by the intuitive method based on the dispersion relation in excitonic medium and the resonance condition described by a boundary problem with ABCs. This intuitive method actually provided the calculation results obtained by the matrix method of the microscopic nonlocal theory, and has a few unknown variables to be considered. Therefore, there should be a simple calculation technique providing the same information as obtained by the microscopic nonlocal theory, especially the retarded correlation functions of excitons, from the calculation results of boundary problems with ABCs.

As such works connecting the two calculation frameworks, i.e., ABC theory and microscopic nonlocal theory (ABC-free theory), the equivalent expressions of the electric field were derived from the two frameworks for semi-infinite and slab systems in Refs. 29 and 102, respectively. Further, in the case of spherical semiconductor nanocrystal, spectra of its cross section were calculated by ABC theory and by the microscopic nonlocal theory in Refs. 76 and 77, and a good agreement between the two results has been verified. The subject of this chapter is to derive the analytical expression of the exciton correlation functions in exciton-photon inhomogeneous systems from the calculation results of boundary problem with ABCs, which do not require the complicated calculation of large matrices. The analytical expression is applicable to deriving the time-ordered and thermal correlation functions by the analytical continuation with the retarded ones. Therefore, the calculation method of this chapter is useful not only for reducing the calculation time but also for the perturbation technique based on the Feynman diagrams. However, we should pay attention the fact that, in the boundary problem, we must use the ABC properly determined from the exciton center-of-mass wavefunctions. In other words, if the ABC cannot be derived from considering set of elementary excitations, the correlation functions cannot be calculated by the present method explained in the following sections. In this chapter, the exciton center-of-mass wavefunctions are assumed as sinusoidal functions whose amplitude is zero at interfaces. Therefore, I can use Pekar's ABC [67] for the boundary problem according to the discussion in Ref. 72.

4.2 Bare correlation functions

I consider a material where the translational symmetry is broken in the z direction, and s-polarized excitons are weakly confined in a finite region. For simplicity, I consider only one relative exciton state with eigenfrequency $\omega_{\rm T}$, and denote the center-of-mass motion by index m. In the present paper, I simply

consider that the exciton is a pure boson, and the system is linear as

$$\hat{H}_{\rm ex} = \sum_m \hbar\Omega_m \hat{b}_m^\dagger \hat{b}_m, \tag{4.1}$$

where $\hat{b}_m$ is the annihilation operator of an exciton in state m, and Ω_m is the eigenfrequency including the center-of-mass kinetic energy. On the other hand, I consider the interaction between the excitons and the electromagnetic fields as

$$\hat{H}_{\rm int} = -\int {\rm d}z\ \hat{E}(z)\hat{P}(z), \tag{4.2}$$

where $\hat{E}(z)$ is the electric field and

$$\hat{P}(z) = \sum_m \mathcal{P} g_m(z)\hat{b}_m + {\rm H.c.}, \tag{4.3}$$

is the excitonic polarization density. The coefficient $\mathcal{P}$ has the relation with the longitudinal-transverse (LT) splitting energy of excitons as $\hbar\omega_{\rm LT} = |\mathcal{P}|^2/\varepsilon_{\rm bg}\varepsilon_0$, and $g_m(z)$ is the exciton center-of-mass wavefunction. The whole Hamiltonian is written as

$$\hat{H} = \hat{H}_{\rm ex} + \hat{H}_{\rm int} + \hat{H}_{\rm em}, \tag{4.4}$$

and $\hat{H}_{\rm em}$ describes the electromagnetic fields and the background dielectrics as treated in the QED theory of excitons (see Chap. 2), and it provides the Maxwell wave equation with quantum fluctuation as discussed in the QED theory of dispersive and absorptive media [21, 18].

I suppose a background system characterized by dielectric function $\varepsilon_{\rm bg}(z,\omega)$ and a resonant contribution from excitons inducing polarization $P(z,\omega)$. The Maxwell wave equation for $\hat{E}(z,\omega)$ is represented as

$$\left[(\partial^2/\partial z^2) + q^2(z,\omega)\right] E(z,\omega) = -\mu_0\omega^2 P(z,\omega), \tag{4.5}$$

where $q^2(z,\omega) = \varepsilon_{\rm bg}(z,\omega)\omega^2/c^2 - {k_\parallel}^2$ and $k_\parallel$ is the in-plane wavenumber. This wave equation can be rewritten as

$$E(z,\omega) = E_0(z,\omega) - \mu_0\omega^2 \int {\rm d}z'\ G(z,z',\omega)P(z',\omega), \tag{4.6}$$

where $E_0(z,\omega)$ is the homogeneous solution of Eq. (4.5), and $G(z,z',\omega)$ is the Green function satisfying

$$\left[(\partial^2/\partial z^2) + q^2(z,\omega)\right] G(z,z',\omega) = \delta(z-z'). \tag{4.7}$$

On the other hand, since the expectation value $E = \langle\hat{E}\rangle$ of the electric field is given in the same form as Eq. (4.6) according to the linear response theory, the retarded correlation function of $\hat{E}$ in the $\hat{H}_{\rm em}$ system corresponds to the Green's function satisfying Eq. (4.7) as discussed in Chap. 6 of Ref. 53:

$$\mu_0\omega^2 G(z,z',\omega) = \int_0^\infty {\rm d}t\ \frac{{\rm e}^{{\rm i}\omega t}}{{\rm i}\hbar} \left\langle[\hat{E}_0(z,t), \hat{E}_0(z',0)]\right\rangle_{\rm em}, \tag{4.8}$$

where the time representation of the electric field is defined as

$$\hat{E}_0(z,t) \equiv {\rm e}^{{\rm i}\hat{H}_{\rm em}t/\hbar}\hat{E}(z){\rm e}^{-{\rm i}\hat{H}_{\rm em}t/\hbar}. \tag{4.9}$$

Furthermore, under the rotating wave approximation (RWA), $G(z,z',\omega)$ is also equal to the time-ordered correlation function of $\hat{E}$:

$$\mu_0\omega^2 G(z,z',\omega) \simeq \int_{-\infty}^\infty {\rm d}t\ \frac{{\rm e}^{{\rm i}\omega t}}{{\rm i}\hbar} \left\langle {\rm T}\hat{E}_0(z,t)\hat{E}_0(z',0)\right\rangle_{\rm em}, \tag{4.10}$$

where T is the time-ordering operator. Therefore, under the RWA, the correlation function of $\hat{E}$ in the background system can be obtained by finding the Green function satisfying Eq. (4.7), which has already been known for general multilayer systems [65] (or see App. D).

Next, I discuss the correlation functions of exciton. The exciton correlation function in $\hat{H}_{\rm ex}$ system is derived as

$$\begin{aligned}\mathfrak{G}^{\mathrm{R}(0)}_{m,m'}(\omega) &= \frac{1}{\mathrm{i}\hbar}\int_0^\infty \mathrm{d}t\ \mathrm{e}^{\mathrm{i}\omega t}\,\langle[\hat{b}^{(0)}_m(t), \hat{b}^{(0)\dagger}_{m'}(0)]\rangle_{\rm ex} \\ &= \frac{\delta_{m,m'}}{\hbar(\omega - \Omega_m + \mathrm{i}\delta)},\end{aligned} \tag{4.11}$$

where the time representation is written as

$$\hat{b}^{(0)}_m(t) \equiv \mathrm{e}^{\mathrm{i}\hat{H}_{\rm ex}t/\hbar}\hat{b}_m\mathrm{e}^{-\mathrm{i}\hat{H}_{\rm ex}t/\hbar}, \tag{4.12a}$$

$$\hat{b}^{(0)\dagger}_m(t) \equiv \mathrm{e}^{\mathrm{i}\hat{H}_{\rm ex}t/\hbar}\hat{b}^\dagger_m\mathrm{e}^{-\mathrm{i}\hat{H}_{\rm ex}t/\hbar}. \tag{4.12b}$$

This function is identical to the time-ordered exciton correlation function as long as we do not consider the interaction with the electromagnetic fields:

$$\mathfrak{G}^{\mathrm{R}(0)}_{m,m'}(\omega) = \mathfrak{G}^{(0)}_{m,m'}(\omega) = \int_{-\infty}^\infty \mathrm{d}t\ \frac{\mathrm{e}^{\mathrm{i}\omega t}}{\mathrm{i}\hbar}\,\langle[\hat{b}^{(0)}_m(t), \hat{b}^{(0)\dagger}_{m'}(0)]\rangle_{\rm ex}\,. \tag{4.13}$$

According to the linear response theory, the excitonic contribution in the optical susceptibility is derived as a nonlocal from as [31, 78]

$$\begin{aligned}\chi(z,z',\omega) &= \frac{-1}{\mathrm{i}\hbar\varepsilon_0}\int_0^\infty \mathrm{d}t\ \mathrm{e}^{\mathrm{i}\omega t}\,\langle[\hat{P}_0(z,t), \hat{P}_0(z',0)]\rangle_{\rm ex}\,, \\ &= \varepsilon_{\rm bg}\omega_{\rm LT}\sum_m\left[\frac{g_m(z)g^*_m(z')}{\Omega_m - \omega - \mathrm{i}\delta} + \frac{g^*_m(z)g_m(z')}{\Omega_m + \omega + \mathrm{i}\delta}\right].\end{aligned} \tag{4.14}$$

This susceptibility characterizes $\hat{P}(z,\omega)$ at position z induced by $\hat{E}(z',\omega)$ at another position z' as

$$P(z,\omega) = \varepsilon_0\int_{-\infty}^\infty \mathrm{d}z'\ \chi(z,z',\omega)E(z',\omega). \tag{4.15}$$

Here, in the case of bulk system, we can consider the exciton center-of-mass wavefunction as $g_m = \mathrm{e}^{\mathrm{i}k_m z}/\sqrt{L}$, where L is the normalization length and $k_m = 2\pi m/L$ for $m = 0,\ \pm1,\ \pm2,\ \ldots$. In this situation, the nonlocal susceptibility [Eq. (4.14)] is diagonal in the k-space, but it depends not only on ω but also on k due to the nonlocality as

$$\begin{aligned}\chi(k,k',\omega) &= \frac{1}{L}\int_{-\infty}^\infty \mathrm{d}z\int_{-\infty}^\infty \mathrm{d}z'\ \mathrm{e}^{-\mathrm{i}kz}\chi(z,z',\omega)\mathrm{e}^{\mathrm{i}k'z'} \\ &= \delta_{k,k'}\frac{2\varepsilon_{\rm bg}\omega_{\rm LT}\Omega(k)}{\Omega(k)^2 - (\omega + \mathrm{i}\delta)^2} = \delta_{k,k'}\chi(k,\omega),\end{aligned} \tag{4.16}$$

where I suppose $\Omega(k) = \Omega(-k)$ for simplicity. Substituting Eqs. (4.15) and (4.16) into the Maxwell wave equation [Eq. (4.5)], we can obtain the polariton dispersion relation in bulk system as

$$\frac{c^2({k_\parallel}^2 + k^2)}{\omega^2} = \varepsilon_{\rm bg} + \chi(k,\omega). \tag{4.17}$$

4.3 Correlation functions in homogeneous system

First, I discuss the exciton correlation functions in the homogeneous exciton-photon system, i.e., in the infinite system. Due to the translational symmetry in the z direction, the wavenumber k is a good quantum number as well as the one in x-y plane, and the exciton center-of-mass motion should be represented as a plane wave as $g_k(z) = \mathrm{e}^{\mathrm{i}kz}/\sqrt{L}$. Therefore, it is convenient to describe all the physical quantities in the k-space as

$$\hat{E}_k \equiv \int_{-\infty}^{\infty} \mathrm{d}z \, \frac{\mathrm{e}^{-\mathrm{i}kz}}{\sqrt{L}} \hat{E}(z), \tag{4.18}$$

$$\hat{P}_k \equiv \int_{-\infty}^{\infty} \mathrm{d}z \, \frac{\mathrm{e}^{-\mathrm{i}kz}}{\sqrt{L}} \hat{P}(z) = \mathcal{P}\hat{b}_k + \mathcal{P}^*\hat{b}^\dagger_{-k}. \tag{4.19}$$

Further, the interaction Hamiltonian, Eq. (4.2), is rewritten as

$$\hat{H}_{\mathrm{int}} = -\sum_k \hat{P}_k \hat{E}_{-k}, \tag{4.20}$$

and also the exciton Hamiltonian, Eq. (4.1), is represented as

$$\hat{H}_{\mathrm{ex}} = \sum_k \hbar\Omega(k) \, \hat{b}^\dagger_k \, \hat{b}_k. \tag{4.21}$$

From these Hamiltonians, the Heisenberg equation of excitons is derived as

$$\mathrm{i}\hbar\frac{\partial}{\partial t}\hat{b}_k(t) = \hbar\Omega(k)\hat{b}_k(t) - \mathcal{P}^*\hat{E}_k(t), \tag{4.22}$$

and the ω-representation of the expectation $\langle\hat{b}_k(t)\rangle$ is obtained as

$$[\Omega(k) - \omega - \mathrm{i}\delta] \, \langle\hat{b}_k(\omega)\rangle = \mathcal{P}^* E_k(\omega)/\hbar, \tag{4.23}$$

where δ means the infinitesimal damping and its fluctuation operator disappears by taking the expectation. On the other hand, in the homogeneous case, $\varepsilon_{\mathrm{bg}}(z) = \varepsilon_{\mathrm{bg}}$, the Green's function $G(z, z', \omega)$ satisfying Eq. (4.7) is diagonal in the k-space, and easily derived as

$$G_{k,k'}(\omega) \equiv \frac{1}{L}\int_{-\infty}^{\infty}\mathrm{d}z\int_{-\infty}^{\infty}\mathrm{d}z' \, \mathrm{e}^{-\mathrm{i}kz}G(z,z',\omega)\mathrm{e}^{\mathrm{i}k'z'} = \frac{\delta_{k,k'}}{(q+\mathrm{i}\delta)^2 - k^2}. \tag{4.24}$$

Therefore, Eq. (4.6) is rewritten as

$$E_k(\omega) = E_0(k,\omega) - \mu_0\omega^2 \frac{\mathcal{P}\,\langle\hat{b}_k(\omega)\rangle + \mathcal{P}^*\,\langle\hat{b}^\dagger_{-k}(\omega)\rangle}{(q+\mathrm{i}\delta)^2 - k^2}. \tag{4.25}$$

Substituting this into Eq. (4.23), the self-consistent equation for the exciton amplitude is obtained as

$$[\Omega(k) + \Sigma_k(\omega) - \omega - \mathrm{i}\delta] \, \langle\hat{b}_k(\omega)\rangle + \mathrm{e}^{-\mathrm{i}2\theta}\Sigma_k(\omega) \, \langle\hat{b}^\dagger_{-k}(\omega)\rangle = \mathcal{P}^* E_0(k,\omega)/\hbar, \tag{4.26}$$

where θ is the phase of $\mathcal{P}$, and the self-energy $\Sigma_k(\omega)$ is represented as

$$\Sigma_k(\omega) = \frac{\omega_{\mathrm{LT}}\omega^2}{(\omega+\mathrm{i}\delta)^2 - v^2k^2}, \tag{4.27}$$

where $v \equiv c/\sqrt{\varepsilon_{\mathrm{bg}}}$ is the light speed in the background medium. Further, together with the equation for $\hat{b}^\dagger_{-k}(\omega) = \{\hat{b}_{-k}(-\omega^*)\}^\dagger$, this equation is rewritten as

$$\begin{bmatrix} \Omega(k) + \Sigma_k(\omega) - \omega - \mathrm{i}\delta & \mathrm{e}^{-\mathrm{i}2\theta}\Sigma_k(\omega) \\ \mathrm{e}^{\mathrm{i}2\theta}\Sigma_k(\omega) & \Omega(k) + \Sigma_k(\omega) + \omega + \mathrm{i}\delta \end{bmatrix} \begin{bmatrix} \langle\hat{b}_k(\omega)\rangle \\ \langle\hat{b}^\dagger_{-k}(\omega)\rangle \end{bmatrix} = \begin{bmatrix} \mathcal{P}^* \\ \mathcal{P} \end{bmatrix} E_0(k,\omega)/\hbar, \tag{4.28}$$

and, according to the linear response theory, the retarded correlation functions of excitons are obtained as the inverse of the coefficient matrix as

$$\begin{bmatrix} \mathfrak{G}^{\mathrm{R}}_{11,k}(\omega) & \mathfrak{G}^{\mathrm{R}}_{12,k}(\omega) \\ \mathfrak{G}^{\mathrm{R}}_{21,k}(\omega) & \mathfrak{G}^{\mathrm{R}}_{22,k}(\omega) \end{bmatrix} = \frac{-1/\hbar}{\Omega(k)^2 - (\omega + \mathrm{i}\delta)^2 + 2\Omega(k)\Sigma_k(\omega)} \times \begin{bmatrix} \Omega(k) + \Sigma_k(\omega) + \omega + \mathrm{i}\delta & -\mathrm{e}^{-\mathrm{i}2\theta}\Sigma_k(\omega) \\ -\mathrm{e}^{\mathrm{i}2\theta}\Sigma_k(\omega) & \Omega(k) + \Sigma_k(\omega) - \omega - \mathrm{i}\delta \end{bmatrix}, \tag{4.29}$$

where these correlation functions are defined as

$$\mathrm{i}\hbar\mathfrak{G}^{\mathrm{R}}_{11,k}(t-t') \equiv \theta(t-t')\left\langle[\hat{b}_k(t), \hat{b}^\dagger_k(t')]\right\rangle, \tag{4.30a}$$

$$\mathrm{i}\hbar\mathfrak{G}^{\mathrm{R}}_{12,k}(t-t') \equiv \theta(t-t')\left\langle[\hat{b}_k(t), \hat{b}_{-k}(t')]\right\rangle, \tag{4.30b}$$

$$\mathrm{i}\hbar\mathfrak{G}^{\mathrm{R}}_{21,k}(t-t') \equiv \theta(t-t')\left\langle[\hat{b}^\dagger_{-k}(t), \hat{b}^\dagger_k(t')]\right\rangle, \tag{4.30c}$$

$$\mathrm{i}\hbar\mathfrak{G}^{\mathrm{R}}_{22,k}(t-t') \equiv \theta(t-t')\left\langle[\hat{b}^\dagger_{-k}(t), \hat{b}_{-k}(t')]\right\rangle. \tag{4.30d}$$

4.4 Correlation functions in inhomogeneous system

Next, I discuss the correlation functions in exciton-photon inhomogeneous system. Due to the interaction with the electromagnetic fields, the bare center-of-mass motion states of excitons are not diagonalized in such systems, although the wavenumber is a good quantum number in homogeneous system as discussed in the previous section. Therefore, I represent the correlation function as the matrix form $\mathfrak{G}^{\mathrm{R}}_{ij}(\omega)$ on basis of the center-of-mass motion states, where $i, j = \{1, 2\}$ are the indices used in Eqs. (4.30). As the result of Ref. 78, the retarded correlation functions in inhomogeneous system is obtained by the matrix inversion as

$$\begin{bmatrix} \mathfrak{G}^{\mathrm{R}}_{11}(\omega) & \mathfrak{G}^{\mathrm{R}}_{12}(\omega) \\ \mathfrak{G}^{\mathrm{R}}_{21}(\omega) & \mathfrak{G}^{\mathrm{R}}_{22}(\omega) \end{bmatrix}^{-1} = -\hbar \begin{bmatrix} \mathbf{S}(\omega) & \mathbf{\Sigma}'(\omega) \\ \{\mathbf{\Sigma}'(-\omega^*)\}^* & \{\mathbf{S}(-\omega^*)\}^* \end{bmatrix} \tag{4.31}$$

the matrix $\mathbf{S}(\omega)$ is defined as

$$S_{m,m'} \equiv (\Omega_m - \omega - \mathrm{i}\delta)\delta_{m,m'} + \Sigma_{m,m'}(\omega). \tag{4.32}$$

Further, the self-energy tensors $\mathbf{\Sigma}(\omega)$ and $\mathbf{\Sigma}'(\omega)$ are derived as

$$\Sigma_{m,m'}(\omega) = \varepsilon_{\mathrm{bg}}\omega_{\mathrm{LT}}(\omega/c)^2 \int_{-\infty}^{\infty}\mathrm{d}z \int_{-\infty}^{\infty}\mathrm{d}z'\; g^*_m(z)G(z,z',\omega)g_{m'}(z'), \tag{4.33a}$$

$$\Sigma'_{m,m'}(\omega) = \mathrm{e}^{-\mathrm{i}2\theta}\varepsilon_{\mathrm{bg}}\omega_{\mathrm{LT}}(\omega/c)^2 \int_{-\infty}^{\infty}\mathrm{d}z \int_{-\infty}^{\infty}\mathrm{d}z'\; g^*_m(z)G(z,z',\omega)g^*_{m'}(z'). \tag{4.33b}$$

These describe the retarded interaction not only between the same exciton states ($m = m'$) but also between the different states ($m \neq m'$).

In a numerical demonstration, I consider a CuCl film with thickness d, and suppose the background dielectric constant $\varepsilon_{\mathrm{bg}} = {n_{\mathrm{bg}}}^2 = 5.59$ inside of the film. In the case that the background is a homogeneous medium, $\varepsilon_{\mathrm{bg}}(z) = \varepsilon_{\mathrm{bg}}$, the Green's function satisfying Eq. (4.7) is obtained by the Fourier transform of Eq. (4.24) as

$$G(z,z',\omega) = \frac{\mathrm{e}^{\mathrm{i}q|z-z'|}}{\mathrm{i}2q}. \tag{4.34}$$

On the other hand, as discussed in Ref. 65 (or in App. D), in general multilayer systems, the Green's function from a focusing layer to the same one is written as

$$\begin{aligned}\mathrm{i}2qG(z,z',\omega) = \mathrm{e}^{\mathrm{i}q|z-z'|} + \mathrm{e}^{\mathrm{i}qz}\tilde{R}_L\left[\mathrm{e}^{\mathrm{i}qz'} + \mathrm{e}^{\mathrm{i}qd}\tilde{R}_R\mathrm{e}^{\mathrm{i}q(d-z')}\right]\tilde{M} \\ + \mathrm{e}^{-\mathrm{i}q(z-d)}\tilde{R}_R\left[\mathrm{e}^{\mathrm{i}q(d-z')} + \mathrm{e}^{\mathrm{i}qd}\tilde{R}_L\mathrm{e}^{\mathrm{i}qz'}\right]\tilde{M},\end{aligned} \tag{4.35}$$

where I consider that the left interface of the focusing layer is at $z = 0$, and right at $z = d$. In Eq. (4.35), $\tilde{R}_{L/R}$ is the generalized reflection coefficient [65] from the focusing layer to the left-/right-hand interface, and $\tilde{M} = [1 - \tilde{R}_L \tilde{R}_R \mathrm{e}^{\mathrm{i}2qd}]^{-1}$. In the case of three-layer systems where the background dielectric constants are respectively given as ε_L, $\varepsilon_{\mathrm{bg}}$, and ε_R, when we focus on the middle layer, $\tilde{R}_{L/R}$ is simply expressed as the Fresnel reflection coefficient:

$$\tilde{R}_{L/R} = \frac{q - k_{L/R}}{q + k_{L/R}}, \tag{4.36}$$

where $k_{L/R}$ is the wavenumber in the left/right region:

$$k_{L/R} = \left[\varepsilon_{L/R}(\omega/c)^2 - {k_\parallel}^2\right]^{1/2}. \tag{4.37}$$

In this chapter, I discuss only the fields perpendicular to the layers, i.e., $k_\parallel = 0$, and I consider the wavefunctions of the exciton center-of-mass motion as sinusoidal functions whose amplitudes are zero at the interfaces of the focusing layer:

$$g_m(z) = \begin{cases} \sqrt{2/d}\sin(k_m z) & 0 < z < d \\ 0 & \text{otherwise} \end{cases} \tag{4.38}$$

where $k_m = m\pi/d$, $m = 1, 2, \ldots$. The exciton translational mass is $m_{\mathrm{ex}} = 2.3m_0$, where m_0 is the free electron mass. The bare exciton frequencies are given as $\hbar\omega_{\mathrm{T}} = 3.2022$ eV and $\Omega_m = \omega_{\mathrm{T}} + \hbar {k_m}^2/2m_{\mathrm{ex}}$. The LT splitting energy is $\hbar\omega_{\mathrm{LT}} = 5.7$ meV.

4.5 Analytical expression of correlation functions

As explained in Sec. 4.1, in principle, the nonlocal theory requires the complete set of elementary excitations in excitonic materials, and, in order to derive the exciton correlation functions, we must numerically calculate the inverse of a large matrix whose size is the number of all excitation states. Therefore, even by using the technique describing nonresonant contributions as background media, a large number of exciton center-of-mass motion states must be considered in order to discuss macroscopic materials. For example, in the case of CuCl film with 1 μm thickness, about 500 states of exciton center-of-mass motion must be considered for good numerical precision. The required number of states is doubled, if we double the film thickness. On the other hand, as discussed in Chap. 3, the poles of the correlation functions can be calculated from the dispersion relation and self-sustaining condition with ABC, which do not require the numerical calculation of large matrices.

As seen in Eq. (4.29), the divergence condition of the correlation function in bulk system is written as $\Omega(k)^2 - (\omega + \mathrm{i}\delta)^2 + 2\Omega(k)\Sigma_k(\omega) = 0$, and we can find that it is just identical to Eq. (4.17), the dispersion relation of bulk polaritons. Therefore, the pole $\tilde{\omega} = \omega_{\mathrm{res}} - \mathrm{i}\gamma$ of correlation functions in inhomogeneous system can be reflected by replacing k with the complex wavenumber $\tilde{k} = k - \mathrm{i}{d_{\mathrm{eff}}}^{-1}$, which satisfies Eq. (4.17) together with $\tilde{\omega}$. This means that the exciton correlation function $\mathfrak{G}^{\mathrm{R}}_{ij,mm'}(\omega)$ in inhomogeneous system could be represented with that in homogeneous system [$\mathfrak{G}^{\mathrm{R}}_{ij}(k,\omega)$, Eq. (4.29)] as

$$\mathfrak{G}^{\mathrm{R}}_{ij,mm'}(\omega) = \sum_\lambda \mathfrak{G}^{\mathrm{R}}_{ij}(\tilde{k}_{\lambda,1},\omega) C_\lambda v^*_m(\{\tilde{k}_{\lambda,i}\}) v_{m'}(\{\tilde{k}_{\lambda,i}\}), \tag{4.39}$$

where λ denotes an exciton-photon coupled mode, C_λ is the weight of exciton component in state λ, and $v_m(\{\tilde{k}_{\lambda,i}\})$ is the base transformation coefficient from λ to a exciton center-of-mass motion state m. In

the limit of infinite system, the coefficient should become $v_k(\{\tilde{k}_{\lambda,i}\}) = \delta_{k_\lambda,k}$, and then Eq. (4.39) becomes

$$\mathfrak{G}^{\mathrm{R}}_{ij,kk'}(\omega) = \delta_{k,k'}\mathfrak{G}^{\mathrm{R}}_{ij}(k,\omega)[C_{\mathrm{UBP}} + C_{\mathrm{LBP}}], \tag{4.40}$$

where C_{UBP} and C_{LBP} are the exciton components of upper and lower branch polariton states, respectively. When we consider $C_{\mathrm{UBP/LBP}}$ as the Hopfield coefficient [19], $C_{\mathrm{UBP}} + C_{\mathrm{LBP}} = 1$ is obtained, and then Eq. (4.40) becomes identical to the bulk one.

From Eq. (3.38), the field representation in the ABC problem of self-sustaining condition, the polariton field of an exciton-photon coupled mode λ should be written as

$$P(\{\tilde{k}_{\lambda,i}\}, z) = \sum_{i=1}^{2} \chi_{\lambda,i}\left[A_{\lambda,i}\mathrm{e}^{\mathrm{i}\tilde{k}_{\lambda,i}(z-d)} + B_{\lambda,i}\mathrm{e}^{-\mathrm{i}\tilde{k}_{\lambda,i}z}\right]. \tag{4.41}$$

Therefore, the transformation coefficient $v_m(\{\tilde{k}_{\lambda,i}\})$ is obtained as

$$v_m(\{\tilde{k}_{\lambda,i}\}) = \frac{1}{N_\lambda}\int_0^d \mathrm{d}z\ P(\{\tilde{k}_{\lambda,i}\}, z)g^*_m(z), \tag{4.42}$$

where N_λ is the factor for the normalization condition (without the orthogonality)

$$\sum_m v_m(\{\tilde{k}_{\lambda,i}\})v^*_m(\{\tilde{k}_{\lambda,i}\}) = 1. \tag{4.43}$$

Since I consider the exciton center-of-mass wavefunction as Eq. (4.38) , the coefficient is represented as

$$\begin{aligned} v_m(\{\tilde{k}_{\lambda,i}\}) &= \sum_{i=1}^{2}\frac{\chi_{\lambda,i}}{N_\lambda}\sqrt{\frac{2}{d}}\int_0^d \mathrm{d}z\left[A_{\lambda,i}\mathrm{e}^{\mathrm{i}\tilde{k}_{\lambda,i}(z-d)} + B_{\lambda,i}\mathrm{e}^{-\mathrm{i}\tilde{k}_{\lambda,i}z}\right]\sin(q_m z) \\ &= \sum_{i=1}^{2}\frac{\chi_{\lambda,i}}{N_\lambda}\sqrt{\frac{2}{d}}\left[(-1)^m A_{\lambda,i} - B_{\lambda,i}\right]\frac{q_m}{{\tilde{k}_{\lambda,i}}^2 - {q_m}^2}\left[\mathrm{e}^{-\mathrm{i}(\tilde{k}_{\lambda,i}-q_m)d} - 1\right], \end{aligned} \tag{4.44a}$$

$$v^*_m(\{\tilde{k}_{\lambda,i}\}) = \sum_{i=1}^{2}\frac{\chi_{\lambda,i}}{N_\lambda}\sqrt{\frac{2}{d}}\left[(-1)^m A_{\lambda,i} - B_{\lambda,i}\right]\frac{q_m}{{\tilde{k}_{\lambda,i}}^2 - {q_m}^2}\left[\mathrm{e}^{\mathrm{i}(\tilde{k}_{\lambda,i}-q_m)d} - 1\right]. \tag{4.44b}$$

Here, it is worth to note that we must not use the conjugate of the complex wavenumber $\tilde{k}_{\lambda,i}$ in the latter representation, and also $\chi_{\lambda,i}$, $A_{\lambda,i}$, and $B_{\lambda,i}$ are not changed, because they are determined by $\tilde{k}_{\lambda,i}$ and $\tilde{\omega}_\lambda$. Further, the normalization factor N_λ is determined from these representations for satisfying Eq. (4.43).

4.6 Numerical verification

As demonstrations, I numerically calculated the exciton correlation function $\mathfrak{G}^{\mathrm{R}}_{11,mm'}(\omega)$ by the matrix inversion method and from the phenomenologically introduced analytical expression, Eq. (4.39). Figs. 4.1 - 4.6 show the comparison of the two calculation results. In these calculations, I used Eq. (4.38) as the exciton center-of-mass wavefunction, and considered that the CuCl film is existing in vacuum. As seen in these figures, it can be said that Eq. (4.39) provides a good approximation of the exciton correlation functions for nano- to macro-scale thicknesses. However, as seen in Fig. 4.5, there are some deviations between the two calculation results. Although the deviations are five orders of magnitude smaller than the maximum value (about 10000 in Fig. 4.5), the deviation significantly modifies the spectra of correlation functions for nonresonant exciton states ($m = 3$, 12, and 61 are the resonant exciton states for $d = 100$, 1000, and 5000 nm, respectively). In the application of the analytical expression into the nonlinear and thermal processes of excitons in inhomogeneous systems, these deviations may significantly affect the calculation results.

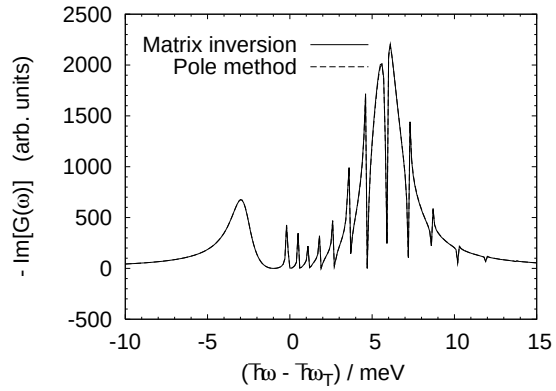

Figure 4.1: Imaginary part of exciton correlation function. $d = 100$ nm, $m = 1$, $m' = 1$.

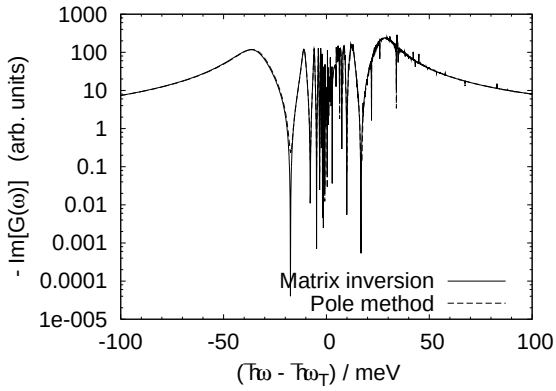

Figure 4.2: Imaginary part of exciton correlation function. $d = 1000$ nm, $m = 12$, $m' = 12$.

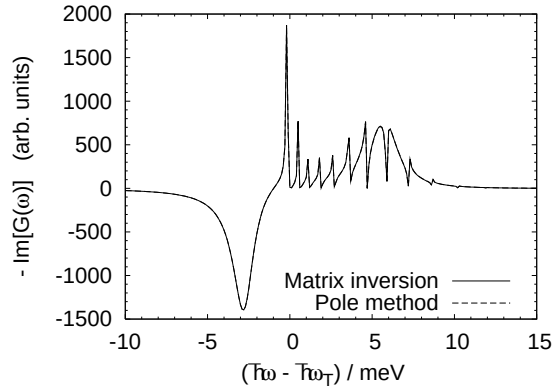

Figure 4.3: Imaginary part of exciton correlation function. $d = 100$ nm, $m = 1$, $m' = 3$.

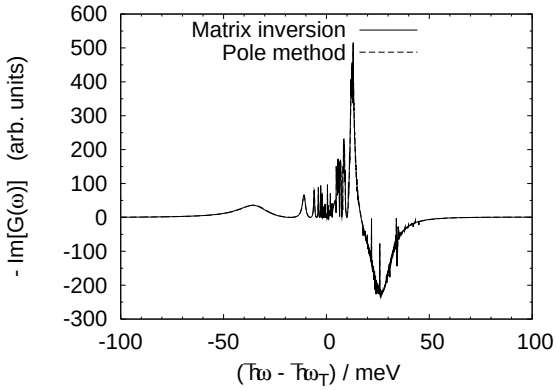

Figure 4.4: Imaginary part of exciton correlation function. $d = 1000$ nm, $m = 12$, $m' = 10$.

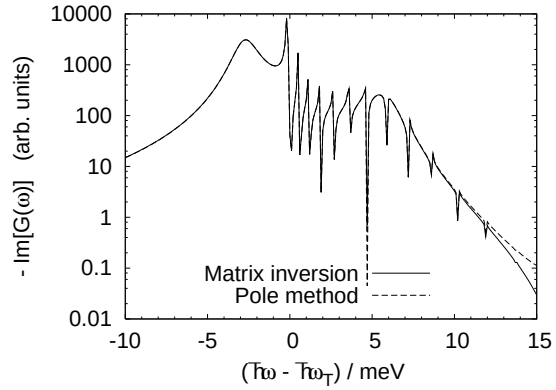

Figure 4.5: Imaginary part of exciton correlation function. $d = 100$ nm, $m = 3$, $m' = 3$.

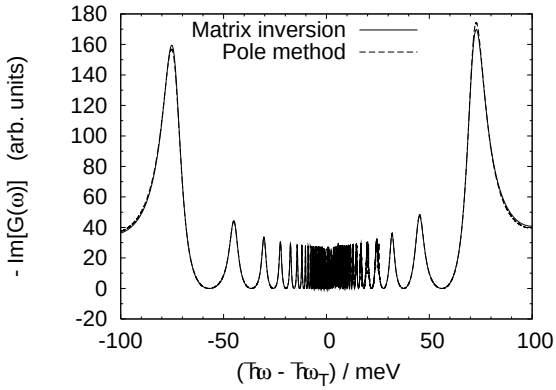

Figure 4.6: Imaginary part of exciton correlation function. $d = 5000$ nm, $m = 61$, $m' = 61$.

4.7 Discussion

In the matrix inversion method, the calculation time is proportional to the third power of the number of considered exciton states. In contrast, in the analytical method based on the poles of correlation functions, the calculation time is linearly proportional to the number of states when we calculate the poles $\{\tilde{\omega}_\lambda\}$ (or complex wavenumber $\{\tilde{k}_{\lambda,i}\}$) from the dispersion relation and the self-sustaining condition. However, there remains a little deviation from the results of the matrix inversion method. In order to remove the deviation, the analytical expression of the correlation functions should be systematically derived from Eq. (4.31), the strict expression, although Eq. (4.39) has been intuitively introduced in this thesis.

As part of the derivation of the analytical expression represented with the poles $\{\tilde{\omega}_\lambda\}$ or the complex wavenumbers $\{\tilde{k}_{\lambda,i}\}$, in Chap. 3, I numerically verified the equivalence between the correlation function method for calculating $\{\tilde{\omega}_\lambda\}$ and the intuitive method for the poles, which is based on the dispersion relation and the self-sustaining condition. The derivation of the analytical expression has close connections with the discussion of the microscopic derivation of ABCs [70, 71, 72] and also with the equivalence between ABC theory and ABC-Free theory (microscopic nonlocal theory) [29, 102]. From the detailed analytical calculations in these previous works, the equivalence of the two calculation methods for poles would be verified systematically, and also the analytical expression of correlation functions would be derived precisely. These tasks are essential for the perturbation calculations based on the correlation functions obtained in the present QED theory.

Although Pekar's ABC [67] was used for the actual calculations in this chapter, other ABCs can also be treated in the self-sustaining condition, if the ABCs have been properly derived from the microscopic viewpoint. In other words, in order to apply the present analytical method into practical problems in the future, the general derivation method of ABCs from given exciton center-of-mass wavefunctions should be established. Further, in addition to the excitonic layer considered in this chapter, the present method can be applied to other structures, such as multilayers, spheres, photonic crystals, and so on. If the analytical expression of the retarded correlation functions of excitons is properly obtained, the time-ordered and temperature correlation functions would be derived by the analytic continuation, and then the present method could be applied to the discussions of nonlinear and thermal processes in exciton-photon inhomogeneous systems.

Chapter 5

Conclusion

In the present thesis, for the future discussions of nonclassical light generation from condensed matters and of nonclassical states of exciton-polaritons, I have constructed (1) QED theory of excitons in inhomogeneous systems. Although I discussed the present QED theory only under the linear response scheme, this theory would extended to a calculation method applicable to general perturbation in the exciton-photon inhomogeneous systems, because the retarded correlation functions of excitons can be obtained by the present QED theory. In order to derive time-ordered and thermal correlation functions by the analytical continuation from the retarded ones, I tried to obtain the poles of the retarded correlation functions in the exciton-photon inhomogeneous system. A pole is characterized by a resonance frequency and a radiative decay rate, and, as a part of the discussion of the poles, I have explicitly elucidated the condition of (2) crossover of radiative decay schemes of excitons. Last, from the obtained information of the poles, I discussed (3) analytical expression of exciton correlation functions in the exciton-photon inhomogeneous systems for the future development of general perturbation theory. I summarize these topics in Sec. 5.1, and finally I suggest the remaining problems and the future perspectives in Sec. 5.2.

5.1 Summary

From the following three research works in this thesis, it can be said that a QED theory for excitons with center-of-mass motion and nonradiative damping in arbitrary-structured 3D systems has been established including the actual calculation method for practical materials. Further, although the present thesis concentrated on only the linear optical process of excitons, the present QED theory has already been applied to the theoretical study of entangled-photon generation from nano-structures [46], and also has a potential to provide a systematic calculation method for general perturbation in the exciton-photon inhomogeneous systems, because the exciton correlation functions can be obtained in the present theory.

(1) QED theory of excitons in inhomogeneous systems

I have constructed a QED theory for excitons whose center-of-mass motion is confined in arbitrary-structured 3D dielectrics, and therefore it can be applied to optical processes of excitons from nano-structures to bulk-like systems. This theory is based on the two theoretical frameworks: the series of QED theories for dispersive and absorptive dielectrics [21, 18], and the semiclassical microscopic nonlocal theory [31]. In the same line as the former, the present theory has a good correspondence with the fluctuation dissipation theorem, and it provides the retarded correlation functions of excitons and of electromagnetic fields in the inhomogeneous systems. Further, in the same line as the nonlocal theory,

the present theory reduces the problem into a linear equation set, although the previous QED theories [23, 24, 25, 26, 27, 28] for spatially-dispersive media are based on the Maxwell wave equations with nonlocal susceptibility, which is an integro-differential equation. Compared to the semiclassical nonlocal theory [31], the present theory considers the fluctuation operators due to the exciton and background nonradiative damping, which do not appear in the semiclassical framework.

(2) Crossover of radiative decay schemes of excitons

According to Fermi's golden rule, the radiative decay rate of excitons increases together with the crystal size (exciton superradiance). However, in a thick film where the exciton-polariton picture is suited, the decay rate is inversely proportional to the thickness, because the decay time should be proportional to the time of flight of polaritons. The present thesis explicitly provides the crossover condition between these two radiative decay schemes. The condition means that the crossover occurs when an apparent propagation speed of superradiant excitons reaches the group velocity of polaritons. In other words, the photon emitted by the electron-hole recombination cannot go outside of the film without reabsorption, when the propagation speed looks beyond the polariton group velocity. I used two methods to calculate the thickness dependence of the radiative decay rate and resonance frequency of exciton-photon coupled modes. One method is calculating the poles of exciton correlation functions, which are obtained by the present QED theory in Topic (1). The other is an intuitive method based on the dispersion relation and self-sustaining condition for the exciton-photon coupled mode, which is characterized by a complex frequency and a complex wavenumber. I verify that the latter method actually reproduces results of the former, and the crossover condition has been obtained by analyzing the dispersion relation of the latter.

(3) Correlation functions in exciton-photon inhomogeneous systems

While the retarded correlation functions of excitons are evaluated by matrix inversion in the present QED theory, I have shown an analytical expression of it, which is represented with the complex wavenumbers and wavefunctions of polariton fields obtained in Topic (2). The calculation of the poles can be performed in a finite time regardless of the crystal size, although, in the matrix inversion method, the calculation time increases together with the crystal size. I have numerically demonstrated that the analytical expression shows good agreement with the strict correlation functions calculated by the matrix inversion method. However, there remains a little deviation from the strict results. By deriving the precise analytical expression and obtaining time-ordered and thermal correlation functions, we can apply the present QED theory into nonlinear, relaxation, emission processes of excitons or exciton-polaritons in inhomogeneous systems. It is worth to note that the calculation method of poles is based on a boundary problem with ABCs, although ABCs are not required in the microscopic nonlocal theory in principle. This means that we must use proper ABCs corresponding to the considering center-of-mass wavefunctions in the pole calculation.

5.2 Remaining problems and future perspectives

As seen in Chap. 2, the present QED theory considers the excitons as pure bosons, and describes only its linear optical process under the discussion in the present thesis. In order to apply this theory into nonlinear or relaxation processes, we must introduce exciton-exciton interactions as performed in

the semiclassical framework [34, 37, 31] or in Ref. 46, where the entangled-photon generation from nanostructures has been discussed by using the present QED theory. While the phenomenological introduction of the exciton-exciton interactions is useful for simplicity and qualitative discussions, the representation of the interaction should also be derived from the non-bosonic property of excitons by considering a general electron-hole system as discussed in Refs. 103, 104, and 105. Although the exciton correlation functions obtained in the present QED theory is useful for discussing nonlinear and relaxation processes if the representation of the exciton-exciton interaction is properly obtained, the nonlinearity may not be described as the exciton-exciton interaction in particular problems. In such situations, we must rediscuss the present QED theory for non-bosonic excitons, and derive the correlation functions under the first-order perturbation in the exciton-photon interaction.

There is another problem whether the exciton-photon interaction should be represented as the product of current density and vector potential $\boldsymbol{J}(\boldsymbol{r})\cdot\boldsymbol{A}(\boldsymbol{r})$ or the one of polarization and electric field $\boldsymbol{P}(\boldsymbol{r})\cdot\boldsymbol{E}(\boldsymbol{r})$. As explained in Chap. 2, the latter representation includes the exchange interaction between electrons and holes or the dipole-dipole interaction, which is the origin of the exciton LT splitting. The present QED theory does not consider the second term of Eq. (2.2), which is proportional to the square of $\boldsymbol{A}(\boldsymbol{r})$, in deriving the motion equation of excitons. As the result of this approximation, I assume $\omega \simeq \omega_\mu$ in deriving Eq. (2.37), and the polariton dispersion relation [Eq. (3.34)] cannot be properly derived if only $\boldsymbol{J}(\boldsymbol{r})\cdot\boldsymbol{A}(\boldsymbol{r})$ is considered. On the other hand, although representation $\boldsymbol{P}(\boldsymbol{r})\cdot\boldsymbol{E}(\boldsymbol{r})$ correctly provides Eq. (3.34), its representation is only an approximation under the resonant linear optical process. This problem concerning the interaction representation should be discussed in detail by considering the gauge transformation as discussed in Ref. 16, or by considering $\boldsymbol{A}(\boldsymbol{r})^2$ term as in Refs. 19 and 31.

As seen in Chap. 3, the method based on the dispersion relation and the self-sustaining condition was intuitively introduced, although it exactly provides the same complex frequencies as calculated by the correlation function method in numerical precision. The equivalence of the two methods should be systematically verified by a detailed analysis of the correlation function method. Further, such analysis will provide a precise expression of the retarded correlation functions of excitons, while only its approximation was intuitively proposed in Chap. 4. In these analytical discussions, some calculation ideas would be obtained from the previous studies about the first-principle derivations of ABCs [70, 71, 72] and the equivalence between ABC theory and ABC-free theory (microscopic nonlocal theory) [29, 102]. Although, in the self-sustaining condition, we must use additional boundary conditions (ABCs) properly determined from the exciton eigenstates, only a few ABCs have been derived from the first-principle calculations. The general ABC derivation method should also be developed for the future applications.

From the precise expression of the retarded functions, the time-ordered and thermal ones are derived by the analytic continuation. The former can be applied to discussing general nonlinear processes by using the Feynman diagram technique, while the retarded and time-ordered correlation functions are identical under the rotating-wave approximation. On the other hand, the thermal correlation functions can be applied to, for example, the discussion of BEC of excitons or polaritons including the exciton-photon interaction in inhomogeneous systems. However, for such discussions, we must consider the quasi-thermal equilibrium state, where only the excitonic system is in equilibrium and the radiation one is not. When we simply connect to the thermal correlation function from the retarded one analytically, it represents the full equilibrium state including the radiation system, i.e., the thermal radiation. Therefore, the analytical continuation to the thermal correlation function in the quasi-equilibrium should also be developed for the future applications.

Appendix A

Retarded Correlation Function

Retarded correlation (Green's) function is an essential concept not only in this thesis but also in general physics. In this appendix, I explain its basic knowledge, i.e., the relation with the linear response theory, Kramers-Kronig relations, and Langevin equation.

A.1 Linear response theory

The linear response theory is the first-order perturbation theory providing physical quantities modulated by perturbation, and their coefficients are represented by the retarded correlation functions. More detailed discussions are shown in Chap. 5 of Ref. 106, Appendix 2 of Ref. 107, and many other textbooks.

I consider a perturbation H', an unperturbed system H_0, and the density matrix ρ_0 in thermal equilibrium of H_0 system. In the interaction representation, H' and the density matrix $\rho(t)$ in whole system are written as

$$\tilde{H}'(t) = \mathrm{e}^{\mathrm{i}H_0 t/\hbar} H' \mathrm{e}^{-\mathrm{i}H_0 t/\hbar}, \tag{A.1}$$

$$\tilde{\rho}_{\mathrm{int}}(t) = \mathrm{e}^{\mathrm{i}H_0 t/\hbar} \rho(t) \mathrm{e}^{-\mathrm{i}H_0 t/\hbar}, \tag{A.2}$$

and the density matrix is modulated by the perturbation as

$$\mathrm{i}\hbar \frac{\partial \tilde{\rho}_{\mathrm{int}}(t)}{\partial t} = \left[\tilde{H}'(t), \tilde{\rho}_{\mathrm{int}}(t)\right] \tag{A.3}$$

$$\tilde{\rho}_{\mathrm{int}}(t) = \rho_0 + \frac{1}{\mathrm{i}\hbar} \int_{-\infty}^{t} \mathrm{d}t' \left[\tilde{H}'(t'), \tilde{\rho}_{\mathrm{int}}(t')\right] \tag{A.4}$$

$$= \rho_0 + \frac{1}{\mathrm{i}\hbar} \int_{-\infty}^{t} \mathrm{d}t' \left[\tilde{H}'(t'), \rho_0\right] + O(H'^2). \tag{A.5}$$

Therefore, when we suppose the perturbation as the product of external field f and internal quantity B as

$$H' = Bf(t), \tag{A.6}$$

the expectation value of quantity A is derived in the first-order perturbation as

$$\langle A(t)\rangle \simeq \langle A\rangle_0 + \frac{1}{\mathrm{i}\hbar}\int_{-\infty}^{t} \mathrm{d}t'\ \mathrm{tr}\left\{\left[\tilde{H}'(t'),\rho_0\right]\tilde{A}(t)\right\} \tag{A.7}$$

$$= \langle A\rangle_0 + \frac{1}{\mathrm{i}\hbar}\int_{-\infty}^{t} \mathrm{d}t' \left\langle\left[\tilde{A}(t),\tilde{H}'(t')\right]\right\rangle_0 \tag{A.8}$$

$$= \langle A\rangle_0 + \frac{1}{\mathrm{i}\hbar}\int_{-\infty}^{t} \mathrm{d}t' \left\langle\left[\tilde{A}(t),\tilde{B}(t')\right]\right\rangle_0 f(t') \tag{A.9}$$

$$= \int_{-\infty}^{\infty} \mathrm{d}t'\ G^{\mathrm{R}}(t-t')f(t'), \tag{A.10}$$

where $G^{\mathrm{R}}(t-t')$ is the retarded correlation function between A and B:

$$G^{\mathrm{R}}(t-t') = \frac{\theta(t-t')}{\mathrm{i}\hbar}\left\langle\left[\tilde{A}(t),\tilde{B}(t')\right]\right\rangle_0. \tag{A.11}$$

Further, the Fourier transform of $A(t)$ is written as

$$\int_{-\infty}^{\infty}\mathrm{d}t\ \frac{\mathrm{e}^{\mathrm{i}\omega t}}{2\pi}\langle A(t)\rangle = \langle A(\omega)\rangle \simeq G^{\mathrm{R}}(\omega)f(\omega) = G^{\mathrm{R}}(\omega)\int_{-\infty}^{\infty}\mathrm{d}t\ \frac{\mathrm{e}^{\mathrm{i}\omega t}}{2\pi}f(t), \tag{A.12}$$

where the ω-representation of the retarded correlation function is defined as

$$G^{\mathrm{R}}(\omega) \equiv \int_{-\infty}^{\infty}\mathrm{d}t\ \mathrm{e}^{\mathrm{i}\omega(t-t')}G^{\mathrm{R}}(t-t') = \frac{1}{\mathrm{i}\hbar}\int_{t'}^{\infty}\mathrm{d}t\ \mathrm{e}^{\mathrm{i}\omega(t-t')}\left\langle\left[\tilde{A}(t),\tilde{B}(t')\right]\right\rangle_0. \tag{A.13}$$

We should pay attention to the fact that the factor $(2\pi)^{-1}$ does not appear in this definition in contrast to Eq. (A.12).

In this way, according to the linear response theory, by calculating the retarded correlation function (A.11) or (A.13), the expectation value of physical quantity A can be directly obtained from external field f as Eq. (A.10) or (A.12).

A.2 Kramers-Kronig Relations

As explained in the previous section, a retarded correlation function plays as a response function having the causality (providing a finite value only for $t > t'$). In this section, I explain the Kramers-Kronig relations, which is derived by the causality of response functions. More detailed discussions are shown in Sec. 7.10 of Ref. 68, Chap. XII of Ref. 50, and many other textbooks.

I consider the above response relations (A.10) and (A.12). First, if the response function $G^{\mathrm{R}}(t)$ is a real function, we obtain the following equation:

$$G^{\mathrm{R}}(\omega) = \{G^{\mathrm{R}}(-\omega^*)\}^* = G^{\mathrm{R}^*}(-\omega). \tag{A.14}$$

Further, when the frequency is complex as $\omega = \omega_1 + \mathrm{i}\omega_2$, $G^{\mathrm{R}}(\omega)$ [(A.13)] is a regular function for $\omega_2 > 0$ if $G^{\mathrm{R}}(t)$ is real and continuous, although $G^{\mathrm{R}}(\omega)$ diverges for $\omega_2 < 0$. This is because the real and imaginary parts of $G^{\mathrm{R}}(\omega) = G_1^{\mathrm{R}}(\omega) + \mathrm{i}G_2^{\mathrm{R}}(\omega)$ are written as

$$G_1^{\mathrm{R}}(\omega) = \int_0^{\infty}\mathrm{d}t\ \cos(\omega_1 t)\mathrm{e}^{-\omega_2 t}G^{\mathrm{R}}(t), \tag{A.15a}$$

$$G_2^{\mathrm{R}}(\omega) = \int_0^{\infty}\mathrm{d}t\ \sin(\omega_1 t)\mathrm{e}^{-\omega_2 t}G^{\mathrm{R}}(t), \tag{A.15b}$$

and then they satisfy the Cauchy-Riemann equations

$$\frac{\partial G_1^{\mathrm{R}}}{\partial \omega_1} = \frac{\partial G_2^{\mathrm{R}}}{\partial \omega_2}, \tag{A.16a}$$

$$\frac{\partial G_1^{\mathrm{R}}}{\partial \omega_2} = -\frac{\partial G_2^{\mathrm{R}}}{\partial \omega_1}. \tag{A.16b}$$

On the other hand, from the physical viewpoint, the response function $G^{\mathrm{R}}(t)$ should vanish in the limit of $t \to \infty$. Further, I consider $G^{\mathrm{R}}(t)$ is differentiable at $t = 0^+$. In this situation, by partially integrating Eq. (A.13), $G^{\mathrm{R}}(\omega)$ is written as

$$G^{\mathrm{R}}(\omega) = \left[\frac{\mathrm{i}G^{\mathrm{R}}(t)}{\omega} + \frac{1}{\omega^2} \frac{\mathrm{d}G^{\mathrm{R}}(t)}{\mathrm{d}t} + \cdots \right]_{t \to 0^+}. \tag{A.17}$$

Since the response function gives $G^{\mathrm{R}}(0^-) = 0$ for the causality, we obtain $G^{\mathrm{R}}(0^+) = 0$ owing to the continuity. Therefore, the first term of (A.17) is zero, and we obtain for enoughly large ω as

$$G_1^{\mathrm{R}}(\omega) = O(\omega^{-2}), \tag{A.18a}$$

$$G_2^{\mathrm{R}}(\omega) = O(\omega^{-3}). \tag{A.18b}$$

As the result, $G^{\mathrm{R}}(\omega)$ vanishes in the limit of $|\omega| \to \infty$.

Since $G^{\mathrm{R}}(\omega)$ is regular for $\omega_2 > 0$ and vanishes at $\omega \to \infty$, we obtain the equation as

$$\frac{1}{\mathrm{i}\pi} \int_{-\infty}^{\infty} \mathrm{d}\omega' \, \frac{G^{\mathrm{R}}(\omega)}{\omega' - \omega + \mathrm{i}0} = 0. \tag{A.19}$$

Here, by using the equality

$$\frac{1}{x \pm \mathrm{i}0} = \mathrm{P}\frac{1}{x} \mp \mathrm{i}\pi\delta(x), \tag{A.20}$$

we can derive the following relation

$$\frac{\mathrm{P}}{\mathrm{i}\pi} \int_{-\infty}^{\infty} \mathrm{d}\omega' \, \frac{G^{\mathrm{R}}(\omega)}{\omega' - \omega} - G^{\mathrm{R}}(\omega) = 0 \tag{A.21}$$

$$\frac{\mathrm{P}}{\pi} \int_{-\infty}^{\infty} \mathrm{d}\omega' \, \frac{G_2^{\mathrm{R}}(\omega) - \mathrm{i}G_1^{\mathrm{R}}(\omega)}{\omega' - \omega} = G_1^{\mathrm{R}}(\omega) + \mathrm{i}G_2^{\mathrm{R}}(\omega), \tag{A.22}$$

where P means the primitive integration. Therefore, we can obtain the Kramers-Kronig relations:

$$G_1^{\mathrm{R}}(\omega) = \frac{\mathrm{P}}{\pi} \int_{-\infty}^{\infty} \mathrm{d}\omega' \, \frac{G_2^{\mathrm{R}}(\omega')}{\omega' - \omega}, \tag{A.23a}$$

$$G_2^{\mathrm{R}}(\omega) = -\frac{\mathrm{P}}{\pi} \int_{-\infty}^{\infty} \mathrm{d}\omega' \, \frac{G_1^{\mathrm{R}}(\omega')}{\omega' - \omega}. \tag{A.23b}$$

These relations are derived from the causality of the response function.

A.3 Langevin equation

Last, I discuss the response relation of dispersive systems, which have tight connection with the QED theory for dielectrics. In order to discuss such systems, we must consider the Langevin equation, and its detailed explanation is shown in Chap. 15 of Ref. 108, Ref. 109, or other textbooks.

In this section, I consider boson operator $\hat{a}$ with eigenfrequency Ω, and it interacts with reservoir of oscillators $\hat{b}_j$ with frequency ω_j. The unperturbed Hamiltonian is written as

$$H_0 = \hbar\Omega \hat{a}^\dagger \hat{a} + \sum_j \hbar\omega_j \hat{b}_j^\dagger \hat{b}_j + \hbar \sum_j \left(g_j \hat{a}^\dagger \hat{b}_j + g_j^* \hat{b}_j^\dagger \hat{a} \right). \tag{A.24}$$

The Heisenberg equations are derived as

$$\frac{\partial}{\partial t}\hat{a}(t) = -\mathrm{i}\Omega\hat{a}(t) - \mathrm{i}\sum_j g_j\hat{b}_j(t), \tag{A.25a}$$

$$\frac{\partial}{\partial t}\hat{b}_j(t) = -\mathrm{i}\omega_j\hat{b}_j(t) - \mathrm{i}g_j^*\hat{a}(t). \tag{A.25b}$$

The latter differential equation is solved as

$$\hat{b}_j(t) = \hat{b}_j(t_0)\mathrm{e}^{-\mathrm{i}\omega_j(t-t_0)} - \mathrm{i}g_j^*\int_{t_0}^{t}\mathrm{d}t'\ \mathrm{e}^{-\mathrm{i}\omega_j(t-t')}\hat{a}(t'), \tag{A.26}$$

and, by substituting it into the former equation, we obtain

$$\frac{\partial}{\partial t}\hat{a}(t) = -\mathrm{i}\Omega\hat{a}(t) - \int_{t_0}^{t}\mathrm{d}t'\ \frac{\gamma(t-t')}{2}\hat{a}(t') + \hat{f}(t), \tag{A.27}$$

where $\gamma(t-t')$ and $\hat{f}(t)$ are respectively defined as

$$\frac{\gamma(t-t')}{2} \equiv \sum_j |g_j|^2\mathrm{e}^{-\mathrm{i}\omega_j(t-t')} = \frac{\gamma^*(t'-t)}{2}, \tag{A.28}$$

$$\hat{f}(t) \equiv -\mathrm{i}\sum_j g_j\hat{b}_j(t_0)\mathrm{e}^{-\mathrm{i}\omega_j(t-t_0)}. \tag{A.29}$$

The commutation relation of $\hat{f}(t)$ is derived as

$$\left[\hat{f}(t), \hat{f}^\dagger(t')\right] = \frac{\gamma(t-t')}{2}. \tag{A.30}$$

Here, for a simple example, I suppose that $\gamma(t-t')$ has no value except for $t=t'$ as

$$\frac{\gamma(t-t')}{2} = \Gamma\delta(t-t'). \tag{A.31}$$

This treatment is called the Markov approximation, and Eq. (A.27) is rewritten as

$$\frac{\partial}{\partial t}\hat{a}(t) = -\mathrm{i}\Omega\hat{a}(t) - \frac{\Gamma}{2}\hat{a}(t) + \hat{f}(t). \tag{A.32}$$

The Markov approximation means that $\hat{a}$ does not keep its previous memory, and its amplitude does not return to $\hat{a}$. Therefore, the amplitude monochromatically decreases. Eq. (A.32) is called the Langevin equation, and $\hat{f}$ is the fluctuation operator. Here, Eq. (A.32) is solved as

$$\hat{a}(t) = \hat{a}\ \mathrm{e}^{-\mathrm{i}(\Omega-\mathrm{i}\Gamma/2)(t-t_0)} + \int_{t_0}^{t}\mathrm{d}t'\ \mathrm{e}^{-\mathrm{i}(\Omega-\mathrm{i}\Gamma/2)(t-t')}\hat{f}(t'), \tag{A.33}$$

and then, for $t > t'$, the commutation relation between $\hat{a}(t)$ and $\hat{a}^\dagger(f')$ is derived as

$$\begin{aligned}
[\hat{a}(t), \hat{a}^\dagger(t')] &= \mathrm{e}^{-\mathrm{i}\Omega(t-t')-\Gamma(t+t'-2t_0)/2} + \Gamma\int_{t_0}^{t}\mathrm{d}s\int_{t_0}^{t'}\mathrm{d}s'\ \mathrm{e}^{-\mathrm{i}(\Omega-\mathrm{i}\Gamma/2)(t-s)}\mathrm{e}^{\mathrm{i}(\Omega+\mathrm{i}\Gamma/2)(t'-s')}\delta(s-s') \\
&= \mathrm{e}^{-\mathrm{i}\Omega(t-t')-\Gamma(t+t'-2t_0)/2} + \Gamma\mathrm{e}^{-\mathrm{i}\Omega(t-t')-\Gamma(t+t')/2}\int_{t_0}^{t'}\mathrm{d}s\ \mathrm{e}^{\Gamma s} \\
&= \mathrm{e}^{-\mathrm{i}\Omega(t-t')-\Gamma(t-t')/2}.
\end{aligned} \tag{A.34}$$

We can see that this correctly provides the equal-time commutation relation $[\hat{a}(t), \hat{a}^\dagger(t)] = 1$, which must identical to that in the Schrödinger representation. On the other hand, it is worth to note that, if

the Langevin equation (A.32) does not have the fluctuation operator $\hat{f}(t)$, the equal-time commutation relation does not match with the Schrödinger one. From Eq. (A.34), the retarded correlation function of $\hat{a}$ is obtained as

$$G^{\mathrm{R}}(t-t') \equiv \frac{\theta(t-t')}{\mathrm{i}\hbar}\left\langle\left[\hat{a}(t),\hat{a}^{\dagger}(t')\right]\right\rangle_0 = \frac{\theta(t-t')}{\mathrm{i}\hbar}\mathrm{e}^{-\mathrm{i}\Omega(t-t')-\Gamma(t-t')/2}, \tag{A.35}$$

$$G^{\mathrm{R}}(\omega) = \frac{1}{\hbar(\omega-\Omega+\mathrm{i}\Gamma/2)} \tag{A.36}$$

As discussed in the previous section, this function has the extreme value $\Omega-\mathrm{i}\Gamma/2$ in the lower half side of the complex ω-plane, because Eq. (A.28) provides a real positive value for $t=t'$.

Last, I show the ω Fourier transform of the Langevin equation (A.32). By defining the Fourier transforms of $\hat{a}(t)$ and $\hat{f}(t)$ as

$$\hat{a}(\omega) \equiv \frac{1}{2\pi}\int_{-\infty}^{\infty}\mathrm{d}t\ \mathrm{e}^{\mathrm{i}\omega t}\hat{a}(t) \tag{A.37}$$

$$\hat{f}(\omega) \equiv \frac{1}{2\pi}\int_{-\infty}^{\infty}\mathrm{d}t\ \mathrm{e}^{\mathrm{i}\omega t}\hat{f}(t), \tag{A.38}$$

Eq. (A.32) is rewritten as

$$\hat{a}(\omega) = \frac{\hat{f}(\omega)}{\mathrm{i}\Omega+\gamma(\omega)/2-\mathrm{i}\omega}, \tag{A.39}$$

where I consider that the interaction between $\hat{a}$ and $\hat{b}$ initially exists as $t_0\to\infty$, and $\gamma(\omega)$ is defined as

$$\gamma(\omega) = \int_{-\infty}^{t}\mathrm{d}t'\ \mathrm{e}^{\mathrm{i}\omega(t-t')}\gamma(t-t') = \int_{0}^{\infty}\mathrm{d}t\ \mathrm{e}^{\mathrm{i}\omega t}\gamma(t). \tag{A.40}$$

From Eq. (A.28), we obtain the relation

$$\gamma^*(\omega) = \int_0^{\infty}\mathrm{d}t\ \mathrm{e}^{-\mathrm{i}\omega t}\gamma^*(t) = \int_0^{\infty}\mathrm{d}t\ \mathrm{e}^{-\mathrm{i}\omega t}\gamma(-t) = \int_{-\infty}^{0}\mathrm{d}t\ \mathrm{e}^{\mathrm{i}\omega t}\gamma(t), \tag{A.41}$$

and the the commutation relation of $\hat{f}(\omega)$ is obtained as

$$\left[\hat{f}(\omega),\hat{f}^{\dagger}(\omega')\right] = \delta(\omega-\omega')\frac{1}{2\pi}\int_{-\infty}^{\infty}\mathrm{d}t\ \mathrm{e}^{\mathrm{i}\omega t}\frac{\gamma(t)}{2} = \delta(\omega-\omega')\frac{1}{2\pi}\frac{\gamma(\omega)+\gamma^*(\omega)}{2}. \tag{A.42}$$

Appendix B

Vacuum Fluctuation in QED of Dielectrics

In this appendix, I discuss the source of the vacuum fluctuation in the QED theory for dispersive and absorptive dielectrics established in the pioneering work by Huttner and Barnett [21]. As seen in Eq. (1.11) or (1.26), the commutator of noise operator $\hat{J}_{\rm NT}(z,\omega)$ vanishes in the limit of zero absorption ${\rm Im}[\varepsilon(\omega)] \to 0$. However, as see in Eq. (1.27), the commutator of the vector potential $\hat{A}(z,\omega)$ does not vanish in the same limit, and then we must take the zero absorption limit after expectation values of focusing observables are obtained. Although this result reflects the existence of the vacuum fluctuation in the electromagnetic fields, the noise operator $\hat{J}_{\rm NT}(z,\omega)$ should describe only the fluctuation originating from the absorption in dielectrics. Therefore, there is a following question: What describes the vacuum fluctuation in the series of QED theories?

I consider a homogeneous medium with dielectric function $\varepsilon(\omega)$, and discuss transverse fields propagating in the z direction. The Maxwell wave equation for the vector potential $\hat{A}(z,\omega)$ is represented in Eq. (1.20) with noise operator $\hat{J}_{\rm NT}(z,\omega)$. This operator satisfies commutation relation (1.26), and the one of $\hat{A}(z,\omega)$ is derived as Eq. (1.27). Since the Green's function $G_0(z,z',\omega)$ satisfying Eq. (1.24) is represented as Eq. (1.25), the vector potential is written from Eq. (1.23) as

$$\hat{A}^+(z,\omega) = \frac{1}{{\rm i}2\kappa}\int_{-\infty}^{\infty} {\rm d}z'\ \hat{J}_{\rm NT}(z',\omega)\ {\rm e}^{{\rm i}\kappa|z-z'|} = \hat{A}^+_>(z,\omega) + \hat{A}^+_<(z,\omega), \tag{B.1}$$

where $\kappa = \sqrt{\varepsilon(\omega)}\omega/c$ and I define forward and backward fields as follows:

$$\hat{A}^+_>(z,\omega) = \frac{1}{{\rm i}2\kappa}\int_{-\infty}^{z} {\rm d}z'\ \hat{J}_{\rm NT}(z',\omega)\ {\rm e}^{{\rm i}\kappa(z-z')}, \tag{B.2a}$$

$$\hat{A}^+_<(z,\omega) = \frac{1}{{\rm i}2\kappa}\int_{z}^{\infty} {\rm d}z'\ \hat{J}_{\rm NT}(z',\omega)\ {\rm e}^{{\rm i}\kappa(z'-z)}. \tag{B.2b}$$

These fields are also represented with the fields at another position z_1 as

$$\hat{A}^+_>(z,\omega) = {\rm e}^{{\rm i}\kappa(z-z_1)}\hat{A}^+_>(z_1,\omega) + \frac{1}{{\rm i}2\kappa}\int_{z_1}^{z} {\rm d}z'\ \hat{J}_{\rm NT}(z',\omega)\ {\rm e}^{{\rm i}\kappa(z-z')}, \tag{B.3a}$$

$$\hat{A}^+_<(z,\omega) = {\rm e}^{{\rm i}\kappa(z_1-z)}\hat{A}^+_<(z_1,\omega) + \frac{1}{{\rm i}2\kappa}\int_{z}^{z_1} {\rm d}z'\ \hat{J}_{\rm NT}(z',\omega)\ {\rm e}^{{\rm i}\kappa(z'-z)}. \tag{B.3b}$$

The former relation means that $\hat{A}^+_>(z_1,\omega)$ feels phase shift ${\rm iRe}[\kappa](z-z_1)$ and amplitude decay ${\rm e}^{-{\rm Im}[\kappa](z-z_1)}$ during the propagation from z_1 to z, and also is affected by the fluctuation $\hat{J}_{\rm NT}(z',\omega)$ in $z_1 < z' < z$. The latter relation is also interpreted in the same way.

Next, I discuss commutation relations between the forward and backward fields. As seen in Eq. (1.26), the noise operator $\hat{J}_{\rm NT}(z,\omega)$ has a correlation with itself only at the save position. Therefore, forward

field $\hat{A}^{+}_{>}(z,\omega)$ and backward field $\hat{A}^{+}_{<}(z',\omega)$ have a correlation only in the case of $z > z'$:

$$\begin{aligned}
&\left[\hat{A}^{+}_{>}(z,\omega), \hat{A}^{-}_{<}(z',\omega')\right] \\
&= \frac{1}{4\kappa\kappa'^{*}} \int_{-\infty}^{z} \mathrm{d}x \int_{z'}^{\infty} \mathrm{d}x' \ \mathrm{e}^{\mathrm{i}\kappa(z-x)} \left[\hat{J}_{\mathrm{NT}}(x,\omega), \{\hat{J}_{\mathrm{NT}}(x',\omega'^{*})\}^{\dagger}\right] \mathrm{e}^{-\mathrm{i}\kappa'^{*}(x'-z')} \\
&= \delta(\omega-\omega') \ \theta(z-z') \ \frac{\mathrm{i}\mu_0\hbar\omega^2 \ \mathrm{Im}[\varepsilon(\omega)]}{4\pi c^2|\kappa|^2 S} \ \frac{\mathrm{e}^{\mathrm{iRe}[\kappa](z'-z)} - \mathrm{e}^{\mathrm{iRe}[\kappa](z-z')}}{2\mathrm{Re}[\kappa]} \ \mathrm{e}^{-\mathrm{Im}[\kappa](z-z')} \\
&= \delta(\omega-\omega') \ \theta(z-z') \ \frac{\mathrm{i}\mu_0\hbar \ \mathrm{Im}[\kappa]}{4\pi|\kappa|^2 S} \left[\mathrm{e}^{\mathrm{iRe}[\kappa](z'-z)} - \mathrm{e}^{\mathrm{iRe}[\kappa](z-z')}\right] \mathrm{e}^{-\mathrm{Im}[\kappa](z-z')}, \qquad \text{(B.4)}
\end{aligned}$$

where $\theta(z-z')$ is the step function providing unity only for $z > z'$, and I used the relation $\mathrm{Im}[\varepsilon(\omega)](\omega/c)^2 = 2\ \mathrm{Re}[\kappa]\ \mathrm{Im}[\kappa]$ to derive the above equations. On the other hand, the commutator between $\hat{A}^{+}_{>}(z,\omega)$ and itself is derived as

$$\begin{aligned}
&\left[\hat{A}^{+}_{>}(z,\omega), \hat{A}^{-}_{>}(z',\omega')\right] \\
&= \frac{1}{4\kappa\kappa'^{*}} \int_{-\infty}^{z} \mathrm{d}x \int_{-\infty}^{z'} \mathrm{d}x' \left[\hat{J}_{\mathrm{NT}}(x,\omega), \{\hat{J}_{\mathrm{NT}}(x',\omega'^{*})\}^{\dagger}\right] \mathrm{e}^{\mathrm{i}\kappa(z-x)} \ \mathrm{e}^{-\mathrm{i}\kappa'^{*}(z'-x')} \\
&= \delta(\omega-\omega') \ \frac{1}{4|\kappa|^2} \ \frac{\mu_0\hbar\omega^2 \ \mathrm{Im}[\varepsilon(\omega)]}{\pi c^2 S} \mathrm{e}^{\mathrm{iRe}[\kappa](z-z')} \ \mathrm{e}^{-\mathrm{Im}[\kappa](z+z')} \int_{-\infty}^{z} \mathrm{d}x \int_{-\infty}^{z'} \mathrm{d}x' \ \delta(x-x') \ \mathrm{e}^{2\mathrm{Im}[\kappa]x}. \qquad \text{(B.5)}
\end{aligned}$$

Here, since the integrations with respect to x and x' are performed as

$$\begin{aligned}
\int_{-\infty}^{z} \mathrm{d}x \int_{-\infty}^{z'} \mathrm{d}x' \ \delta(x-x') \ \mathrm{e}^{2\mathrm{Im}[\kappa]x} &= \theta(z-z') \int_{-\infty}^{z'} \mathrm{d}x \ \mathrm{e}^{2\mathrm{Im}[\kappa]x} + \theta(z'-z) \int_{-\infty}^{z} \mathrm{d}x \ \mathrm{e}^{2\mathrm{Im}[\kappa]x} \\
&= \frac{\theta(z-z')\mathrm{e}^{2\mathrm{Im}[\kappa]z'}}{2\mathrm{Im}[\kappa]} + \frac{\theta(z'-z)\mathrm{e}^{2\mathrm{Im}[\kappa]z}}{2\mathrm{Im}[\kappa]}, \qquad \text{(B.6)}
\end{aligned}$$

I obtain

$$\begin{aligned}
\mathrm{e}^{-\mathrm{Im}[\kappa](z+z')} \int_{-\infty}^{z} \mathrm{d}x \int_{-\infty}^{z'} \mathrm{d}x' \ \delta(x-x') \ \mathrm{e}^{2\mathrm{Im}[\kappa]x} &= \frac{\theta(z-z')\mathrm{e}^{-\mathrm{Im}[\kappa](z-z')}}{2\mathrm{Im}[\kappa]} + \frac{\theta(z'-z)\mathrm{e}^{-\mathrm{Im}[\kappa](z'-z)}}{2\mathrm{Im}[\kappa]} \\
&= \frac{\mathrm{e}^{-\mathrm{Im}[\kappa]|z-z'|}}{2\mathrm{Im}[\kappa]}. \qquad \text{(B.7)}
\end{aligned}$$

Therefore, Eq. (B.5) becomes

$$\left[\hat{A}^{+}_{>}(z,\omega), \hat{A}^{-}_{>}(z',\omega')\right] = \delta(\omega-\omega') \ \frac{\mu_0\hbar \ \mathrm{Re}[\kappa]}{4\pi|\kappa|^2 S} \ \mathrm{e}^{\mathrm{iRe}[\kappa](z-z')} \ \mathrm{e}^{-\mathrm{Im}[\kappa]|z-z'|}, \qquad \text{(B.8)}$$

and this commutator has a finite value even in the limit of $\mathrm{Im}[\kappa] \to 0$. On the other hand, by the same procedure, the commutation relation between $\hat{A}^{+}_{<}(z,\omega)$ and itself is obtained as

$$\left[\hat{A}^{+}_{<}(z,\omega), \hat{A}^{-}_{<}(z',\omega')\right] = \delta(\omega-\omega') \ \frac{\mu_0\hbar \ \mathrm{Re}[\kappa]}{4\pi|\kappa|^2 S} \ \mathrm{e}^{\mathrm{iRe}[\kappa](z'-z)} \ \mathrm{e}^{-\mathrm{Im}[\kappa]|z'-z|}. \qquad \text{(B.9)}$$

This also has a finite value in the zero absorption limit.

Next, I describe $\hat{A}^{+}_{>}(z,\omega)$ by using $\hat{A}^{+}_{>}(z',\omega)$ at different position $z' < z$ as

$$\hat{A}^{+}_{>}(z,\omega) = \mathrm{e}^{\mathrm{i}\kappa(z-z')}\hat{A}^{+}_{>}(z',\omega) + \frac{1}{\mathrm{i}2\kappa} \int_{z'}^{z} \mathrm{d}x \ \hat{J}_{\mathrm{NT}}(x,\omega) \ \mathrm{e}^{\mathrm{i}\kappa(z-x)}. \qquad \text{(B.10)}$$

In this situation, Eq. (B.8) is also written as

$$\begin{aligned}
\left[\hat{A}^{+}_{>}(z,\omega), \hat{A}^{-}_{>}(z',\omega')\right] &= \mathrm{e}^{\mathrm{i}\kappa(z-z')} \left[\hat{A}^{+}_{>}(z',\omega), \hat{A}^{-}_{>}(z',\omega')\right] \\
&\quad + \frac{1}{\mathrm{i}2\kappa} \int_{z'}^{z} \mathrm{d}x \ \left[\hat{j}(x,\omega), \hat{A}^{-}_{>}(z',\omega')\right] \mathrm{e}^{\mathrm{i}\kappa(z-x)}, \qquad \text{(B.11)}
\end{aligned}$$

and we can find that Eq. (B.8) is obtained from only the first term, and the second term provides no contribution. This is because $\hat{A}^{+}_{>}(z',\omega)$ is described by $\hat{J}_{\rm NT}(x,\omega)$ only in $-\infty < x < z'$, and then it has no correlation with $\hat{J}_{\rm NT}(x,\omega)$ in $z' < x < z$. On the other hand, by introducing another position $z'' < z,\ z'$, Eq. (B.8) is rewritten as

$$\left[\hat{A}^{+}_{>}(z,\omega),\hat{A}^{-}_{>}(z',\omega')\right] = \mathrm{e}^{\mathrm{i}\kappa(z-z'')}\ \mathrm{e}^{-\mathrm{i}\kappa'^{*}(z'-z'')}\left[\hat{A}^{+}_{>}(z'',\omega),\hat{A}^{-}_{>}(z'',\omega')\right] + \frac{1}{4\kappa\kappa'^{*}}\int_{z''}^{z}\mathrm{d}x\int_{z''}^{z'}\mathrm{d}x'\left[\hat{j}(x,\omega),\hat{j}^{\dagger}(x',\omega')\right]\mathrm{e}^{\mathrm{i}\kappa(z-x)}\ \mathrm{e}^{-\mathrm{i}\kappa'^{*}(z'-x')}, \quad \text{(B.12)}$$

where I neglect the commutators between $\hat{J}_{\rm NT}(x,\omega)$ and $\hat{A}^{\pm}(z,\omega)$ for the same reason as in the above discussion. From the first term of Eq. (B.12), we obtain

$$\delta(\omega-\omega')\ \frac{\mu_0\hbar\ \mathrm{Re}[\kappa]}{4\pi|\kappa|^2 S}\ \mathrm{e}^{\mathrm{iRe}[\kappa](z-z')}\ \mathrm{e}^{-\mathrm{Im}[\kappa](z+z'-2z'')}, \quad \text{(B.13)}$$

and the second term becomes

$$\delta(\omega-\omega')\ \frac{\mu_0\hbar\ \mathrm{Re}[\kappa]}{4\pi|\kappa|^2 S}\ \mathrm{e}^{\mathrm{iRe}[\kappa](z-z')}\ \left[\mathrm{e}^{-\mathrm{Im}[\kappa]|z-z'|}-\mathrm{e}^{-\mathrm{Im}[\kappa](z+z'-2z'')}\right]. \quad \text{(B.14)}$$

Here, we can find that the second term vanishes in the limit of $\mathrm{Im}[\kappa]\to 0$, although the first term has a finite value. Therefore, the vacuum fluctuation comes from the noise operator $\hat{J}_{\rm NT}(x,\omega)$ in $-\infty < x < z''$ for arbitrary z'', and we can conclude that the vacuum fluctuation is described by $\hat{J}_{\rm NT}(x,\omega)$ at the infinite distance $x\to\infty$ in the series of QED theories for dispersive and absorptive dielectrics and also in the present QED theory for excitons.

Appendix C

Direct Derivation of Green's Function for Integro-Differential Equation

In this appendix, I show a direct derivation of the Green's function satisfying Eq. (2.88), the integro-differential equation or the wave equation with the nonlocal susceptibility under the RWA. The Green's function satisfying Eq. (2.58) without the RWA can be also derived directly by the same procedure. The calculation is based on the fact that the nonlocal susceptibility is represented as a summation of separable functions with respect to the two positions. Actually, the radiation Green's function for a quantum well system with DBR cavity has already been derived in Ref. 81.

I explain the general calculation idea in Sec. C.1, and the Green's function satisfying Eq. (2.88) is derived in Sec. C.2.

C.1 General calculation idea

I consider an arbitrary operator $\hat{O}$, and suppose that its Green's function $g(x, x')$ is already known and satisfies $\hat{O}g(x, x') = \delta(x - x')$. From this Green's function, I try to derive the Green's function $G(x, x')$ satisfying

$$\hat{O}G(x, x') + \sum_m A_m(x) \int \mathrm{d}y \; B_m(y)G(y, x') = \delta(x - x'). \tag{C.1}$$

First, by operating on this equation from the left with $\hat{O}^{-1}$, I obtain

$$G(x, x') + \sum_m \left[\int \mathrm{d}y' \; g(x, y')A_m(y') \right] H_m(x') = g(x, x'), \tag{C.2}$$

where $H_m(x')$ is defined as

$$H_n(x') \equiv \int \mathrm{d}y \; B_n(y)G(y, x'). \tag{C.3}$$

Next, by multiplying both sides of Eq. (C.2) by $B_n(x)$ and integrating with respect to x, I obtain

$$H_n(x') + \sum_m \left[\int \mathrm{d}x \int \mathrm{d}y' \; B_n(x)g(x, y')A_m(y') \right] H_m(x') = h_n(x'), \tag{C.4}$$

where $h_n(x')$ is defined as

$$h_n(x') \equiv \int \mathrm{d}x \; B_n(x)g(x, x'). \tag{C.5}$$

Next, I express the coefficient appearing in the second term of Eq. (C.4) by

$$C_{n,m} \equiv \int \mathrm{d}x \int \mathrm{d}y \; B_n(x)g(x, y')A_m(y'), \tag{C.6}$$

and then Eq. (C.4) is rewritten as

$$H_n(x') + \sum_m C_{n,m} H_m(x') = h_n(x'). \tag{C.7}$$

Therefore, by calculating the inverse matrix of the coefficient as $\mathbf{D} = (\mathbf{1} + \mathbf{C})^{-1}$, Eq. (C.7) is rewritten as

$$H_m(x') = \sum_n D_{m,n} h_n(x'). \tag{C.8}$$

Substituting this into Eq. (C.2), I obtain the representation of the Green's function as

$$G(x, x') = g(x, x') - \sum_{m,n} h'_m(x) D_{m,n} h_n(x'), \tag{C.9}$$

where $h'_m(x)$ is defined as

$$h'_m(x) \equiv \int \mathrm{d}y' \; g(x, y') A_m(y'). \tag{C.10}$$

C.2 Green's function for nonlocal media

Along the same line as the previous section, I derive the Green's function satisfying Eq. (2.88), the wave equation with the nonlocal susceptibility under the RWA. First, I suppose that the Green's function $\mathbf{G}_0(\boldsymbol{r}, \boldsymbol{r}', \omega)$ satisfying Eq. (1.59), the wave equation with local dielectric function $\varepsilon_{\mathrm{bg}}(\boldsymbol{r}, \omega)$, is already known. By substituting Eq. (2.77) into Eq. (2.88), I obtain the equation to be solved as

$$\begin{aligned} \boldsymbol{\nabla} \times \boldsymbol{\nabla} \times \mathbf{G}(\boldsymbol{r}, \boldsymbol{r}', \omega) - \frac{\omega^2}{c^2} \varepsilon_{\mathrm{bg}}(\boldsymbol{r}, \omega) \mathbf{G}(\boldsymbol{r}, \boldsymbol{r}', \omega) \\ - \sum_\mu \frac{\mu_0 \omega^2 \boldsymbol{\mathcal{P}}_\mu(\boldsymbol{r})}{\hbar\omega_\mu - \hbar\omega - \mathrm{i}\Gamma_\mu(\omega)/2} \int \mathrm{d}\boldsymbol{r}'' \; \boldsymbol{\mathcal{P}}^*_\mu(\boldsymbol{r}'') \cdot \mathbf{G}(\boldsymbol{r}'', \boldsymbol{r}', \omega) = \delta(\boldsymbol{r} - \boldsymbol{r}') \mathbf{1}. \end{aligned} \tag{C.11}$$

Here, we can consider that the functions and variables appearing in the previous section correspond as follows:

$$G(x, x') \to \mathbf{G}(\boldsymbol{r}, \boldsymbol{r}', \omega), \tag{C.12}$$

$$g(x, x') \to \mathbf{G}_0(\boldsymbol{r}, \boldsymbol{r}', \omega), \tag{C.13}$$

$$h_\mu(x') \to \int \mathrm{d}\boldsymbol{r} \; \boldsymbol{\mathcal{P}}^*_\mu(\boldsymbol{r}) \cdot \mathbf{G}_0(\boldsymbol{r}, \boldsymbol{r}', \omega) = \frac{\{\boldsymbol{\mathcal{F}}_\mu(\boldsymbol{r}', \omega)\}^{\mathrm{t}}}{\mu_0 \omega^2}, \tag{C.14}$$

$$h'_\mu(x) \to -\frac{\mu_0 \omega^2}{\hbar\omega_\mu - \hbar\omega} \int \mathrm{d}\boldsymbol{r}' \; \mathbf{G}_0(\boldsymbol{r}, \boldsymbol{r}', \omega) \cdot \boldsymbol{\mathcal{P}}_\mu(\boldsymbol{r}') = -\frac{\boldsymbol{\mathcal{E}}_\mu(\boldsymbol{r}, \omega)}{\hbar\omega_\mu - \hbar\omega - \mathrm{i}\Gamma_\mu(\omega)/2}, \tag{C.15}$$

$$C_{\mu,\mu'} \to -\frac{\mu_0 \omega^2}{\hbar\omega_{\mu'} - \hbar\omega - \mathrm{i}\Gamma_{\mu'}(\omega)/2} \int \mathrm{d}\boldsymbol{r} \int \mathrm{d}\boldsymbol{r}' \; \boldsymbol{\mathcal{P}}^*_\mu(\boldsymbol{r}) \cdot \mathbf{G}_0(\boldsymbol{r}, \boldsymbol{r}', \omega) \cdot \boldsymbol{\mathcal{P}}_{\mu'}(\boldsymbol{r}') = \frac{\Sigma_{\mu,\mu'}(\omega)}{\hbar\omega_{\mu'} - \hbar\omega - \mathrm{i}\Gamma_{\mu'}(\omega)/2}, \tag{C.16}$$

where $\Sigma_{\mu,\mu'}(\omega)$, $\boldsymbol{\mathcal{E}}_\mu(\boldsymbol{r}, \omega)$, and $\boldsymbol{\mathcal{F}}_\mu(\boldsymbol{r}, \omega)$ are defined as Eqs. (2.62a), (2.68a), and (2.68b), respectively. Since the elements of $\mathbf{1} + \mathbf{C}$ correspond to $S^{11}_{\mu,\mu'}(\omega)$ [Eq. (2.61a)] as

$$[\mathbf{1} + \mathbf{C}]_{\mu,\mu'} \to \frac{S^{11}_{\mu,\mu'}(\omega)}{\hbar\omega_{\mu'} - \hbar\omega - \mathrm{i}\Gamma_{\mu'}(\omega)/2}, \tag{C.17}$$

the inverse matrix $\mathbf{D}$ corresponds to $\widetilde{\mathbf{W}}(\omega) = [\mathbf{S}^{11}(\omega)]^{-1}$ as

$$D_{\mu,\mu'} \to [\hbar\omega_\mu - \hbar\omega - \mathrm{i}\Gamma_\mu(\omega)/2] \, \widetilde{W}_{\mu,\mu'}(\omega). \tag{C.18}$$

Therefore, from Eq. (C.9) and the above relations, the Green's function satisfying Eq. (2.88) is derived as Eq. (2.87).

Appendix D

Green's Function for Multilayer System

In this appendix, I show and derive the expression of the Green's function $G(z, z', \omega)$ satisfying Eq. (3.3) in the case of multilayer system. The details and the Green's function for other structures with high symmetry are discussed in Ref. 65.

First, I show the expression of $G(z, z', \omega)$ in Sec. D.1. The general reflection and transmission coefficients appearing in the expression are discussed in Sec. D.2, and the derivation of $G(z, z', \omega)$ is explained in Sec. D.3.

D.1 Expression of Green's function

I consider general multilayer system shown in Fig. D.1. Layer i has a thickness d_i and a dielectric function $\varepsilon_i(\omega)$. I suppose the in-plane wavenumber as $k_\parallel$, and the wavenumber in the z direction is written as

$$k_i = \sqrt{\varepsilon_i(\omega)\omega^2/c^2 - {k_\parallel}^2}. \tag{D.1}$$

When we consider that z and z' are in layers j and i, respectively, the Green's function satisfying Eq. (3.3) is represented as

$$G(z, z', \omega) = \frac{1}{\mathrm{i}2k_i}\mathcal{G}_{j,i}(z, z'), \tag{D.2}$$

where $\mathcal{G}_{j,i}$ is the propagator represented as follows. In case $i = j$, the propagator is written as

$$\begin{aligned}\mathcal{G}_{i,i}(z, z') = {} & \mathrm{e}^{\mathrm{i}k_i|z-z'|} + \mathrm{e}^{\mathrm{i}k_i(z-z_{i-1})}\tilde{R}_{i-1,i}\left[\mathrm{e}^{-\mathrm{i}k_i(z_{i-1}-z')} + \mathrm{e}^{\mathrm{i}k_i d_i}\tilde{R}_{i+1,i}\mathrm{e}^{\mathrm{i}k_i(z_i-z')}\right]\tilde{M}_i \\ & + \mathrm{e}^{-\mathrm{i}k_i(z-z_i)}\tilde{R}_{i+1,i}\left[\mathrm{e}^{\mathrm{i}k_i(z_i-z')} + \mathrm{e}^{\mathrm{i}k_i d_i}\tilde{R}_{i-1,i}\mathrm{e}^{-\mathrm{i}k_i(z_{i-1}-z')}\right]\tilde{M}_i. \end{aligned} \tag{D.3}$$

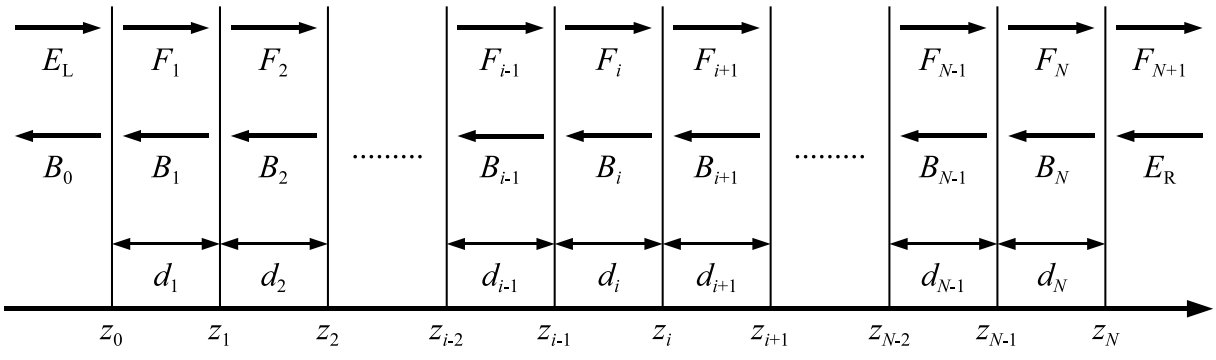

Figure D.1: Schematic view of considering multilayer system.

Here, $\tilde{R}_{j,i}$ is the general reflection coefficient from layer i to the interface with layer j, which is discussed in Sec. D.2, and the factor $\tilde{M}_i$ is defined as

$$\tilde{M}_i = \left[1 - \tilde{R}_{i-1,i}\tilde{R}_{i+1,i}\mathrm{e}^{\mathrm{i}2k_i d_i}\right]^{-1}. \tag{D.4}$$

In case $j > i$, the propagator is represented as

$$\mathcal{G}_{j,i}(z,z') = \left[\mathrm{e}^{\mathrm{i}k_j(z-z_{j-1})} + \mathrm{e}^{\mathrm{i}k_j d_j}\tilde{R}_{j+1,j}\mathrm{e}^{-\mathrm{i}k_j(z-z_j)}\right]\tilde{T}_{j,i}\left[\mathrm{e}^{\mathrm{i}k_i(z_i-z')} + \mathrm{e}^{\mathrm{i}k_i d_i}\tilde{R}_{i-1,i}\mathrm{e}^{-\mathrm{i}k_i(z_{i-1}-z')}\right]\tilde{M}_i, \tag{D.5}$$

and, especially in case $j = N+1$, it is written as

$$\mathcal{G}_{N+1,i}(z,z') = \mathrm{e}^{\mathrm{i}k_{N+1}(z-z_N)}\tilde{T}_{N+1,i}\left[\mathrm{e}^{\mathrm{i}k_i(z_i-z')} + \mathrm{e}^{\mathrm{i}k_i d_i}\tilde{R}_{i-1,i}\mathrm{e}^{-\mathrm{i}k_i(z_{i-1}-z')}\right]\tilde{M}_i. \tag{D.6}$$

Here, $\tilde{T}_{j,i}$ is the general transmission coefficient from layer i to layer j discussed in Sec. D.2, and it is represented with the ones connecting neighboring layers as

$$\tilde{T}_{j,i} = \tilde{T}_{j,j-1}\ \mathrm{e}^{\mathrm{i}k_{j-1}d_{j-1}}\ \tilde{T}_{j-1,j-2}\cdots\tilde{T}_{i+2,i+1}\ \mathrm{e}^{\mathrm{i}k_{i+1}d_{i+1}}\ \tilde{T}_{i+1,i}. \tag{D.7}$$

On the other hand, in case $j < i$, the propagator is represented as

$$\mathcal{G}_{j,i}(z,z') = \left[\mathrm{e}^{-\mathrm{i}k_j(z-z_j)} + \mathrm{e}^{\mathrm{i}k_j d_j}\tilde{R}_{j-1,j}\mathrm{e}^{\mathrm{i}k_j(z-z_{j-1})}\right]\tilde{T}_{j,i}\left[\mathrm{e}^{-\mathrm{i}k_i(z_{i-1}-z')} + \mathrm{e}^{\mathrm{i}k_i d_i}\tilde{R}_{i+1,i}\mathrm{e}^{\mathrm{i}k_i(z_i-z')}\right]\tilde{M}_i, \tag{D.8}$$

and, especially in case $i = 0$, it is written as

$$\mathcal{G}_{0,i}(z,z') = \mathrm{e}^{-\mathrm{i}k_0(z-z_0)}\tilde{T}_{0,i}\left[\mathrm{e}^{-\mathrm{i}k_i(z_{i-1}-z')} + \mathrm{e}^{\mathrm{i}k_i d_i}\tilde{R}_{i+1,i}\mathrm{e}^{\mathrm{i}k_i(z_i-z')}\right]\tilde{M}_i. \tag{D.9}$$

The general transmission coefficient has the relation

$$\tilde{T}_{j,i} = \tilde{T}_{j,j+1}\ \mathrm{e}^{\mathrm{i}k_{j+1}d_{j+1}}\ \tilde{T}_{j+1,j+2}\cdots\tilde{T}_{i-2,i-1}\ \mathrm{e}^{\mathrm{i}k_{i-1}d_{i-1}}\ \tilde{T}_{i-1,i}. \tag{D.10}$$

As seen in the above representations, the Green's function has the reciprocal relation

$$G(z,z',\omega) = \frac{\mathcal{G}_{j,i}(z,z')}{\mathrm{i}2k_i} = \frac{\mathcal{G}_{i,j}(z',z)}{\mathrm{i}2k_j} = G(z',z,\omega), \tag{D.11}$$

because of the reciprocity of Eq. (3.3). The dyadic Green's function satisfying Eq. (1.59) for general multilayer system is shown in Sec. 7.4 of Ref. 65.

D.2 General reflection and transmission coefficients

In this section, I derive general reflection and transmission coefficients including the effect of multiple reflections in multilayer structure. I also consider the system shown in Fig. D.1. I denote the electric field $E_i(z)$ in layer $i = 1, \ldots, N$ as a sum of the forward propagating field $F_i(z)$ and backward one $B_i(z)$ as

$$E_i(z) = F_i(z) + B_i(z), \tag{D.12}$$

and I define the amplitudes $\tilde{F}_i$ and $\tilde{B}_i$ of these fields as

$$F_i(z) = \mathrm{e}^{\mathrm{i}k_i(z-z_{i-1})}\ \tilde{F}_i, \tag{D.13a}$$

$$B_i(z) = \mathrm{e}^{-\mathrm{i}k_i(z-z_i)}\ \tilde{B}_i. \tag{D.13b}$$

On the other hand, the electric field in layers 0 and $N+1$ are respectively written as

$$E_0(z) = E_\mathrm{L}\ \mathrm{e}^{\mathrm{i}k_0(z-z_0)} + B_0(z), \tag{D.14}$$

$$E_{N+1}(z) = F_{N+1}(z) + E_\mathrm{R}\ \mathrm{e}^{-\mathrm{i}k_{N+1}(z-z_N)}, \tag{D.15}$$

where I consider that the incident fields E_L and E_R are given.

D.2.1 For incident field only from left

First, I consider that the field is incident on the system only from the left-hand side ($E_{\mathrm{L}} \neq 0$, $E_{\mathrm{R}} = 0$). In this situation, the fields in layers N and $N+1$ have the following relations at interface $z = z_N$:

$$F_{N+1}(z_N) = T_{N+1,N}\ F_N(z_N), \tag{D.16}$$
$$B_N(z_N) = R_{N+1,N}\ F_N(z_N), \tag{D.17}$$

where $R_{N+1,N}$ and $T_{N+1,N}$ are Fresnel reflection and transmission coefficients from layer N to layer $N+1$, respectively, and they are represented for $j = i \pm 1$ as

$$R_{j,i} = \frac{k_i - k_j}{k_i + k_j}, \tag{D.18a}$$
$$T_{j,i} = \frac{2k_i}{k_i + k_j}. \tag{D.18b}$$

In the following paragraph, I derive the general reflection and transmission coefficients $\tilde{R}_{i+1,i}$ and $\tilde{T}_{i+1,i}$ providing the relations at interface $z = z_i$ as

$$F_{i+1}(z_i) = \tilde{T}_{i+1,i}\ F_i(z_i), \tag{D.19}$$
$$B_i(z_i) = \tilde{R}_{i+1,i}\ F_i(z_i). \tag{D.20}$$

Here, I rewrite (D.20) by using Eqs. (D.13) as

$$\tilde{B}_i = \tilde{R}_{i+1,i}\ \mathrm{e}^{\mathrm{i}k_i d_i}\ \tilde{F}_i, \tag{D.21}$$

and consider that $\tilde{B}_i$ is already known. On the other hand, by using the Fresnel coefficients, the boundary conditions at $z = z_{i-1}$ are obtained as

$$F_i(z_{i-1}) = T_{i,i-1}\ F_{i-1}(z_{i-1}) + R_{i-1,i}\ B_i(z_{i-1}), \tag{D.22}$$
$$B_{i-1}(z_{i-1}) = T_{i-1,i}\ B_i(z_{i-1}) + R_{i,i-1}\ F_{i-1}(z_{i-1}), \tag{D.23}$$

and they are rewritten as

$$\tilde{F}_i = T_{i,i-1}\ F_{i-1}(z_{i-1}) + R_{i-1,i}\ \mathrm{e}^{\mathrm{i}k_i d_i}\ \tilde{B}_i, \tag{D.24}$$
$$B_{i-1}(z_{i-1}) = T_{i-1,i}\ \mathrm{e}^{\mathrm{i}k_i d_i}\ \tilde{B}_i + R_{i,i-1}\ F_{i-1}(z_{i-1}). \tag{D.25}$$

Substituting Eq. (D.21) into Eq. (D.24), the following relation is obtained:

$$F_i(z_{i-1}) = \tilde{F}_i = \tilde{T}_{i,i-1}\ F_{i-1}(z_{i-1}), \tag{D.26}$$

where the general transmission coefficient $\tilde{T}_{i,i-1}$ is represented with the general reflection coefficient $\tilde{R}_{i+1,i}$ as

$$\tilde{T}_{i,i-1} = \frac{T_{i,i-1}}{1 - R_{i-1,i}\ \tilde{R}_{i+1,i}\ \mathrm{e}^{\mathrm{i}2k_i d_i}}. \tag{D.27}$$

Further, substituting Eq. (D.26) into Eq. (D.21), we obtain

$$\tilde{B}_i = \tilde{R}_{i+1,i}\ \mathrm{e}^{\mathrm{i}k_i d_i}\ \tilde{T}_{i,i-1}\ F_{i-1}(z_{i-1}), \tag{D.28}$$

and, substituting this into Eq. (D.25), the following relation is obtained:

$$B_{i-1}(z_{i-1}) = \tilde{R}_{i,i-1}\ F_{i-1}(z_{i-1}), \tag{D.29}$$

where the general reflection coefficient $\tilde{R}_{i,i-1}$ is represented as

$$\tilde{R}_{i,i-1} = R_{i,i-1} + \frac{T_{i-1,i}\ \mathrm{e}^{\mathrm{i}k_i d_i}\ \tilde{R}_{i+1,i}\ \mathrm{e}^{\mathrm{i}k_i d_i}\ T_{i,i-1}}{1 - R_{i-1,i}\ \tilde{R}_{i+1,i}\ \mathrm{e}^{\mathrm{i}2k_i d_i}}. \tag{D.30}$$

Therefore, $\tilde{R}_{i,i-1}$ is obtained from $\tilde{R}_{i+1,i}$, and then all $\tilde{R}_{i,i-1}$ ($i = N,\ \ldots,\ 1$) are obtained from $\tilde{R}_{N+1,N} = R_{N+1,N}$. Further, $\tilde{T}_{i,i-1}$ ($i = N,\ \ldots,\ 1$) is obtained from the derived $\tilde{R}_{i+i,i}$ by using Eq. (D.27), and $\tilde{T}_{N+1,N} = T_{N+1,N}$.

Next, I denote the electric field in each layer by the incident field E_{L}. The forward field in layer 1 is written as

$$\tilde{F}_1 = \tilde{T}_{1,0}\ E_{\mathrm{L}}. \tag{D.31}$$

By rewriting Eq. (D.26) as

$$\tilde{F}_i = \tilde{T}_{i,i-1}\ \mathrm{e}^{\mathrm{i}k_{i-1}d_{i-1}}\ \tilde{F}_{i-1}, \tag{D.32}$$

the forward field in layer i is represented as

$$\tilde{F}_i = \tilde{T}_{i,i-1}\ \mathrm{e}^{\mathrm{i}k_{i-1}d_{i-1}}\ \tilde{F}_{i-1} = \tilde{T}_{i,0}\ E_{\mathrm{L}} \qquad (i = 1,\ \ldots,\ N+1), \tag{D.33}$$

where the transmission coefficient from layer 0 to i is written as

$$\tilde{T}_{i,0} = \tilde{T}_{i,i-1} \left[\prod_{j=1}^{i-1} \mathrm{e}^{\mathrm{i}k_j d_j}\ \tilde{T}_{j,j-1} \right]. \tag{D.34}$$

Further, the transmission coefficient of the whole multilayer is obtained as $\tilde{T}_{N+1,0}$. On the other hand, since the backward field is represented as Eq. (D.21), the backward field in layer i is represented as

$$\tilde{B}_i = \tilde{R}_{i+1,i}\ \mathrm{e}^{\mathrm{i}k_i d_i}\ \tilde{F}_i = \tilde{R}_{i+1,i}\ \mathrm{e}^{\mathrm{i}k_i d_i}\ \tilde{T}_{i,0}\ E_{\mathrm{L}} \qquad (i = 1,\ \ldots,\ N), \tag{D.35}$$

and the one in layer 0 is written as

$$\tilde{B}_0 = \tilde{R}_{1,0}\ E_{\mathrm{L}}. \tag{D.36}$$

D.2.2 For incident field only from right

Next, I discuss the case that the incident field propagates from the right-hand side ($E_{\mathrm{L}} = 0$, $E_{\mathrm{R}} \neq 0$). In the same manner as the previous subsection, the forward field in layer 1 is represented by the Fresnel reflection coefficient $R_{0,1}$ as

$$\tilde{F}_1 = F_1(z_0) = R_{0,1}\ B_1(z_0) = R_{0,1}\ \mathrm{e}^{\mathrm{i}k_1 d_1}\ \tilde{B}_1, \tag{D.37}$$

and I try to derive the general reflection coefficient $\tilde{R}_{i-1,i}$ providing

$$\tilde{F}_i = \tilde{R}_{i-1,i}\ \mathrm{e}^{\mathrm{i}k_i d_i}\ \tilde{B}_i. \tag{D.38}$$

From the boundary conditions at $z = z_i$, I obtain

$$F_{i+1}(z_i) = T_{i+1,i}\ F_i(z_i) + R_{i,i+1}\ B_{i+1}(z_i) = T_{i+1,i}\ \mathrm{e}^{\mathrm{i}k_i d_i}\ \tilde{F}_i + R_{i,i+1}\ B_{i+1}(z_i), \tag{D.39}$$

$$\tilde{B}_i = B_i(z_i) = T_{i,i+1}\ B_{i+1}(z_i) + R_{i+1,i}\ F_i(z_i) = T_{i,i+1}\ B_{i+1}(z_i) + R_{i+1,i}\ \mathrm{e}^{\mathrm{i}k_i d_i}\ \tilde{F}_i. \tag{D.40}$$

Substituting Eq. (D.38) into Eq. (D.40), the general transmission coefficient $\tilde{T}_{i,i+1}$ providing

$$\tilde{B}_i = B_i(z_i) = \tilde{T}_{i,i+1}\ B_{i+1}(z_i) \tag{D.41}$$

is represented with $\tilde{R}_{i-1,i}$ as

$$\tilde{T}_{i,i+1} = \frac{T_{i,i+1}}{1 - R_{i+1,i}\ \tilde{R}_{i-1,i}\ \mathrm{e}^{\mathrm{i}2k_i d_i}}. \tag{D.42}$$

Substituting this into Eq. (D.38), I obtain

$$\tilde{F}_i = \tilde{R}_{i-1,i}\ \mathrm{e}^{\mathrm{i}k_i d_i}\ \tilde{T}_{i,i+1}\ B_{i+1}(z_i), \tag{D.43}$$

and then, substituting this into Eq. (D.39), the general reflection coefficient $\tilde{R}_{i,i+1}$ providing

$$F_{i+1}(z_i) = \tilde{R}_{i,i+1}\ B_{i+1}(z_i) \tag{D.44}$$

is obtained as

$$\tilde{R}_{i,i+1} = R_{i,i+1} + \frac{T_{i+1,i}\ \mathrm{e}^{\mathrm{i}k_i d_i}\ \tilde{R}_{i-1,i}\ \mathrm{e}^{\mathrm{i}k_i d_i}\ T_{i,i+1}}{1 - R_{i+1,i}\ \tilde{R}_{i-1,i}\ \mathrm{e}^{\mathrm{i}2k_i d_i}}. \tag{D.45}$$

Therefore $\tilde{R}_{i,i+1}$ is obtained from $\tilde{R}_{i-1,i}$, and all the reflection coefficients is derived from $\tilde{R}_{0,1} = R_{0,1}$.

Next, I try to describe the forward and backward fields by E_{R}. The backward field in layer N is written as

$$\tilde{B}_N = \tilde{T}_{N,N+1}\ E_{\mathrm{R}}, \tag{D.46}$$

and then the backward field in layer i is represented as

$$\tilde{B}_i = \tilde{T}_{i,i+1}\ \mathrm{e}^{\mathrm{i}k_{i+1}d_{i+1}}\ \tilde{B}_{i+1} = \tilde{T}_{i,N+1}\ E_{\mathrm{R}}, \tag{D.47}$$

where the transmission coefficient $\tilde{T}_{i,N+1}$ from $N+1$ to i is written as

$$\tilde{T}_{i,N+1} = \tilde{T}_{i,i+1}\left[\prod_{j=i+1}^{N} \mathrm{e}^{\mathrm{i}k_j d_j}\ \tilde{T}_{j,j+1}\right]. \tag{D.48}$$

The transmission coefficients of the whole multilayer is $\tilde{T}_{0,N+1}$, and it should be identical to $\tilde{T}_{N+1,0}$ obtained in the previous subsection. On the other hand, the backward field in layer i is represented as

$$\tilde{F}_i = \tilde{R}_{i-1,i}\ \mathrm{e}^{\mathrm{i}k_i d_i}\ \tilde{B}_i = \tilde{R}_{i-1,i}\ \mathrm{e}^{\mathrm{i}k_i d_i}\ \tilde{T}_{i,N+1}\ E_{\mathrm{R}} \qquad (i = 1,\ \ldots,\ N), \tag{D.49}$$

and the one in layer $N+1$ is

$$\tilde{F}_{N+1} = \tilde{R}_{N,N+1}\ E_{\mathrm{R}}. \tag{D.50}$$

D.3 Derivation of Green's function

First, I consider the case of $j = i$. The propagator $\mathcal{G}_{i,i}(z, z')$ should be written as

$$\mathcal{G}_{i,i}(z, z') = \mathrm{e}^{\mathrm{i}k_i|z-z'|} + \mathrm{e}^{\mathrm{i}k_i(z-z_{i-1})}F_{i,i}(z') + \mathrm{e}^{-\mathrm{i}k_i(z-z_i)}B_{i,i}(z'), \tag{D.51}$$

where functions $F_{i,i}(z')$ and $B_{i,i}(z')$ are unknowns to be determined. From Eq. (D.38) at interface $z = z_{i-1}$, I obtain

$$F_{i,i}(z') = \tilde{R}_{i-1,i}\left[\mathrm{e}^{\mathrm{i}k_i(z_i-z')} + \mathrm{e}^{\mathrm{i}k_i d_i}B_{i,i}(z')\right], \tag{D.52}$$

and the following relation is also obtained from Eq. (D.20) at $z = z_i$:

$$B_{i,i}(z') = \tilde{R}_{i+1,i}\left[\mathrm{e}^{\mathrm{i}k_i(z_i-z')} + \mathrm{e}^{\mathrm{i}k_i d_i}F_{i,i}(z')\right]. \tag{D.53}$$

Solving these two equations, the two unknown functions are determined as

$$F_{i,i}(z') = \tilde{R}_{i-1,i}\left[\mathrm{e}^{-\mathrm{i}k_i(z_{i-1}-z')} + \mathrm{e}^{\mathrm{i}k_i d_i}\tilde{R}_{i+1,i}\mathrm{e}^{\mathrm{i}k_i(z_i-z')}\right]\tilde{M}_i, \tag{D.54}$$

$$B_{i,i}(z') = \tilde{R}_{i+1,i}\left[\mathrm{e}^{\mathrm{i}k_i(z_i-z')} + \mathrm{e}^{\mathrm{i}k_i d_i}\tilde{R}_{i-1,i}\mathrm{e}^{-\mathrm{i}k_i(z_{i-1}-z')}\right]\tilde{M}_i, \tag{D.55}$$

and then we obtain Eq. (D.3).

Next, I consider the case of $j > i$. The propagator $\mathcal{G}_{j,i}(z, z')$ should be written as

$$\mathcal{G}_{j,i}(z, z') = \mathrm{e}^{\mathrm{i}k_j(z-z_{j-1})}F_{j,i}(z') + \mathrm{e}^{-\mathrm{i}k_j(z-z_j)}B_{j,i}(z'), \tag{D.56}$$

and the two unknown functions $F_{j,i}(z')$ and $B_{j,i}(z')$ are determined as follows. From Eq. (D.20) at $z = z_j$, I obtain

$$B_{j,i}(z') = \tilde{R}_{j+1,j}\mathrm{e}^{\mathrm{i}k_j d_j}F_{j,i}(z'). \tag{D.57}$$

On the other hand, from Eq. (D.19) at $z = z_{j-1}$, $F_{j,i}(z')$ is represented as

$$\begin{aligned} F_{j,i}(z') &= \tilde{T}_{j,j-1}\mathrm{e}^{\mathrm{i}k_{j-1}d_{j-1}}F_{j-1,i}(z') \\ &= \tilde{T}_{j,i}\left[\mathrm{e}^{\mathrm{i}k_i(z_i-z')} + \mathrm{e}^{\mathrm{i}k_i d_i}F_{i,i}(z')\right] \\ &= \tilde{T}_{j,i}\frac{B_{i,i}(z')}{\tilde{R}_{i+1,i}} \\ &= \tilde{T}_{j,i}\left[\mathrm{e}^{\mathrm{i}k_i(z_i-z')} + \mathrm{e}^{\mathrm{i}k_i d_i}\tilde{R}_{i-1,i}\mathrm{e}^{-\mathrm{i}k_i(z_{i-1}-z')}\right]\tilde{M}_i. \end{aligned} \tag{D.58}$$

Therefore, $\mathcal{G}_{j,i}(z, z')$ is represented as Eq. (D.5). The propagator in the case of $j > i$ is also obtained by the same procedure.

Appendix E

Numerical Calculation of Poles

For calculating the poles for exciton-photon inhomogeneous systems as discussed in Chap. 3, we should use proper algorithm to correctly obtain the poles. Especially, in order to reproduce the retarded correlation functions of excitons, we must calculate all the poles of the system. I show the algorithm of the matrix method in Sec. E.1, and the one of the intuitive method in Sec. E.2.

E.1 Matrix method

When we calculate the poles of exciton correlation functions by the matrix method, in the previous studies based on the microscopic nonlocal theory [33, 35, 38], the poles have been calculated under the condition that the determinant of the coefficient matrix [Eq. (3.18)] of the linear equation set is zero for a trial complex frequency $\tilde{\omega}$. However, this calculation algorithm cannot provide the poles at a large film thickness, for example, thicker than 300 nm in the case of CuCl film. Therefore, this algorithm is not applicable to the crossover discussion between the two radiative decay schemes.

On the other hand, I used another algorithm and succeeded to calculate the poles for micrometer-order thickness. This algorithm is as follows.

1. I calculate complex eigenvalues of the coefficient matrix for a initial frequency. The number of eigenvalues is equal to the number of exciton states considered in the matrix calculation. Usually, these eigenvalues are approximately equal to the strict frequencies of the poles. Therefore, for all obtained eigenvalues, I perform the following processes by considering one of the eigenvalues as a trial frequency.
2. For a given trial frequency, I calculate the eigenvalues of the coefficient matrix.
3. Among the obtained eigenvalues, I select a value mostly close to the trial frequency.
4. If the difference between the selected value and the trial one is sufficiently close to each other, I consider the calculated value is the complex frequency characterizing a pole of the correlation functions. Otherwise, I perform processes 2, 3, and 4 by considering the selected value as the new trial frequency.

In the actual calculation for CuCl film, I used $\hbar\omega - \hbar\omega_{\mathrm{T}} = 0$, 6, 100, and -100 meVas initial frequencies. These frequency approximately correspond to the band edge of bare exciton dispersion, band edge of upper polariton branch, eigenenergies of upper and lower polaritons at the phase-matching wavenumber $k = \sqrt{\varepsilon_{\mathrm{bg}}}\omega_{\mathrm{T}}/c$, respectively. By using these four initial values, when I consider 200 states of exciton center-of-mass motion, 200 values are obtained for most thicknesses. However, only 199 or 198 values

were obtained at particular thicknesses, because the exciton-photon coupled modes with much photon component cannot be numerically calculated in this matrix method as explained in Chap. 3. In order to obtain such photon-like modes, we must use the intuitive method explained in the next section.

E.2 Intuitive method

In the intuitive method based on the dispersion relation and the self-sustaining condition, we can obtain infinite number of poles regardless of the crystal size. This is because I used the effective mass approximation for the exciton center-of-mass kinetic energy, although the dispersion relation of excitons is actually periodic by shifting the wavenumber by the unit of reciprocal lattice vector. Therefore, we should consider the first Brillouin zone as the range of the wavenumber in the actual calculation, and then the number of wavenumbers are equal to the number of atomic layers in the considering film.

In actual calculation for poles in a film with thickness d, I used the following algorithm.

1. I consider an positive integer $n = 1, 2, \ldots$, and use $k = n\pi/d$ as an initial wavenumber. Further, I consider a small quantity (10^{-8}) as the initial value of α. For all integers smaller than the number of atomic layers, I perform the following processes in the exciton-like case and in the photon-like one, independently.
2. For a trial complex wavenumber $\tilde{k} = k - \mathrm{i}\alpha/d$, I obtain two complex frequencies with positive real parts satisfying Eq. (3.34), the dispersion relation. In the exciton-like case, I select the frequency with smaller imaginary absolute, and select the other in the photon-like case.
3. From the selected complex frequency, I obtain two complex wavenumbers satisfying Eq. (3.34), and one of them should be equal to the trial wavenumber.
4. Considering the trial wavenumber as $\tilde{k}_1$ and the other as $\tilde{k}_2$, I solve the ABC problem [Eqs. (3.39)], and then obtain B_1/F_1.
5. Using B_1/F_1, I renew the trial wavenumber $\tilde{k}$ as Eq. (3.44). Here, it is worth to note that the real part of the renewed wavenumber is not determined uniquely, because $\tilde{k} + m\pi/d$ also satisfies Eq. (3.43) for arbitrary integer m. Therefore, I define the range of the real part of $\tilde{k}$ as $(n - 1/2)\pi/d < k < (n + 1/2)\pi/d$ or $(n - 1)\pi/d < k < n\pi/d$. We should independently consider both of the ranges to obtain all the poles in the system.
6. If the renewed $\tilde{k}$ and the trial complex wavenumber are sufficiently close to each other, I consider the obtained value as the wavenumber of a pole, and corresponding frequency is the pole. Otherwise, I perform processes 2–5 again.

When we want to categorize the poles as upper and lower branches instead of exciton- and photon-like modes, we should select the frequency with larger real part part as the upper branch, and the other as the lower branch in process 2.

Appendix F

Definitions of Fourier Transform and Longitudinal & Transverse Fields

I explain the definition of Fourier transform and that of longitudinal and transverse fields discussed in this thesis. I show the definition of the spatial Fourier transform in Sec. F.1, and the temporal one in Sec. F.2. I explain the definition of longitudinal and transverse fields in Sec. F.3.

F.1 Spatial Fourier transform

I define the Fourier transform of function f between spatial position $\boldsymbol{r}$ and wavevector $\boldsymbol{k}$ as

$$f(\boldsymbol{r}) = \frac{1}{(2\pi)^{3/2}} \int \mathrm{d}\boldsymbol{k}\ f(\boldsymbol{k})\ \mathrm{e}^{\mathrm{i}\boldsymbol{k}\cdot\boldsymbol{r}}, \tag{F.1a}$$

$$f(\boldsymbol{k}) = \frac{1}{(2\pi)^{3/2}} \int \mathrm{d}\boldsymbol{r}\ f(\boldsymbol{r})\ \mathrm{e}^{-\mathrm{i}\boldsymbol{k}\cdot\boldsymbol{r}}. \tag{F.1b}$$

On the other hand, in a finite system with volume V, the wavenumber is discrete, and I denote the function in the k-space as

$$f_{\boldsymbol{k}} = \frac{(2\pi)^{3/2}}{\sqrt{V}} f(\boldsymbol{k}). \tag{F.2}$$

For this definition, the Fourier transform is represented as

$$f(\boldsymbol{r}) = \frac{1}{\sqrt{V}} \sum_{\boldsymbol{k}} f_{\boldsymbol{k}}\ \mathrm{e}^{\mathrm{i}\boldsymbol{k}\cdot\boldsymbol{r}}, \tag{F.3a}$$

$$f_{\boldsymbol{k}} = \frac{1}{\sqrt{V}} \int \mathrm{d}\boldsymbol{r}\ f(\boldsymbol{r})\ \mathrm{e}^{-\mathrm{i}\boldsymbol{k}\cdot\boldsymbol{r}}. \tag{F.3b}$$

Further, when we consider $\boldsymbol{r}$ as a discrete position in a lattice consisting of N unit cells with volume Ω, I denote the function in the real space as

$$f_{\boldsymbol{r}} = \sqrt{\Omega} f(\boldsymbol{r}). \tag{F.4}$$

In this case, the Fourier transform is represented as

$$f_{\boldsymbol{r}} = \frac{1}{\sqrt{N}} \sum_{\boldsymbol{k}} f_{\boldsymbol{k}}\ \mathrm{e}^{\mathrm{i}\boldsymbol{k}\cdot\boldsymbol{r}}, \tag{F.5a}$$

$$f_{\boldsymbol{k}} = \frac{1}{\sqrt{N}} \sum_{\boldsymbol{r}} f_{\boldsymbol{r}}\ \mathrm{e}^{-\mathrm{i}\boldsymbol{k}\cdot\boldsymbol{r}}. \tag{F.5b}$$

On the other hand, when I consider a function $G(\boldsymbol{r}, \boldsymbol{r}')$ connecting two functions $f(\boldsymbol{r})$ and $g(\boldsymbol{r})$ as

$$g(\boldsymbol{r}) = \int \mathrm{d}\boldsymbol{r}\ G(\boldsymbol{r}, \boldsymbol{r}') f(\boldsymbol{r}'), \tag{F.6}$$

I define the Fourier transform of $G(\boldsymbol{r}, \boldsymbol{r}')$ as

$$G(\boldsymbol{r}, \boldsymbol{r}') = \frac{1}{(2\pi)^3} \int \mathrm{d}\boldsymbol{k} \int \mathrm{d}\boldsymbol{k}'\ \mathrm{e}^{\mathrm{i}\boldsymbol{k}\cdot\boldsymbol{r}}\ G(\boldsymbol{k}, \boldsymbol{k}')\ \mathrm{e}^{-\mathrm{i}\boldsymbol{k}'\cdot\boldsymbol{r}'}, \tag{F.7a}$$

$$G(\boldsymbol{k}, \boldsymbol{k}') = \frac{1}{(2\pi)^3} \int \mathrm{d}\boldsymbol{r} \int \mathrm{d}\boldsymbol{r}'\ \mathrm{e}^{-\mathrm{i}\boldsymbol{k}\cdot\boldsymbol{r}}\ G(\boldsymbol{r}, \boldsymbol{r}')\ \mathrm{e}^{\mathrm{i}\boldsymbol{k}'\cdot\boldsymbol{r}'}. \tag{F.7b}$$

The definitions for finite and discrete systems are the same as mentioned above.

F.2 Temporal Fourier transform

I define the Fourier transform of function f between time t and frequency ω as

$$f(t) = \int_{-\infty}^{\infty} \mathrm{d}\omega\ f(\omega)\ \mathrm{e}^{-\mathrm{i}\omega t}, \tag{F.8a}$$

$$f(\omega) = \frac{1}{2\pi} \int_{-\infty}^{\infty} \mathrm{d}t\ f(t)\ \mathrm{e}^{\mathrm{i}\omega t}. \tag{F.8b}$$

Especially in the case that $f(t)$ is a real function, I define positive- and negative-frequency Fourier components of $f(t)$ for $\omega > 0$ as

$$f^{+}(\omega) = \frac{1}{2\pi} \int_{-\infty}^{\infty} \mathrm{d}t\ f(t)\ \mathrm{e}^{\mathrm{i}\omega t}, \tag{F.9a}$$

$$f^{-}(\omega) = \frac{1}{2\pi} \int_{-\infty}^{\infty} \mathrm{d}t\ f(t)\ \mathrm{e}^{-\mathrm{i}\omega t}, \tag{F.9b}$$

respectively. These functions have a relation as

$$\left\{ f^{+}(\omega^*) \right\}^* = f^{-}(\omega), \tag{F.10}$$

and the time representation is represented as

$$f(t) = \int_{0}^{\infty} \mathrm{d}\omega\ \left[f^{+}(\omega)\ \mathrm{e}^{-\mathrm{i}\omega t} + f^{-}(\omega)\ \mathrm{e}^{\mathrm{i}\omega t} \right]. \tag{F.11}$$

On the other hand, for correlation functions appearing in the linear response theory discussed in Sec. A.1, I define the temporal Fourier transform as

$$G(t) = \frac{1}{2\pi} \int_{-\infty}^{\infty} \mathrm{d}\omega\ G(\omega)\ \mathrm{e}^{-\mathrm{i}\omega t}, \tag{F.12a}$$

$$G(\omega) = \int_{-\infty}^{\infty} \mathrm{d}t\ G(t)\ \mathrm{e}^{\mathrm{i}\omega t}. \tag{F.12b}$$

This definition or Eq. (A.13) is suitable for simplifying the representation as seen in Eq. (A.12).

F.3 Longitudinal and transverse fields

I define that a vector function $\boldsymbol{X}(\boldsymbol{r})$ satisfying

$$\boldsymbol{\nabla} \cdot \boldsymbol{X}(\boldsymbol{r}) = 0 \tag{F.13}$$

is transverse, and a vector function satisfying

$$\boldsymbol{\nabla} \times \boldsymbol{X}(\boldsymbol{r}) = \boldsymbol{0} \tag{F.14}$$

is longitudinal. The reason of these definitions is as follows. By expanding $\boldsymbol{X}(\boldsymbol{r})$ by plane waves as

$$\boldsymbol{X}(\boldsymbol{r}) = \frac{1}{(2\pi)^{3/2}} \int \mathrm{d}\boldsymbol{k}\ \boldsymbol{X}(\boldsymbol{k})\ \mathrm{e}^{\mathrm{i}\boldsymbol{k}\cdot\boldsymbol{r}}, \tag{F.15}$$

its divergence and rotation are represented as

$$\boldsymbol{\nabla} \cdot \boldsymbol{X}(\boldsymbol{r}) = \frac{1}{(2\pi)^{3/2}} \int \mathrm{d}\boldsymbol{k}\ \mathrm{i}\boldsymbol{k} \cdot \boldsymbol{X}(\boldsymbol{k})\ \mathrm{e}^{\mathrm{i}\boldsymbol{k}\cdot\boldsymbol{r}}, \tag{F.16}$$

$$\boldsymbol{\nabla} \times \boldsymbol{X}(\boldsymbol{r}) = \frac{1}{(2\pi)^{3/2}} \int \mathrm{d}\boldsymbol{k}\ \mathrm{i}\boldsymbol{k} \times \boldsymbol{X}(\boldsymbol{k})\ \mathrm{e}^{\mathrm{i}\boldsymbol{k}\cdot\boldsymbol{r}}. \tag{F.17}$$

Here, the condition $\boldsymbol{\nabla} \cdot \boldsymbol{X}(\boldsymbol{r}) = 0$ means that $\boldsymbol{X}(\boldsymbol{k})$ is parallel to the propagation direction $\boldsymbol{k}$, and $\boldsymbol{\nabla} \times \boldsymbol{X}(\boldsymbol{r}) = \boldsymbol{0}$ means that $\boldsymbol{k}$ and $\boldsymbol{X}(\boldsymbol{k})$ are perpendicular to each other. Therefore, the above definitions for longitudinal and transverse fields are reasonable.

From Eq. (F.15), the longitudinal component of $\boldsymbol{X}(\boldsymbol{r})$ is represented as

$$\begin{aligned}
\boldsymbol{X}_{\mathrm{L}}(\boldsymbol{r}) &\equiv \frac{1}{(2\pi)^{3/2}} \int \mathrm{d}\boldsymbol{k}\ \frac{\boldsymbol{k}\boldsymbol{k}}{k^2} \cdot \boldsymbol{X}(\boldsymbol{k})\ \mathrm{e}^{\mathrm{i}\boldsymbol{k}\cdot\boldsymbol{r}} \\
&= -\frac{1}{(2\pi)^{3/2}} \int \mathrm{d}\boldsymbol{k}\ \frac{\boldsymbol{\nabla}\boldsymbol{\nabla}}{k^2} \cdot \boldsymbol{X}(\boldsymbol{k})\ \mathrm{e}^{\mathrm{i}\boldsymbol{k}\cdot\boldsymbol{r}} \\
&= -\frac{1}{(2\pi)^{3}} \int \mathrm{d}\boldsymbol{r}' \int \mathrm{d}\boldsymbol{k}\ \frac{\boldsymbol{\nabla}\boldsymbol{\nabla}}{k^2} \cdot \boldsymbol{X}(\boldsymbol{r}')\ \mathrm{e}^{\mathrm{i}\boldsymbol{k}\cdot(\boldsymbol{r}-\boldsymbol{r}')}.
\end{aligned} \tag{F.18}$$

Here, from the Fourier transform between $1/4\pi r$ and $1/k^2$ as

$$\int \mathrm{d}\boldsymbol{r}\ \frac{\mathrm{e}^{-\mathrm{i}\boldsymbol{k}\cdot\boldsymbol{r}}}{4\pi r} = \frac{1}{k^2}, \tag{F.19a}$$

$$\frac{1}{(2\pi)^3} \int \mathrm{d}\boldsymbol{k}\ \frac{\mathrm{e}^{\mathrm{i}\boldsymbol{k}\cdot\boldsymbol{r}}}{k^2} = \frac{1}{4\pi r}, \tag{F.19b}$$

$\boldsymbol{X}_{\mathrm{L}}(\boldsymbol{r})$ is rewritten as

$$\boldsymbol{X}_{\mathrm{L}}(\boldsymbol{r}) = -\int \mathrm{d}\boldsymbol{r}'\ \frac{\boldsymbol{\nabla}'\boldsymbol{\nabla}'}{4\pi|\boldsymbol{r}-\boldsymbol{r}'|} \cdot \boldsymbol{X}(\boldsymbol{r}') = \int \mathrm{d}\boldsymbol{r}'\ \boldsymbol{\delta}_{\mathrm{L}}(\boldsymbol{r}-\boldsymbol{r}') \cdot \boldsymbol{X}(\boldsymbol{r}'), \tag{F.20}$$

where $\boldsymbol{\delta}_{\mathrm{L}}(\boldsymbol{r}-\boldsymbol{r}')$ is the delta function extracting the longitudinal component as

$$\boldsymbol{\delta}_{\mathrm{L}}(\boldsymbol{r}-\boldsymbol{r}') \equiv -\frac{\boldsymbol{\nabla}'\boldsymbol{\nabla}'}{4\pi|\boldsymbol{r}-\boldsymbol{r}'|}. \tag{F.21}$$

On the other hand, by using the delta function extracting the transverse component

$$\boldsymbol{\delta}_{\mathrm{T}}(\boldsymbol{r}-\boldsymbol{r}') \equiv \boldsymbol{1}\ \delta(\boldsymbol{r}-\boldsymbol{r}') + \frac{\boldsymbol{\nabla}'\boldsymbol{\nabla}'}{4\pi|\boldsymbol{r}-\boldsymbol{r}'|}, \tag{F.22}$$

the transverse field is represented as

$$\boldsymbol{X}_{\mathrm{T}}(\boldsymbol{r}) = \int \mathrm{d}\boldsymbol{r}'\ \boldsymbol{\delta}_{\mathrm{T}}(\boldsymbol{r}-\boldsymbol{r}') \cdot \boldsymbol{X}(\boldsymbol{r}'). \tag{F.23}$$

These functions satisfy Eqs. (F.13) and (F.14) as

$$\boldsymbol{\nabla} \times \boldsymbol{X}_{\mathrm{L}}(\boldsymbol{r}) = \frac{1}{(2\pi)^{3/2}} \int \mathrm{d}\boldsymbol{k}\ \mathrm{i}\boldsymbol{k} \times \frac{\boldsymbol{k}\boldsymbol{k}}{k^2} \cdot \boldsymbol{X}(\boldsymbol{k})\ \mathrm{e}^{\mathrm{i}\boldsymbol{k}\cdot\boldsymbol{r}}, = \boldsymbol{0} \tag{F.24}$$

$$\boldsymbol{\nabla} \cdot \boldsymbol{X}_{\mathrm{T}}(\boldsymbol{r}) = \frac{1}{(2\pi)^{3/2}} \int \mathrm{d}\boldsymbol{k}\ \mathrm{i}\boldsymbol{k} \cdot \left(\boldsymbol{1} - \frac{\boldsymbol{k}\boldsymbol{k}}{k^2}\right) \cdot \boldsymbol{X}(\boldsymbol{k})\ \mathrm{e}^{\mathrm{i}\boldsymbol{k}\cdot\boldsymbol{r}} = 0. \tag{F.25}$$

References

[1] Keiichi Edamatsu, Goro Oohata, Ryosuke Shimizu, and Tadashi Itoh, *Generation of ultraviolet entangled photons in a semiconductor*, Nature **431**(7005), 167–170 (Sep 2004).

[2] S. Strauf, P. Michler, M. Klude, D. Hommel, G. Bacher, and A. Forchel, *Quantum Optical Studies on Individual Acceptor Bound Excitons in a Semiconductor*, Phys. Rev. Lett. **89**(17), 177403, 4 pages (Oct 2002).

[3] Paolo Schwendimann, Cristiano Ciuti, and Antonio Quattropani, *Statistics of polaritons in the nonlinear regime*, Phys. Rev. B **68**(16), 165324, 10 pages (Oct 2003).

[4] J. Ph. Karr, A. Baas, R. Houdré, and E. Giacobino, *Squeezing in semiconductor microcavities in the strong-coupling regime*, Phys. Rev. A **69**(3), 031802, 4 pages (Mar 2004).

[5] S. A. Moskalenko and D. W. Snoke, *Bose-Einstein Condensation of Excitons and Biexcitons: And Coherent Nonlinear Optics With Excitons* (Cambridge University Press, United Kingdom, 2000).

[6] David Snoke, *Spontaneous Bose Coherence of Excitons and Polaritons*, Science **292**(5597), 1368–1372 (Nov 2002).

[7] Hui Deng, Gregor Weihs, Charles Santori, Jacqueline Bloch, and Yoshihisa Yamamoto, *Condensation of Semiconductor Microcavity Exciton Polaritons*, Science **298**(5591), 199–202 (Oct 2002).

[8] J. Kasprzak, M. Richard, S. Kundermann, A. Baas, P. Jeambrun, J. M. J. Keeling, F. M. Marchetti, M. H. Szymańska, R. André, J. L. Staehli, V. Savona, P. B. Littlewood, B. Deveaud, and Le Si Dang, *Bose-Einstein condensation of exciton polaritons*, Nature **443**(7110), 409–414 (Sep 2006).

[9] Hui Deng, David Press, Stephan Gotzinger, Glenn S. Solomon, Rudolf Hey, Klaus H. Ploog, and Yoshihisa Yamamoto, *Quantum Degenerate Exciton-Polaritons in Thermal Equilibrium*, Phys. Rev. Lett. **97**(14), 146402, 4 pages (Oct 2006).

[10] R. Balili, V. Hartwell, D. Snoke, L. Pfeiffer, and K. West, *Bose-Einstein Condensation of Microcavity Polaritons in a Trap*, Science **316**(5827), 1007–1010 (May 2007).

[11] F. M. Marchetti, J. Keeling, M. H. Szymańska, and P. B. Littlewood, *Thermodynamics and Excitations of Condensed Polaritons in Disordered Microcavities*, Phys. Rev. Lett. **96**(6), 066405, 4 pages (Feb 2006).

[12] M. H. Szymańska, J. Keeling, and P. B. Littlewood, *Nonequilibrium Quantum Condensation in an Incoherently Pumped Dissipative System*, Phys. Rev. Lett. **96**(23), 230602, 4 pages (Jun 2006).

[13] I. A. Shelykh, Yuri G. Rubo, G. Malpuech, D. D. Solnyshkov, , and A. Kavokin, *Polarization and Propagation of Polariton Condensates*, Phys. Rev. Lett. **97**(6), 066402, 4 pages (Aug 2006).

[14] G. Malpuech, D. D. Solnyshkov, H. Ouerdane, M. M. Glazov, and I. Shelykh, *Bose Glass and Superfluid Phases of Cavity Polaritons*, Phys. Rev. Lett. **98**(20), 206402, 4 pages (May 2007).

[15] D. Sarchi and V. Savona, *Spectrum and thermal fluctuations of a microcavity polariton Bose-Einstein condensate*, Phys. Rev. B **77**(4), 045304, 8 pages (Jan 2008).

[16] Claude Cohen-Tannoudji, Jacques Dupont-Roc, and Gilbert Grynberg, *Photons and Atoms: Introduction to Quantum Electrodynamics* (Wiley, New York, 1989).

[17] Seng-Tiong Ho and Prem Kumar, *Quantum optics in dielectric: macroscopic electromagnetic-field and medium operators for a linear dispersive lossy medium - a microscopic derivation of the operators and their commutation relations*, J. Opt. Soc. Am. B **10**(9), 1620–1636 (Sep 1993).

[18] Ludwig Knöll, Stefan Scheel, and Dirk-Gunnar Welsch, *QED in Dispersing and Absorbing Dielectric Media*, in *Coherence and Statistics of Photons and Atoms*, edited by Jan Peřina, Wiley Series in Lasers and Applications (Wiley, New York, 2001), chapter 1, pages 1–64, for update, see arXiv:quant-ph/0006121.

[19] J. J. Hopfield, *Theory of the Contribution of Excitons to the Complex Dielectric Constant of Crystals*, Phys. Rev. **112**(5), 1555–1567 (Dec 1958).

[20] B. Huttner and S. M. Barnett, *Dispersion and Loss in a Hopfield Dielectric*, Europhys. Lett. **18**(6), 487–492 (Mar 1992).

[21] Bruno Huttner and Stephen M. Barnett, *Quantization of the electromagnetic field in dielectrics*, Phys. Rev. A **46**(7), 4306–4322 (Oct 1992).

[22] Vladimir M. Agranovich and Vitaly L. Ginzburg, *Crystal Optics with Spatial Dispersion, and Excitons*, Vol. 42 of *Springer Series in Solid-State Sciences* (Springer-Verlag, Berlin, 1984), Second Corrected and Updated edition.

[23] Omar Di Stefano, Salvatore Savasta, and Raffaello Girlanda, *Electromagnetic-field quantization in absorbing confined systems*, Phys. Rev. A **60**(2), 1614–1625 (Aug 1999).

[24] Omar Di Stefano, Salvatore Savasta, and Raffaello Girlanda, *Microscopic calculation of noise current operators for electromagnetic field quantization in absorbing material systems*, J. Opt. B: Quantum Semiclass. Opt. **3**(4), 288–292 (Aug 2001).

[25] Salvatore Savasta, Omar Di Stefano, and Raffaello Girlanda, *Light quantization for arbitrary scattering systems*, Phys. Rev. A **65**(4), 043801, 11 pages (Mar 2002).

[26] Adam Bechler, *Path-integral quantization of the electromagnetic field in the Hopfield dielectric beyond dipole approximation*, J. Phys. A: Math. Gen. **39**(43), 13553–13573 (Oct 2006).

[27] L. G. Suttorp, *Field quantization in inhomogeneous anisotropic dielectrics with spatio-temporal dispersion*, J. Phys. A: Math. Theor. **40**(13), 3697–3719 (Mar 2007).

[28] Christian Raabe, Stefan Scheel, and Dirk-Gunnar Welsch, *Unified approach to QED in arbitrary linear media*, Phys. Rev. A **75**(5), 053813, 22 pages (May 2007).

[29] Kikuo Cho, *"ABC"-Free Theory of Polariton: From Semi-Infinite Medium to Quantum Well*, J. Phys. Soc. Jpn. **55**(11), 4113–4121 (Nov 1986).

[30] Kikuo Cho, *Nonlocal Theory of Radiation-Matter Interaction: Boundary-Condition-Less Treatment of Maxwell Equations*, Prog. Theor. Phys. Suppl. **106**, 225–233 (1991).

[31] Kikuo Cho, *Optical Response of Nanostructures: Microscopic Nonlocal Theory*, Springer Series in Solid-State Sciences (Springer-Verlag, Berlin, 2003).

[32] Hajime Ishihara and Kikuo Cho, *Nonlinear optical response due to resonant enhancement of the internal field with particular spatial distribution*, Phys. Rev. B **53**(23), 15823–15833 (Jun 1996).

[33] Hajime Ishihara, Hideyuki Asakawa, and Kikuo Cho, *A super coupling of radiation field and excitons confined in spatially periodic structure*, Physica E **7**(3-4), 671–675 (May 2000).

[34] Hajime Ishihara, Tomonari Amakata, and Kikuo Cho, *Anomalous size dependence of degenerate four-wave mixing due to double resonance of internal field and third-order susceptibility*, Phys. Rev. B **65**(3), 035305, 9 pages (Jan 2001).

[35] Hiroshi Ajiki, *Size dependence of exciton-light interaction in a spherical semiconductor from quantum dot to bulk limit*, J. Lumin. **94-95**, 173–176 (Dec 2001).

[36] H. Ishihara, K. Cho, K. Akiyama, N. Tomita, and T. Isu, *Ultra-Fast Radiative Decay of Spatially Extended Non-Dipole Type Excitonic State*, phys. status solidi (a) **190**(3), 849–853 (Apr 2002).

[37] Hajime Ishihara, *Nonlocality-induced anomalous input-intensity dependence of optical response for weakly confined excitons in an ultrathin film*, Phys. Rev. B **67**(11), 113302, 4 pages (Mar 2003).

[38] H. Ishihara, J. Kishimoto, and K. Sugihara, *Anomalous mode structure of a radiation-exciton coupled system beyond the long-wavelength approximation regime*, J. Lumin. **108**(1-4), 343–346 (Jun 2004).

[39] H. Ishihara, A. Syouji, Y. Segawa, and M. Bamba, *Anomalous exciton-radiation coupling in the nano-to-bulk crossover regime*, J. Phys.: Condens. Matter **19**(44), 445008, 20 pages (Oct 2007).

[40] Koich Akiyama, Nobuyuki Tomita, Yoshinori Nomura, and Toshiro Isu, *Observation of a large third-order nonlinear response of exciton polaritons in GaAs thin film*, Appl. Phys. Lett. **75**(4), 475–477 (Jul 1999).

[41] Hajime Ishihara, Kikuo Cho, Koichi Akiyama, Nobuyuki Tomita, Yoshinori Nomura, and Toshiro Isu, *Large Four-Wave Mixing of Spatially Extended Excitonic States in Thin GaAs Layers*, Phys. Rev. Lett. **89**(1), 017402, 4 pages (Jul 2002).

[42] A. Syouji, B. P. Zhang, Y. Segawa, J. Kishimoto, H. Ishihara, and K. Cho, *Interchange of the Quantum States of Confined Excitons Caused by Radiative Corrections in CuCl Films*, Phys. Rev. Lett. **92**(25), 257401, 4 pages (Jun 2004).

[43] M. Ichimiya, M. Ashida, H. Yasuda, H. Ishihara, and T. Itoh, *Ultrafast degenerate four-wave mixing in CuCl ultrathin films*, phys. status solidi (b) **243**(14), 3800–3805 (Oct 2006).

[44] Salvatore Savasta and Raffaello Girlanda, *Hyper-Raman scattering in semiconductors: A quantum optical process in the strong-coupling regime*, Phys. Rev. B **59**(23), 15409–15421 (Jun 1999).

[45] S. Savasta, G. Martino, and R. Girlanda, *Entangled photon pairs from the optical decay of biexcitons*, Solid State Commun. **111**(9), 495–500 (Jul 1999).

[46] Motoaki Bamba and Hajime Ishihara, *Entangled-photon generation via biexcitons in nanostructures*, phys. status solidi (c) **3**(10), 3460–3463 (Nov 2006).

[47] Hiroshi Ajiki and Hajime Ishihara, *Entangled-Photon Generation in Biexcitonic Cavity QED*, J. Phys. Soc. Jpn. **76**(5), 053401, 4 pages (May 2007).

[48] Hisaki Oka and Hajime Ishihara, *Highly Efficient Generation of Entangled Photons by Controlling Cavity Bipolariton States*, Phys. Rev. Lett. **100**(17), 170505, 4 pages (Apr 2008).

[49] Reza Matloob and Rodney Loudon, *Electromagnetic field quantization in absorbing dielectrics. II*, Phys. Rev. A **53**(6), 4567–4582 (Jun 1996).

[50] L. D. Landau and E. M. Lifshitz, *Statistical Physics Part 1*, Vol. 5 of *Course of Theoretical Physics* (Pergmon, Oxford, 1980), 3rd edition, translated by J. B. Sykes and M. J. Kearsley.

[51] Reza Matloob, Rodney Loudon, Stephen M. Barnett, and John Jeffers, *Electromagnetic field quantization in absorbing dielectrics*, Phys. Rev. A **52**(6), 4823–4838 (Dec 1995).

[52] T. Gruner and D.-G. Welsch, *Green-function approach to the radiation-field quantization for homogeneous and inhomogeneous Kramers-Kronig dielectrics*, Phys. Rev. A **53**(3), 1818–1829 (Mar 1996).

[53] A. A. Abrikosov, L. P. Gorkov, and I. E. Dzyaloshinski, *Methods of Quantum Field Theory in Statistical Physics* (Dover, New York, 1975), Revised English edition, translated and edited by Richard A. Silverman.

[54] T. Gruner and D.-G. Welsch, *Correlation of radiation-field ground-state fluctuations in a dispersive and lossy dielectric*, Phys. Rev. A **51**(4), 3246–3256 (Apr 1995).

[55] Stephen M. Barnett, Bruno Huttner, and Rodney Loudon, *Spontaneous emission in absorbing dielectric media*, Phys. Rev. Lett. **68**(25), 3698–3701 (Jun 1992).

[56] Kazuki Koshino and Akira Shimizu, *Spontaneous emission in an absorptive and inhomogeneous cavity*, Phys. Rev. A **53**(6), 4468–4475 (Jun 1996).

[57] S. Savasta and R. Girlanda, *Quantum description of the input and output electromagnetic fields in a polarizable confined system*, Phys. Rev. A **53**(4), 2716–2726 (Apr 1996).

[58] T. Gruner and D.-G. Welsch, *Quantum-optical input-output relations for dispersive and lossy multilayer dielectric plates*, Phys. Rev. A **54**(2), 1661–1677 (Aug 1996).

[59] Stefan Scheel and Dirk-Gunnar Welsch, *Quantum Theory of Light and Noise Polarization in Nonlinear Optics*, Phys. Rev. Lett. **96**(7), 073601, 4 pages (Feb 2006).

[60] S. Scheel and D.-G. Welsch, *Causal nonlinear quantum optics*, J. Phys. B: At. Mol. Opt. Phys. **39**(15), S711–S724 (Jul 2006).

[61] Ho Trung Dung, Ludwig Knöll, and Dirk-Gunnar Welsch, *Three-dimensional quantization of the electromagnetic field in dispersive and absorbing inhomogeneous dielectrics*, Phys. Rev. A **57**(5), 3931–3942 (May 1998).

[62] Martijn Wubs and L. G. Suttorp, *Transient QED effects in absorbing dielectrics*, Phys. Rev. A **63**(4), 043809, 14 pages (Apr 2001).

[63] L. G. Suttorp and Martijn Wubs, *Field quantization in inhomogeneous absorptive dielectrics*, Phys. Rev. A **70**(1), 013816, 18 pages (Jul 2004).

[64] L. G. Suttorp and A. J. van Wonderen, *Fano diagonalization of a polariton model for an inhomogeneous absorptive dielectric*, Europhys. Lett. **67**(5), 766–772 (Sep 2004).

[65] Weng Cho Chew, *Waves and Fields in Inhomogeneous Media*, IEEE Press Series on Electromagnetic Wave (IEEE, New York, 1995), Reprint edition.

[66] Olivier J. F. Martin, Christian Girard, and Alain Dereux, *Generalized Field Propagator for Electromagnetic Scattering and Light Confinement*, Phys. Rev. Lett. **74**(4), 526–529 (Jan 1995).

[67] S. I. Pekar, *The Theory of Electromagnetic Waves in a Crystal in Which Excitons are produced*, Zh. Eksp. Teor. Fiz. **33**, 1022–1036 (Oct 1957), [Sov. Phys. -JETP **6**(4), 785–796 (April 1958)].

[68] John David Jackson, *Classical Electrodynamics* (Wiley, New Jersey, 1998), Third edition.

[69] J. J. Hopfield and D. G. Thomas, *Theoretical and Experimental Effects of Spatial Dispersion on the Optical Properties of Crystals*, Phys. Rev. **132**(2), 563–572 (Oct 1963).

[70] Roland Zeyher, Joseph L. Birman, and Wilhelm Brenig, *Spatial Dispersion Effects in Resonant Polariton Scattering. I. Additional Boundary Conditions for Polarization Fields*, Phys. Rev. B **6**(12), 4613–4616 (Dec 1972).

[71] A. D'Andrea and R. Del Sole, *Wannier-Mott excitons in semi-infinite crystals: Wave functions and normal-incidence reflectivity*, Phys. Rev. B **25**(6), 3714–3730 (Mar 1982).

[72] Kikuo Cho and Masaru Kawata, *Theoretical Analysis of Polariton Interference in a Thin Platelet of CuCl. I. Additional Boundary Condition*, J. Phys. Soc. Jpn. **54**(11), 4431–4443 (Nov 1985).

[73] Kikuo Cho, Andrea D'andrea, Rodolfo Del Sole, and Hajime Ishihara, *Exciton Quantization and Polariton Interference in Thin Films: Comparison of Different Approaches*, J. Phys. Soc. Jpn. **59**(5), 1853–1867 (May 1990).

[74] Z. K. Tang, A. Yanase, Y. Segawa, N. Matsuura, and K. Cho, *Quantization of excitons in CuCl epitaxial thin films: Behavior between a two-dimensional quantum well and the bulk*, Phys. Rev. B **52**(4), 2640–2648 (Jul 1995).

[75] Hiroshi Ajiki and Kikuo Cho, *Longitudinal and transverse components of excitons in a spherical quantum dot*, Phys. Rev. B **62**(11), 7402–7412 (Sep 2000).

[76] Kikuo Cho, Kiyohiko Kawano, Tetsuya Tsuji, and Hiroshi Ajiki, *Optical response of a confined exciton in a sphere with the effect of LT splitting and background polarization: Comparison of two different approaches*, Int. J. Mod. Phys. B **15**(28/30), 3619–3622 (Dec 2001).

[77] Hiroshi Ajiki, Tetsuya Tsuji, Kiyohiko Kawano, and Kikuo Cho, *Optical spectra and exciton-light coupled modes of a spherical semiconductor nanocrystal*, Phys. Rev. B **66**(24), 245322, 12 pages (Dec 2002).

[78] Motoaki Bamba and Hajime Ishihara, *QED of excitons with nonlocal susceptibility in arbitrarily structured dielectrics*, Phys. Rev. B **78**(8), 085109, 22 pages (Aug 2008).

[79] Jonathan K. Jenkins and Shaul Mukamel, *Quantum electrodynamics of molecular nanostructures*, J. Chem. Phys. **98**(9), 7046–7058 (May 1993).

[80] Kikuo Cho, *Mechanisms for LT Splitting of Polarization Waves: a Link between Electron-Hole Exchange Interaction and Depolarization Shift*, J. Phys. Soc. Jpn. **68**(2), 683–691 (Feb 1999).

[81] Kikuo Cho, *Radiation Green's function of a DBR cavity containing a quantum well: vacuum photons and cavity polaritons on equal footing*, J. Lumin. **102-103**, 232–234 (May 2003).

[82] P. Borri, W. Langbein, S. Schneider, U. Woggon, R. L. Sellin, D. Ouyang, and D. Bimberg, *Ultralong Dephasing Time in InGaAs Quantum Dots*, Phys. Rev. Lett. **87**(15), 157401, 4 pages (Sep 2001).

[83] D. Birkedal, K. Leosson, and J. M. Hvam, *Long Lived Coherence in Self-Assembled Quantum Dots*, Phys. Rev. Lett. **87**(22), 227401, 4 pages (Nov 2001).

[84] P. Borri, W. Langbein, U. Woggon, V. Stavarache, D. Reuter, and A. D. Wieck, *Exciton dephasing via phonon interactions in InAs quantum dots: Dependence on quantum confinement*, Phys. Rev. B **71**(11), 115328, 8 pages (Mar 2005).

[85] J. Ishi-Hayase, K. Akahane, N. Yamamoto, M. Sasaki, M. Kujiraoka, and K. Ema, *Long dephasing time in self-assembled InAs quantum dots at over 1.3 μm wavelength*, Appl. Phys. Lett. **88**(26), 261907, 3 pages (Jun 2006).

[86] Y. C. Lee and P. S. Lee, *Coherent radiation from thin films*, Phys. Rev. B **10**(2), 344–348 (Jul 1974).

[87] T. Takagahara, *Excitonic optical nonlinearity and exciton dynamics in semiconductor quantum dots*, Phys. Rev. B **36**(17), 9293–9296 (Dec 1987).

[88] Eiichi Hanamura, *Very large optical nonlinearity of semiconductor microcrystallites*, Phys. Rev. B **37**(3), 1273–1279 (Jan 1988).

[89] Eiichi Hanamura, *Rapid radiative decay and enhanced optical nonlinearity of excitons in a quantum well*, Phys. Rev. B **38**(2), 1228–1234 (Jul 1988).

[90] A. Nakamura, H. Yamada, and T. Tokizaki, *Size-dependent radiative decay of excitons in CuCl semiconducting quantum spheres embedded in glasses*, Phys. Rev. B **40**(12), 8585–8588 (Oct 1989).

[91] Tadashi Itoh, Tsuyoshi Ikehara, and Yasuo Iwabuchi, *Quantum confinement of excitons and their relaxation processes in CuCl microcrystals*, J. Lumin. **45**(1-6), 29–33 (Jan-Feb 1990).

[92] Jasper Knoester, *Optical dynamics in crystal slabs: Crossover from superradiant excitons to bulk polaritons*, Phys. Rev. Lett. **68**(5), 654–657 (Feb 1992).

[93] T. Takagahara, *Nonlocal theory of the size and temperature dependence of the radiative decay rate of excitons in semiconductor quantum dots*, Phys. Rev. B **47**(24), 16639–16642 (Jun 1993).

[94] Gunnar Björk, Stanley Pau, Joseph M. Jacobson, Hui Cao, and Yoshihisa Yamamoto, *Excitonic superradiance to exciton-polariton crossover and the pole approximations*, Phys. Rev. B **52**(24), 17310–17320 (Dec 1995).

[95] V. M. Agranovich, D. M. Basko, and O. A. Dubovsky, *Superradiance of polaritons: Crossover from two-dimensional to three-dimensional crystals*, J. Chem. Phys. **106**(10), 3896–3907 (Mar 1997).

[96] Yosuke Kayanuma, *Quantum-size effects of interacting electrons and holes in semiconductor microcrystals with spherical shape*, Phys. Rev. B **38**(14), 9797–9805 (Nov 1988).

[97] Yueh-Nan Chen and Der-San Chuu, *Decay rate and renormalized frequency shift of superradiant excitons: Crossover from two-dimensional to three-dimensional crystals*, Phys. Rev. B **61**(16), 10815–10819 (Apr 2000).

[98] David K. Shuh, R. Stanley Williams, Yusaburo Segawa, Jun-ichi Kusano, Yoshinobu Aoyagi, and Susumu Namba, *Line-shape and lifetime studies of exciton luminescence from confined CuCl thin films*, Phys. Rev. B **44**(11), 5827–5833 (Sep 1991).

[99] M. Nakayama, S. Wakaiki, K. Mizoguchi, D. Kim, H. Ichida, and Y. Kanematsu, *Ultrafast photoluminescence dynamics of biexcitons in a CuCl thin film grown by vacuum deposition*, phys. status solidi (c) **3**(10), 3464–3467 (Nov 2006).

[100] Pierre Meystre and Murray Sargent III, *Elements of Quantum Optics* (Springer-Verlag, Berlin, 1999), chapter 18, pages 377–390, Third edition.

[101] Kikuo Cho and Hajime Ishihara, *ABC-Theory of an Exciton-Polariton in a Slab*, Journal of the Physical Society of Japan **59**(2), 754–764, 10 pages (Feb 1990).

[102] Hajime Ishihara and Kikuo Cho, *Additional-boundary-condition-free theory of an exciton polariton in a slab*, Phys. Rev. B **41**(3), 1424–1434, 10 pages (Jan 1990).

[103] Satoru Okumura and Tetsuo Ogawa, *Boson representation of two-exciton correlations: An exact treatment of composite-particle effects*, Phys. Rev. B **65**(3), 035105, 17 pages (Dec 2001).

[104] M. Combescot, O. Betbeder-Matibet, and R. Combescot, *Exciton-exciton scattering: Composite boson versus elementary boson*, Phys. Rev. B **75**(17), 174305, 21 pages (May 2007).

[105] M. Combescot, M. A. Dupertuis, and O. Betbeder-Matibet, *Polariton-polariton scattering: Exact results through a novel approach*, Europhys. Lett. **79**(1), 17001, 6 pages (Jun 2007).

[106] Alexander L. Fetter and John Dirk Walecka, *Quantum Theory of Many-Particle Systems* (Dover, New York, 1971), Reprint edition.

[107] S. Doniach and E. H. Sondheimer, *Green's Functions for Solid State Physicists* (Imperial College Press, Singapore, 1998), Reprint edition.

[108] Pierre Meystre and Murray Sargent III, *Elements of Quantum Optics* (Springer-Verlag, Berlin, 1999), Third edition.

[109] C. W. Gardiner and P. Zoller, *Quantum Noise: A Handbook Of Markovian And Non-markovian Quantum Stochastic Methods With Applications To Quantum Optics*, Springer Series in Synergetics (Springer-Verlag, Berlin, 2004), Third edition.

List of Publications

Articles

1. Kikuo Cho, Jun Ushida, and Motoaki Bamba, *Optical Response of Photonic Crystals Requiring High Precision Band Calculation in the Form of $k(\omega)$ Including Evanescent Waves*, Journal of the Physical Society of Japan, Vol. 74, No. 11, pp. 3088–3092 (November 2005).
2. Motoaki Bamba and Hajime Ishihara, *QED of excitons with nonlocal susceptibility in arbitrary-structured dielectrics*, Physical Review B, Vol. 78, No. 8, Art. No. 085109, 22 pages (August 2008); selected for Virtual Journal of Nanoscale Science & Technology, Vol. 18, Issue 8 (August 2008).
3. Motoaki Bamba and Hajime Ishihara, *Breakdown of Fermi's Golden Rule in Exciton-Photon Interaction*, Journal of the Physical Society of Japan, Vol. 78, No. 4, to be published (2009).
4. Motoaki Bamba and Hajime Ishihara, *Crossover of exciton-photon coupled modes in finite crystal*, to be submitted.
5. Motoaki Bamba and Hajime Ishihara, *High-performance control of entangled-photon generation by nanostructure design*, in preparation.
6. Motoaki Bamba and Hajime Ishihara, *Thickness dependence of entangled-photon generation via biexcitons*, to be submitted.
7. Motoaki Bamba and Hajime Ishihara, *Exciton correlation function in exciton-photon inhomogeneous system*, in preparation.

Invited paper

1. H. Ishihara, A. Syouji, Y. Segawa and M. Bamba, *Anomalous exciton-radiation coupling in the nano-to-bulk crossover regime*, Journal of Physics: Condensed Matter, Vol. 19, No. 44, Art. No. 445008, 20 pages (October 2007).

Proceedings

1. Motoaki Bamba and Hajime Ishihara, *Entangled-photon generation via biexcitons in nanostructures*, physica status solidi (c), Vol. 3, Issue 10, pp. 3460–3463 (November 2006); Proceedings of EXCON'06.
2. Motoaki Bamba and Hajime Ishihara, *QED theory for excitons with microscopic nonlocality*, physica status solidi (c), Vol. 5, Issue 7, pp. 2387–2390 (June 2008); Proceedings of OECS10.

3. Motoaki Bamba and Hajime Ishihara, *Radiative decay theory: What suppresses exciton superradiance?*, physica status solidi (c), Vol. 6, Issue 1, pp. 128–132 (January 2009); Proceedings of EXCON'08.
4. Motoaki Bamba and Hajime Ishihara, *Radiative decay theory of excitons in nano-to-macro crossover*, to be published; Proceedings of International School of Physics "Enrico Fermi" Course CLXII: Quantum Coherence in Solid State Physics.

Conference presentations

1. K. Cho, J. Ushida, and M. Bamba, *Photonic band calculation in the form of $k(\omega)$ including evanescent waves*, International Symposium on Photonic and Electromagnetic Crystal Structures V, PECS-V (Kyoto, Japan; 7–11 March 2004), Mo-P52, Poster.
2. Motoaki Bamba and Hajime Ishihara, *Entangled-Photon Generation via Biexcitons in Semiconductor Nano-Structures*, Conference on Lasers and Electro-Optics / Quantum Electronics and Laser Science Conference 2006, CLEO/QELS 2006 (Long Beach, California, USA; 21–26 May 2006), JTuD4, Poster.
3. Motoaki Bamba and Hajime Ishihara, *Entangled-photon generation via biexcitons in nanostructures*, 7th International Conference on Excitonic Processes in Condensed Matter, EXCON'06 (Winston-Salem, North Carolina, USA; 25–30 June 2006), PLB-3, Oral.
4. Motoaki Bamba and Hajime Ishihara, *Drastic Interplay between Dephasing and Optical Processes of Confined Excitons*, 16th International Conference on Dynamical Processes in Excited States of Solids, DPC'07 (Segovia, Spain; 17–22 June 2007), Mo-P5-03, Poster.
5. M. Bamba and H. Ishihara, *QED theory for Weakly Confined Excitons with Radiative Relaxation*, 10th Conference on the "Optics of Excitons in Confined Systems," OECS10 (Patti, Messina, Italy; 10–13 September 2007), PMo2, Poster.
6. Motoaki Bamba and Hajime Ishihara, *Radiative Decay Theory of Excitons in Weak-confinement to Bulk Regime*, 8th International Conference on Physics of Light-Matter Coupling in Nanostructures, PLMCN8 (Tokyo, Japan; 7–11 April 2008), ThB-2, Oral.
7. Motoaki Bamba and Hajime Ishihara, *Radiative decay theory: What suppresses exciton superradiance?*, 8th International Conference on Excitonic Processes in Condensed Matter, EXCON'08 (Kyoto, Japan; 22–27 June 2008), OP-III-10, Oralposter.
8. Motoaki Bamba and Hajime Ishihara, *Radiative decay theory of excitons in nano-to-macro crossover*, International School of Physics "Enrico Fermi" Course CLXII, Quantum Coherence in Solid State Physics (Varenna, Italy; 1–11 July 2008), B-10, Poster.

Award

1. Motoaki Bamba, *Radiative relaxation theory of excitons: weak confinement to bulk crossover*, Award for Encouragement of Research in Condensed Matter Photophysics, granted by Association for Condensed Matter Photophysics, (Osaka City University, Japan; 21 December 2007).